Guerreiro, Rita, Ross, Owen A., Kun-Rodrigues, Celia, Hernandez, Dena G., Orme, Tatiana, Eicher, John D., Shepherd, Claire E., Parkkinen, Laura, Darwent, Lee, Heckman, Michael G., Scholz, Sonja W., Troncoso, Juan C., Pletnikova, Olga, Ansorge, Olaf, Clarimon, Jordi, Lleo, Alberto, Morenas-Rodriguez, Estrella, Clark, Lorraine, Honig, Lawrence S., Marder, Karen, Lemstra, Afina, Rogaeva, Ekaterina, St George-Hyslop, Peter, Londos, Elisabet, Zetterberg, Henrik, Barber, Imelda, Braae, Anne, Brown, Kristelle, Morgan, Kevin, Troakes, Claire, Al-Sarraj, Safa, Lashley, Tammaryn, Holton, Janice, Compta, Yaroslau, Van Deerlin, Vivianna, Serrano, Geidy E., Beach, Thomas G., Lesage, Suzanne, Galasko, Douglas, Masliah, Eliezer, Santana, Isabel, Pastor, Pau, Diez-Fairen, Monica, Aguilar, Miquel, Tienari, Pentti J., Myllykangas, Liisa, Oinas, Minna, Revesz, Tamas, Lees, Andrew, Boeve, Brad F., Petersen, Ronald C., Ferman, Tanis J., Escott-Price, Valentina , Graff-Radford, Neill, Cairns, Nigel J., Morris, John C., Pickering-Brown, Stuart, Mann, David, Halliday, Glenda M., Hardy, John, Trojanowski, John Q., Dickson, Dennis W., Singleton, Andrew, Stone, David J. and Bras, Jose 2018. Investigating the genetic architecture of dementia with Lewy bodies: a two-stage genome-wide association study. Lancet Neurology 17 (1) , pp. 64-74. 10.1016/S1474-4422(17)30400-3

Genome-wide association analysis of Dementia with Lewy bodies reveals unique genetic architecture

Rita Guerreiro[1, 2, 3]*, Owen A. Ross[4]*, Celia Kun-Rodrigues[2], Dena Hernandez[5], Tatiana Orme[2], John Eicher[6], Claire Shepherd[7], Laura Parkkinen[8], Lee Darwent[2], Michael G. Heckman[9], Sonja W. Scholz[10], Juan C. Troncoso[11], Olga Pletnikova[11], Olaf Ansorge[8], Jordi Clarimon[12], Alberto Lleo[12], Estrella Morenas-Rodriguez[12], Lorraine Clark[13], Lawrence S Honig[13], Karen Marder[13], Afina Lemstra[14], Ekaterina Rogaeva[15], Peter St. George-Hyslop[15, 16], Elisabet Londos[17], Henrik Zetterberg[18], Imelda Barber[19], Anne Braae[19], Kristelle Brown[19], Kevin Morgan[19], Claire Troakes[20], Safa Al-Sarraj[20], Tammaryn Lashley[21], Janice Holton[21], Yaroslau Compta[22], Vivianna Van Deerlin[23], Geidy E Serrano[24], Thomas G. Beach[24], Suzanne Lesage[25], Douglas Galasko[26], Eliezer Masliah[27], Isabel Santana[28], Pau Pastor[29], Monica Diez-Fairen[29], Miquel Aguilar[29], Pentti J. Tienari[30], Liisa Myllykangas[31], Minna Oinas[32], Tamas Revesz[21], Andrew Lees[21], Brad F Boeve[33], Ronald C. Petersen[33], Tanis J Ferman[34], Valentina Escott-Price[35], Neill Graff-Radford[36], Nigel Cairns[37], John C. Morris[37], Stuart Pickering-Brown[38], David Mann[38], Glenda M. Halliday[39, 40], John Hardy[2], John Q. Trojanowski[23], Dennis W. Dickson[4], Andrew Singleton[5], David Stone[6], Jose Bras[1, 2, 3,✝]

* - Denotes equally contributing authors

✝ - Corresponding author. Email: j.bras@ucl.ac.uk

1 - UK Dementia Research Institute (UK DRI) at UCL, London, UK

2 - Department of Molecular Neuroscience, UCL Institute of Neurology, London, UK

3 - Department of Medical Sciences and Institute of Biomedicine, iBiMED, University of Aveiro, 3810-193 Aveiro, Portugal

4 - Department of Neuroscience, Mayo Clinic, Jacksonville, FL, USA

5 - Laboratory of Neurogenetics, National Institutes on Aging, NIH, Bethesda, MD, USA

6 - Genetics and Pharmacogenomics, Merck Research Laboratories, West Point, Pennsylvania, USA

7 - Neuroscience Research Australia, Sydney, Australia and School of Medical Sciences, Faculty of Medicine, University of New South Wales, Sydney, Australia

8 - Nuffield Department of Clinical Neurosciences, Oxford Parkinson's Disease Centre,

University of Oxford, Oxford, UK
9 - Division of Biomedical Statistics and Informatics, Mayo Clinic, Jacksonville, FL, USA
10 - Neurodegenerative Diseases Research Unit, National Institute of Neurological Disorders and Stroke, National Institutes of Health, Bethesda, Maryland, USA
11 - Department of Pathology (Neuropathology), Johns Hopkins University School of Medicine, Baltimore, MD, USA
12 - Memory Unit, Department of Neurology, IIB Sant Pau, Hospital de la Santa Creu i Sant Pau, Universitat Autonoma de Barcelona, Barcelona, Spain; Centro de Investigacion Biomedica en Red en Enfermedades Neurodegenerativas (CIBERNED), Instituto de Salud Carlos III, Madrid, Spain
13 - Taub Institute for Alzheimer Disease and the Aging Brain and Department of Pathology and Cell Biology, Columbia University, New York, NY, USA
14 - Department of Neurology and Alzheimer Center, Neuroscience Campus Amsterdam, VU University Medical Center, Amsterdam, the Netherlands
15 - Tanz Centre for Research in Neurodegenerative Diseases and department of Medicine, University of Toronto, Ontario, Canada
16 - Department of Clinical Neurosciences, Cambridge Institute for Medical Research, University of Cambridge, Cambridge, UK
17 - Clinical Memory Research Unit, Institution of Clinical Sciences Malmo, Lund University, Sweden
18 - UK Dementia Research Institute at UCL, London UK, Department of Molecular Neuroscience, UCL Institute of Neurology, London, UK and Clinical Neurochemistry Laboratory, Institute of Neuroscience and Physiology, Sahlgrenska Academy at the University of Gothenburg, Molndal, Sweden
19 - Human Genetics, School of Life Sciences, Queen’s Medical Centre, University of Nottingham, Nottingham, UK
20 - Department of Basic and Clinical Neuroscience and Institute of Psychiatry, Psychology and Neuroscience, King’s College London, London, UK
21 - Queen Square Brain Bank, Department of Molecular Neuroscience, UCL Institute of Neurology, London, UK
22 - Queen Square Brain Bank, Department of Molecular Neuroscience, UCL Institute of Neurology, London, UK and Movement Disorders Unit, Neurology Service, Clinical Neuroscience Institute (ICN), Hospital Clinic, University of Barcelona, IDIBAPS, Barcelona, Spain

23 - Department of Pathology and Laboratory Medicine, Center for Neurodegenerative Disease Research, Perelman School of Medicine at the University of Pennsylvania, 3600 Spruce Street, Philadelphia, USA
24 - Banner Sun Health Research Institute, 10515 W Santa Fe Drive, Sun City, AZ 85351, USA
25 - Inserm U1127, CNRS UMR7225, Sorbonne Universites, UPMC Univ Paris 06, UMR and S1127, Institut du Cerveau et de la Moelle epiniere, Paris, France
26 - Department of Neurosciences, University of California, San Diego, La Jolla, CA, United States; Veterans Affairs San Diego Healthcare System, La Jolla, CA, United States
27 - Department of Neurosciences, University of California, San Diego, La Jolla, CA, United States; Department of Pathology, University of California, San Diego, La Jolla, CA, United States
28 - Neurology Service, University of Coimbra Hospital, Coimbra, Portugal
29 - Memory Unit, Department of Neurology, University Hospital Mutua de Terrassa, University of Barcelona, and Fundacio de Docencia I Recerca Mutua de Terrassa, Terrassa, Barcelona, Spain. Centro de Investigacion Biomedica en Red Enfermedades Neurdegenerativas (CIBERNED), Madrid, Spain
30 - Molecular Neurology, Research Programs Unit, University of Helsinki, Department of Neurology, Helsinki University Hospital, Helsinki, Finland
31 - Department of Pathology, Haartman Institute, University of Helsinki and HUSLAB
32 - Department of Neuropathology and Neurosurgery, Helsinki University Hospital and University of Helsinki, Helsinki, Finland
33 - Neurology Department, Mayo Clinic, Rochester, MN, USA
34 - Department of Psychiatry and Department of Psychology, Mayo Clinic, Jacksonville, FL, USA
35 - MRC Centre for Neuropsychiatric Genetics and Genomics, School of Medicine, Cardiff University, Cardiff, UK
36 - Department of Neurology, Mayo Clinic, Jacksonville, FL, USA
37 - Knight Alzheimer’s Disease Research Center, Department of Neurology, Washington University School of Medicine, Saint Louis, MO, USA
38 - Institute of Brain, Behaviour and Mental Health, Faculty of Medical and Human Sciences, University of Manchester, Manchester, UK
39 - Neuroscience Research Australia, Sydney, Australia and School of Medical Sciences, Faculty of Medicine, University of New South Wales,Sydney, Australia
40 - Brain and Mind Centre, Sydney Medical School, The University of Sydney, Sydney,

Australia

Abstract

Background: Dementia with Lewy Bodies (DLB) is the second most common form of dementia in the elderly but has been overshadowed in the research field, in part due to similarities between DLB, Parkinson's (PD) and Alzheimer's diseases (AD). This overlap complicates clinical care in that an accurate diagnosis is not always straightforward, and suggests that these diseases may share common aetiology. We have recently shown that loci implicated in susceptibility to PD and AD also play a role in DLB and that the proportion of genetic correlation between these diseases is very similar, when the major risk locus for AD, *APOE*, is excluded. These results demonstrate not only that DLB is genetically associated with these more common diseases, but also that DLB has a strong and quantifiable genetic component that is unique.

Methods: Here we have performed the first large-scale genome-wide association study of DLB in a combined cohort of 1,743 DLB patients and 5,033 controls. We exploited the recently established Haplotype Reference Consortium panel as the basis for imputation to a total of 8.4 million high-quality imputed genotypes and performed independent replication and a meta-analysis of significant and suggestive results.

Findings: Results confirm previously reported associations (*APOE, SNCA, GBA*) and provide genome-wide significant signals for two novel loci (*BCL7C/STX1B* and *CNTN1*), in addition to several loci with suggestive levels of association. Additionally, using the genome-wide SNP data we estimate the heritable component of DLB to be approximately 36%.

Interpretation: These results allow us to characterize, for the first time, the role of common genomic variability in DLB. They show unequivocally that common genetic variability plays a role in this disease, that this variability is, to some extent, shared with PD and AD and, finally, that there is a genetic component that seems unique to the disease.

Funding

Funded by the Alzheimer's Society, and the Lewy Body Society

Introduction

Dementia with Lewy Bodies (DLB) is the second most common form of dementia following Alzheimer's disease (AD) [1]. Despite this fact, very little attention has been devoted to understanding the pathogenesis of this disorder, particularly when compared with the other common neurodegenerative diseases such as AD and Parkinson's disease (PD).

So far, the only fully penetrant genetic variability that has been identified and replicated as a specific cause of DLB are *SNCA* point mutations and gene dosage. Three major factors may have contributed to this low number of causative mutations: first, DLB, often a disease of old age, is not commonly seen in multiplex kindreds, meaning that successful linkage studies have been rare [2]; second, the accurate clinical diagnosis of DLB is complex, with a relatively high rate of misdiagnosis [3]; and third, because even the largest cohorts of DLB samples have been generally small, in many instances including as little as 100 patients [4,5]. However, it is currently indisputable that DLB has a strong genetic component. The epsilon-4 allele of *APOE* [6,7] is recognized to be a strong risk factor, as are heterozygous mutations and common polymorphisms in the glucocerebrosidase gene (*GBA*)[8]. Both of these results have stemmed from candidate gene association studies; it was known that *APOE* was strongly associated with AD and *GBA* was a strong risk factor for PD/Lewy body disorders. In addition to these genetic associations with susceptibility, we have recently provided evidence that DLB has a heritable component [9].

It has been shown that there is no overlap in common genetic risk between PD and AD [10], a fact that is not entirely surprising given the differences in phenotype. However, it is reasonable to hypothesize that the overlaps and differences in clinical and pathological presentation between DLB with both PD and AD stem, at least in part, from aspects in their underlying genetic architecture and, consequently, disease pathobiology. Specific genes/loci associated with disease as well as strength of association are factors that can be expected to modulate these phenotypic overlaps and differences. However, despite these encouraging findings, large-scale unbiased genetic studies in DLB have not yet been performed, which is likely due to the difficulty in identifying large, homogeneous cohorts of cases.

To address the need for more powerful and comprehensive genetic studies of DLB, we performed the first large-scale genome-wide association study in this disease, using a total of 1,743 cases and 5,033 controls. The majority of cases (n=1,324) were neuropathologically assessed, providing a greater level of diagnostic detail. Controls used were derived from two publicly available datasets and from the Mayo Clinic Florida control database. We performed imputation using the most recent imputation panel provided by the Haplotype Reference

Consortium enabling us to have a detailed overview of common and intermediate frequency genetic variability.

Methods

Participants

All case subjects (n=1,687 in discovery and n=527 in replication stages) were diagnosed according to the consensus criteria for either clinical or pathological diagnosis of DLB [11]. The majority of cases were pathologically diagnosed (n=1,308 in discovery and 350 in replication stages), and these were included only when the likelihood of a diagnosis of DLB was "Intermediate" or "High" [11]. Control subjects (n=4,370 in discovery and n=663 in replication stages) are part of the "General Research Use" controls from the two studies publicly available at dbGaP (The Genetic Architecture of Smoking and Smoking Cessation (phs000404.v1.p1) and Genetic Analysis of Psoriasis and Psoriatic Arthritis (phs000982.v1.p1)) and the Mayo Clinic Florida control database for the replication stage only.

Discovery stage genotyping and quality control

Case subjects (n=1,687) were genotyped in either Illumina Omni2.5M or Illumina OmniExpress genotyping arrays (n=987 and n=700, respectively) (Table 1). Controls (n=4,370) were genotyped in either Illumina Omni2.5M or Illumina Omni1M arrays (n=1,523 and n=2,847 respectively). Autosomal variants with GenTrain scores >0.7 were included in the QC stage. We removed SNPs with a call rate <95%, HWE p-value in controls $<1\times10^{-7}$, or a minor allele frequency (MAF) <0.01. Samples were removed if they had substantial non-European admixture, were duplicates or first- or second-degree relatives of other samples, had a genotype call rate <98% or had substantial cryptic relatedness scores (PI_HAT >0.1).

Population outliers were determined by principal components analysis (PCA), using SNPs passing the aforementioned quality-control filters. After linkage disequilibrium (LD)-based pruning with version 1.9 of PLINK [12] to quasi-independence (variance inflation factor =2), 130,715 SNPs remained in the dataset. Genotypes for these SNPs were combined with 1000Genomes phase 3 genotypes for samples from the YRI, CEU, JPT, and CHB reference populations, and subjected to PCA. Individuals lying farther than ¼ of the distance between CEU and JPT/CHB/YRI when plotted on the first two PCA axes were considered to have substantial non-European admixture and were excluded.

Imputation

We performed imputation using the most recent reference panels provided by the Haplotype Reference Consortium (HRC v1.1 2016). Eagle v2.3 was used to pre-phase haplotypes based on genotype data[13,14]. Imputation was conducted using the Michigan Imputation Server[15]. Following imputation, variants passing a standard imputation quality threshold (R^2 >= 0.3) were kept for further analysis.

Statistical Analysis of discovery stage

We used logistic regression as implemented in PLINK2[12] to test for association of variants with the binary case-control phenotype. Variants were examined under an additive model (i.e. effect of each minor allele) and odds ratios (ORs) and 95% confidence intervals (Cis) were estimated. To control for population stratification, we used coordinates from the top twenty PCA dimensions as covariates in the logistic regression models. We utilized QQ plots and the genomic inflation factor (λ) to test for residual effects of population stratification not fully controlled for by the inclusion of PCA and cohort covariates in the regression model.

Gene-wise burden tests were performed using all variants with an effect in protein sequence and a maximum MAF of 5%, using SKAT-O [16,17] as implemented in EPACTS [18].

Replication genotyping

A total of 527 DLB cases and 663 controls from the Mayo Clinic were included in the replication stage (Table 2). Replication was attempted for top variants showing a p-value in discovery of less than 1×10^{-6}. A total of 32 signals were tested for replication using a Sequenom MassARRAY iPLEX SNP panel (Supplementary Table 1). Power calculations for replication sample size selection were performed using the R package ‘RPower’. An average statistical power of 0.806 (95%CI=0.714-0.864) was estimated for the 32 signals, based on sample size, variant frequency and effect size in the discovery stage and a replication p-value threshold of 0.05. Association in replication was tested using logistic regression models adjusted for age (age at onset for the clinically diagnosed DLB patients, age at death for the high likelihood DLB patients, and age at study for controls) and gender.

A combined analysis of stage 1 and 2 was conducted with GWAMA[19] under a fixed-effects model, using estimates of the allelic odds ratio and 95% confidence intervals.

Phenotypic variance explained

To estimate the phenotypic variance explained by the genotyped SNPs in this cohort we used GREML analysis as implemented in GCTA [20,21]. We used the first ten principal components as covariates and a disease prevalence of 0.1% [22]. We have also estimated the partitioned heritability by chromosome, where a separate genetic relationship matrix was generated for each chromosome. Each matrix was then run in a separate REML analysis. Linear regression was applied to determine the relationship between heritability and chromosome length.

Results

Single variant analysis

Application of quality control filters to the dataset yielded high-quality genotypes at 448,155 SNPs for 1,216 cases and 3,791 controls. After imputation and quality control, genotypes for 8,410,718 variants were available for downstream analyses. QQ plot and genomic inflation factor (λ=1.002) indicated good control of population stratification (Supplementary Figure 1).

Five regions were associated with DLB risk at genome-wide significance ($p<5x10^{-8}$) in the discovery stage (Figure 1; Table 3).

These included the previously described AD and PD loci *APOE* (rs429358, OR=2.4, $p=5.31x10^{-50}$), *SNCA* (rs7681440, OR=0.7412, $p=1.45x10^{-9}$) and *GBA* (rs35749011, OR=2.5, $p=1.77x10^{-9}$). Additionally, loci overlapping *BCL7C/STX1B* (rs897984, OR=0.72, $p=2.64x10^{-10}$) and *GABRB3* (rs1426210, OR=1.32, $p=4.63x10^{-8}$) were also genome-wide significant. Two additional regions surpassed a suggestive threshold of significance ($p=1x10^{-6}$) in the discovery stage, the first overlapping the *SOX17* gene (rs139919032, OR=2.4, $p=1.37x10^{-7}$) and the second overlapping the *CNTN1* gene (rs79329964, OR=1.5, $p=4.35x10^{-7}$). The replication stage of the GWAS design provided independent replication ($p<0.05$) for 4 of the loci (*APOE*, *SNCA*, *GBA*, *CNTN1*), all of which were also genome-wide significant in the combined analysis of both stages (Table 3; Supplementary Table 1). The associations at *GABRB3*, *BCL7C*/*STX1B* and *SOX17* were not replicated. However, combined analysis of the discovery and replication stages showed the *BCL7C*/*STX1B* association to survive genome-wide multiple testing correction ($p=1.19x10^{-8}$; Table 3).

The association observed at the *SNCA* locus represents an independent signal when compared to the top association reported for PD. Despite the independence of the top association signal from the largest PD GWAS, conditional analyses revealed a secondary association peak (rs7681154) in strong LD (r2=0.92) with our lead SNP here with DLB (rs7681440). Indeed, the PD secondary SNP showed similar association in the present DLB GWAS ($p=1.27x10^{-8}$). To gain insight into potential regulatory effects of this distinct SNCA signal, we used eQTL data from GTEx and the Harvard Brain Bank Resource Center to determine whether rs7681154 and rs7681440 influence gene expression as eQTLs. In the GTEx data, the most associated SNP in DLB is a strong eQTL in the cerebellum for *RP11-67M1.1*, a known antisense gene located at the 5'-end of *SNCA*, with the alternative allele showing a reduction in expression of *RP11-67M1.1* (Figure 2a). These results are compatible with a model in which rs7681440 genotypes influence the expression levels of *SNCA* through the action of *RP11-67M1.1*. More specifically, the alternative allele associates with a lower expression of *RP11-67M1.1* and consequently less repression of *SNCA* transcription (higher *SNCA* expression), which is in accordance with a higher frequency of the alternative allele in cases when compared to controls. Additionally, rs7681154 was associated with SNCA expression in cerebellum using the Harvard Brain Bank Resource Center results ($p=2.87x10^{-11}$) (Figure 2b), with the alternate allele associated with increased SNCA expression. Such a relationship between this locus and SNCA expression is supported by the high expression of SNCA in brain and the association of rs7681440 with increased SNCA expression in whole blood ($p=2.13x10^{-38}$) [23,24].

A systematic assessment of genetic loci previously associated with AD or PD showed no evidence of other genome-wide significant associations in this DLB cohort (Supplementary Figures 5 to 64). These include the *TREM2* locus, where the p.Arg47His variant has been shown to have a strong effect in AD [25]. In our cohort this variant did not show genome-wide significant levels of association (OR=3.4; p=0.002), despite the overrepresentation in cases. Similarly, *MAPT*, which is strongly associated with PD and has been previously linked to DLB [26], shows no strong evidence of association in this study (rs17649553; OR=0.86; p=0.0126).

Gene burden analysis

Gene based burden analysis of all low frequency (MAF < 0.05) and rare variants changing the amino acid sequence, showed a single genome-wide significant result comprised of 6 variants at *GBA* (p.Asn409Ser, p.Thr408Met, p.Glu365Lys, p.Arg301His, p.Ile20Val and p.Lys13Arg), ($p=1.29x10^{-13}$). No other gene showed evidence of strong association with disease or overlap with single variant analysis (Table 4).

Estimation of heritability of DLB

Using the first ten principal components as covariates and a disease prevalence of 0.1%, estimation of the phenotypic variance attributed to genetic variants showed a heritable component of DLB of 36% (± 0.03). Results for the chromosome-partitioned heritability are presented in Figure 3. As expected for a common complex disease, we found a strong correlation between chromosome length and heritability ($p = 6.875 \times 10^{-5}$).

Interestingly, the heritability for DLB at chromosome 19 is much higher than what would be expected given chromosome size and likely reflects the role of *APOE*. It should also be noted that chromosomes 5, 6, 7 and 13 all have higher heritability for DLB than expected, while none of them have variants with genome-wide significant results.

Discussion

This is the first comprehensive, unbiased study of common and intermediate frequency genetic variability in DLB. We identified five genome-wide significant associations (*APOE*, *BCL7C/STX1B, SNCA, GBA*, and, *CNTN1*).

The most significant association signal is observed at the *APOE* locus (*APOE E4*) which has been previously shown to be highly associated with DLB [6,7]. As described *APOE E4* is the major genetic risk locus for AD and has been implicated in cognitive impairment within PD although not with PD risk per se. It has also been observed to affect the levels of both β-amyloid and Lewy body pathology in brains of patients [27], and in a small Finnish dataset the E4 association with DLB was largely driven by the subgroup with concomitant AD pathology [28].

The second strongest association is observed at the *SNCA* locus and we were able to confirm the different association profile between DLB and PD that we had previously reported [7]. *SNC*A is the most significant common genetic risk factor for PD, with rs356182 having a meta-analysis p-value of 1.85×10^{-82} (OR:1.34 [1.30-1.38]) in PDGene. This variant is located 3' to the gene [29], while in DLB no association can be found in that region (Figure 4). Additionally, the most associated SNP reported here for the *SNCA* locus (rs7681440) has a meta-analysis p-value>0.05 in PDGene. Interestingly, when performing a conditional analysis on the top PD SNP (rs356182), Nalls and colleagues reported an independent association at the 5' region of the gene (rs7681154, OR:0.841, $p=7.09 \times 10^{-19}$). It is tempting to speculate that these differences may reflect pathobiological differences between the two diseases, perhaps mediated by differential regulation of gene expression. We show that the top DLB locus contains an eQTL in the cerebellum for a *SNCA* antisense gene and *SNCA* itself, with a consistent model of increased *SNCA* expression. However, further investigation of the identified significant eQTLs is needed: the effect was observed for only one brain region, even though other regions are present in the GTEx dataset, many with similar sample sizes, and include regions preferentially affected by Lewy body pathology (substantia nigra, frontal cortex, caudate). This could plausibly result from low overall expression of *SNCA-AS1* and higher cerebellum RNA quality when compared to other assayed brain regions in the GTEx data. Nonetheless, it is interesting to note that both eQTLs' effects fit with a model of increased *SNCA* expression in cases compared to controls.

The top hit at the *GBA* locus (rs35682329) is located 85,781bp downstream of the gene and is in high LD (D': 0.9; R^2: 0.8) with p.Glu365Lys (also reported in the literature as E365K, E326K, rs2230288), which has been suggested as a risk factor for DLB [8]. The top associated variant for PD at this locus is the rs71628662 (PDGene meta-analysis OR:0.52 [0.46-0.58] and p-value 6.86×10^{-28}). This variant is also in high LD with the top SNP identified here (D': 0.9 and R^2:0.8). Interestingly in this study we show that *APOE* and *GBA* have similar effect sizes in DLB (ORs of 2.5 and 2.2, respectively). Gene burden based analysis showed *GBA* as the only genome-wide significant association with DLB risk. The inexistence of other associations should be interpreted with some caution. As we are not ascertaining the complete spectrum of genetic variability, it is possible that other genes will have a significant burden of genetic variants that were simply not captured in our study design, despite using the most recent imputation panel.

An association at the *BCL7C/STX1B* locus has been previously reported for PD [29,30]. The top PD-associated variants at this locus were rs14235 (synonymous) and rs4889603 (intronic), located at *BCKDK* and *SETD1A*, respectively. The top SNP identified in DLB at this locus (rs897984) shows the same direction of association seen in PD (OR=0.93, 95%CI:0.90-0.96) and a meta-analysis p-value of 1.34×10^{-5} (data from PDgene). This is a gene-rich region of the genome (Figure 5) making it difficult to accurately nominate the gene driving the association. Mining data from the GTEx project showed that rs897984 is not an eQTL for any gene in the locus. Nonetheless, in both PD studies, the nominated gene at the locus was *STX1B* likely due to its function as a synaptic receptor [31]. In addition, *STX1B* has a distinctive pattern of expression across tissues, presenting the highest expression in the brain. In this tissue, when compared to the closest genes in the locus (*HSD3B7*, *BCL7C*, *ZNF668*, *MIR4519, CTF1*, *FBXL19*, *ORAI3*, *SETD1A*, *STX4*), *STX1B* also shows the highest levels of expression (Supplementary Figure 3). Mutations in *STX1B* have recently been shown to cause fever associated epileptic syndromes [32] and myoclonic astatic epilepsy [33].

The *CNTN1* locus has been previously associated with PD in a genome-wide study of IBD segments in an Ashkenazi cohort [34], and with cerebral amyloid deposition, assessed with PET imaging in *APOE E4* non-carriers [35]. This locus was also shown to be sub-significantly associated with clinico-pathologic AD dementia [36]. The Contactin 1 protein encoded by *CNTN1* is a glycosylphosphatidylinositol (GPI)-anchored neuronal membrane protein that functions as a cell adhesion molecule with important roles in axonal function [37,38]. Mutations in *CNTN1* were found to cause a familial form of lethal congenital myopathy [39]. Contactin 1 drives Notch signalling activation and modulates neuroinflammation events, possibly participating in the pathogenesis of Multiple Sclerosis and other inflammatory disorders [40]. A functional protein association network analysis of *CNTN1* using STRING shows it is in the same network as *PSEN2* (Supplementary Figure 4), supporting its potential role in neurodegeneration. It is also worth noting that *LRRK2* is located less than 500kb away from the most associated SNP at this locus, which could suggest that the association might be driven by variation at the *LRRK2* locus. We assessed LD across the region and that analysis revealed that rs79329964 is in equilibrium with both p.Gly2019Ser (R^2: 0.000043) as well as with the PD hit at this locus rs76904798 (R^2: 0.003), suggesting it to be an independent association from the PD risk. Although samples were not screened for p.Gly2019Ser directly, the variant was well imputed (R^2=0.94). The exclusion of all samples that carried the p.Gly2019Ser variant showed no significant effect on the association at the *CNTN1* locus. It is worth noting that the p.Gly2019Ser variant showed a higher minor allele frequency in cases when compared to controls (0.0021 and 0.0003 respectively).

In addition to performing a GWAS with clinico-pathologic AD dementia, Beecham and colleagues [36] also analysed commonly comorbid neuropathologic features observed in older individuals with dementia, including Lewy body disease (LBD). In this latter analysis, only the *APOE* locus was found to achieve genome-wide significance. However, when testing known common AD risk variants with coincident neuropathologic features, the authors identified hits at *SORL1* and *MEF2C* as nominally associated. In our cohort of DLB cases we found no genome-wide significant associations between these variants and disease. Similarly, we had previously reported an association at the *SCARB2* locus with DLB [7]. In the larger dataset studied herein, the association remained at the suggestive level and did not reach genome-wide significance (top SNP in the current study rs13141895: p-value=9.58×10^{-4}). No other variant previously reported to be significantly associated with AD or PD in recent GWAS meta-analyses showed a genome-wide significant association with DLB. The top AD or PD variants at the following loci showed nominal ($p<0.05$) association levels: *MAPT*, *BIN1*, *GAK*, *HLA-DBQ*, *CD2AP*, *INPP5D*, *ECHDC3* and *SCIMP*. Additionally, variants previously suggested to be associated with Lewy-related pathology in a Finnish cohort, did not show evidence of association in this study

(Supplementary Table 2).

This is the first large-scale genome-wide association study performed in DLB. We estimate the heritability of DLB to be approximately 36%, which is similar to what is known to occur in PD [41]. This shows that, despite not having multiple causative genes identified so far, genetics plays a relevant role in the common forms of DLB. Additionally, we provide evidence suggesting that novel DLB loci are likely to be found at chromosomes 5, 6, 7 and 13 given the high heritability estimates at these chromosomes. A significant majority of our case cohort in the current study was comprised of cases with neuropathological diagnoses, which provides a greater level of information for diagnostic accuracy. These results provide us with the first glimpse into the molecular pathogenesis of DLB; they reveal that this disorder has a strong genetic component and a unique genetic risk profile. From a molecular perspective, DLB does not simply sit between PD and AD; instead, the combination of risk alleles is unique, with loci that are established risk factors for those diseases having no clear role in DLB (e.g. *MCCC1*, *STK39*, *CLU*, *CR1* or *PICALM*). Further increases in the size of DLB cohorts will likely reveal additional common genetic risk loci, and these will, in turn, improve our understanding of this disease, its commonalities and differences with other neurodegenerative conditions, ultimately allowing us to identify disease-specific targets for future therapeutic approaches.

Contributors

JB, RG, JH and AS designed the study. JB, AS, DS, and OAR obtained funding for the study. JB, RG, OAR, CKR, LD, SWS and DH performed data acquisition. JB, RG, OAR, and CKR analysed and interpreted the data. CS, LP, SWS, OA, JC, LC, LH, KM, AL, PS, WvdF, EL, HH, ER, PGH, EL, HZ, IB, AB, KB, KM, WM, DB, CT, SAS, TL, JH, YC, VVD, JQT, GES, TGB, SL, DG, EM, IS, PP, PJT, LM, MO, TR, AJL, BFB, RCP, TJF, VEP, NGR, NC, JCM, DS, SPB, DM, DWD, GH collected and characterised samples. JB, RG, OAR, CKR, and TO wrote the first draft of the paper. All other co-authors participated in preparation of the paper by reading and commenting on drafts before submission.

Declaration of interests

We declare that we have no conflicts of interest.

Acknowledgments

This work was supported in part by the National Institutes of Neurological Disease and Stroke. Jose Bras and Rita Guerreiro’s work is funded by research fellowships from the Alzheimer's

Society. Tatiana Orme is supported by a scholarship from the Lewy Body Society. For the neuropathologically confirmed samples from Australia, tissues were received from the Sydney Brain Bank, which is supported by Neuroscience Research Australia and the University of New South Wales, and Dr Halliday is funded by an NHMRC senior principal research fellowship. We would like to thank the South West Dementia Brain Bank (SWDBB) for providing brain tissue for this study. The SWDBB is supported by BRACE (Bristol Research into Alzheimer's and Care of the Elderly), Brains for Dementia Research and the Medical Research Council. We acknowledge the Oxford Brain Bank, supported by the Medical Research Council (MRC), Brains for Dementia Research (BDR) (Alzheimer Society and Alzheimer Research UK), Autistica UK and the NIHR Oxford Biomedical Research Centre. The brain samples and/or bio samples were obtained from The Netherlands Brain Bank, Netherlands Institute for Neuroscience, Amsterdam (open access: www.brainbank.nl). All Material has been collected from donors for or from whom a written informed consent for a brain autopsy and the use of the material and clinical information for research purposes had been obtained by the NBB. This study was also partially funded by the Wellcome Trust, Medical Research Council and Canadian Institutes of Health Research (Dr. St. George-Hyslop). Work from Dr. Compta was supported by the CERCA Programme / Generalitat de Catalunya, Barcelona, Catalonia, Spain. The Nottingham Genetics Group is supported by ARUK and The Big Lottery Fund. The effort from Columbia University was supported by the Taub Institute, the Panasci Fund, the Parkinson's Disease Foundation, and NIH grants NS060113 (Dr Clark), P50AG008702 (P.I. Scott Small), P50NS038370 (P.I.R. Burke), and UL1TR000040 (P.I.H. Ginsberg). Dr Ross is supported by the Michael J. Fox Foundation for Parkinson's Research, NINDS R01# NS078086. The Mayo Clinic Jacksonville is a Morris K. Udall Parkinson's Disease Research Center of Excellence (NINDS P50 #NS072187) and is supported by The Little Family Foundation and by the Mangurian Foundation Program for Lewy Body Dementia research and the Alzheimer Disease Research Center (P50 AG016547). The work from the Mayo Clinic Rochester is supported by the National Institute on Aging (P50 AG016574 and U01 AG006786). This work has received support from The Queen Square Brain Bank at the UCL Institute of Neurology; where Dr Lashley is funded by an ARUK senior fellowship. Some of the tissue samples studied were provided by the MRC London Neurodegenerative Diseases Brain Bank and the Brains for Dementia Research project (funded by Alzheimer's Society and ARUK). This research was supported in part by both the NIHR UCLH Biomedical Research Centre and the Queen Square Dementia Biomedical Research Unit. This work was supported in part by the Intramural Research Program of the National Institute on Aging, National Institutes of Health, Department of Health and Human Services;

project AG000951-12. The University of Pennsylvania case collection is funded by the Penn Alzheimer's Disease Core Center (AG10124) and the Penn Morris K. Udall Parkinson's Disease Research Center (NS053488). Tissue samples from UCSD are supported by NIH grant AG05131. The authors thank the brain bank GIE NeuroCEB, the French program “Investissements d'avenir” (ANR-10-IAIHU-06). Dr Tienari and Dr Myllykangas are supported by the Helsinki University Central Hospital, the Folkhälsan Research Foundation and the Finnish Academy. This work was in part supported by the Canadian Consortium on Neurodegeneration in Aging (ER). The Genotype-Tissue Expression (GTEx) Project was supported by the Common Fund of the Office of the Director of the National Institutes of Health, and by NCI, NHGRI, NHLBI, NIDA, NIMH, and NINDS. The data used for the analyses described in this manuscript were obtained from the GTEx Portal on 04/01/17. The authors acknowledge the contribution of data from Genetic Architecture of Smoking and Smoking Cessation accessed through dbGAP. Funding support for genotyping, which was performed at the Center for Inherited Disease Research (CIDR), was provided by 1 X01 HG005274-01. CIDR is fully funded through a federal contract from the National Institutes of Health to The Johns Hopkins University, contract number HHSN268200782096C. Assistance with genotype cleaning, as well as with general study coordination, was provided by the Gene Environment Association Studies (GENEVA) Coordinating Center (U01 HG004446). Funding support for collection of datasets and samples was provided by the Collaborative Genetic Study of Nicotine Dependence (COGEND; P01 CA089392) and the University of Wisconsin Transdisciplinary Tobacco Use Research Center (P50 DA019706, P50 CA084724). The data used for the analyses described in this paper were obtained from the database of Genotypes and Phenotypes (dbGaP), at http://www.ncbi.nlm.nih.gov/gap. Genotype and phenotype data for the Genetic Analysis of Psoriasis and Psoriatic Arthritis study were provided by Dr. James T. Elder, University of Michigan, with collaborators Dr. Dafna Gladman, University of Toronto and Dr. Proton Rahman, Memorial University of Newfoundland, providing samples. This work was supported in part by the Intramural Research Program of the National Institutes of Health (National Institute of Neurological Disorders and Stroke; project ZIA NS003154). Tissue samples for genotyping were provided by the Johns Hopkins Morris K. Udall Center of Excellence for Parkinson’s Disease Research (NIH P50 NS38377) and the Johns Hopkins Alzheimer Disease Research Center (NIH P50 AG05146). This study was supported by grants from the National Institutes of Health, the Canadian Institute for Health Research, and the Krembil Foundation. Additional support was provided by the Babcock Memorial Trust and by the Barbara and Neal Henschel Charitable Foundation. JTE is supported by the Ann Arbor Veterans Affairs Hospital. The authors would like to thank the Genome Aggregation Database (gnomAD) and the groups that provided exome and genome variant data to this resource. A full list of contributing groups can be found at http://gnomad.broadinstitute.org/about.

References

1 Rahkonen T, Eloniemi-Sulkava U, Rissanen S, Vatanen A, Viramo P, Sulkava R. Dementia with Lewy bodies according to the consensus criteria in a general population aged 75 years or older. *J Neurol Neurosurg Psychiatry* 2003; **74**: 720–4.

2 Bogaerts V, Engelborghs S, Kumar-Singh S, *et al.* A novel locus for dementia with Lewy bodies: a clinically and genetically heterogeneous disorder. *Brain* 2007; **130**: 2277–91.

3 Walker Z, Possin KL, Boeve BF, Aarsland D. Lewy body dementias. *Lancet* 2015; **386**: 1683–97.

4 Keogh MJ, Kurzawa-Akanbi M, Griffin H, *et al.* Exome sequencing in dementia with Lewy bodies. *Transl Psychiatry* 2016; **6**: e728.

5 Geiger JT, Ding J, Crain B, *et al.* Next-generation sequencing reveals substantial genetic contribution to dementia with Lewy bodies. *Neurobiol Dis* 2016; **94**: 55–62.

6 Tsuang D, Leverenz JB, Lopez OL, *et al.* APOE ε4 increases risk for dementia in pure synucleinopathies. *JAMA Neurol* 2013; **70**: 223–8.

7 Bras J, Guerreiro R, Darwent L, *et al.* Genetic analysis implicates APOE, SNCA and suggests lysosomal dysfunction in the etiology of dementia with Lewy bodies. *Hum Mol Genet* 2014; **23**: 6139–46.

8 Nalls MA, Duran R, Lopez G, *et al.* A multicenter study of glucocerebrosidase mutations in dementia with Lewy bodies. *JAMA Neurol* 2013; **70**: 727–35.

9 Guerreiro R, Escott-Price V, Darwent L, *et al.* Genome-wide analysis of genetic correlation in dementia with Lewy bodies, Parkinson's and Alzheimer's diseases. *Neurobiol Aging* 2016; **38**: 214.e7–10.

10 Moskvina V, Harold D, Russo G, *et al.* Analysis of genome-wide association studies of Alzheimer disease and of Parkinson disease to determine if these 2 diseases share a common genetic risk. *JAMA Neurol* 2013; **70**: 1268–76.

11 McKeith IG, Dickson DW, Lowe J, *et al.* Diagnosis and management of dementia with Lewy bodies: third report of the DLB Consortium. *Neurology* 2005; **65**: 1863–72.

12 Chang CC, Chow CC, Tellier LC, Vattikuti S, Purcell SM, Lee JJ. Second-generation PLINK: rising to the challenge of larger and richer datasets. *Gigascience* 2015; **4**: 7.

13 McCarthy S, Das S, Kretzschmar W, *et al.* A reference panel of 64,976 haplotypes for genotype imputation. *Nat Genet* 2016; **48**: 1279–83.

14 Loh P-R, Danecek P, Palamara PF, *et al.* Reference-based phasing using the Haplotype Reference Consortium panel. *Nat Genet* 2016; **48**: 1443–8.

15 Das S, Forer L, Schönherr S, *et al.* Next-generation genotype imputation service and methods. *Nat Genet* 2016; **48**: 1284–7.

16 Wu MC, Lee S, Cai T, Li Y, Boehnke M, Lin X. Rare-variant association testing for sequencing data with the sequence kernel association test. *Am J Hum Genet* 2011; **89**: 82–93.

17 Lee S, Emond MJ, Bamshad MJ, *et al.* Optimal unified approach for rare-variant association testing with application to small-sample case-control whole-exome sequencing studies. *Am J Hum Genet* 2012; **91**: 224–37.

18 Kang HM. EPACTS: efficient and parallelizable association container toolbox. 2014.

19 Mägi R, Morris AP. GWAMA: software for genome-wide association meta-analysis. *BMC Bioinformatics* 2010; **11**: 288.

20 Yang J, Benyamin B, McEvoy BP, *et al.* Common SNPs explain a large proportion of the heritability for human height. *Nat Genet* 2010; **42**: 565–9.

21 Lee SH, Wray NR, Goddard ME, Visscher PM. Estimating missing heritability for disease from genome-wide association studies. *Am J Hum Genet* 2011; **88**: 294–305.

22 Zaccai J, McCracken C, Brayne C. A systematic review of prevalence and incidence studies of dementia with Lewy bodies. *Age Ageing* 2005; **34**: 561–6.

23 GTEx Consortium. Human genomics. The Genotype-Tissue Expression (GTEx) pilot analysis: multitissue gene regulation in humans. *Science* 2015; **348**: 648–60.

24 Westra H-J, Peters MJ, Esko T, *et al.* Systematic identification of trans eQTLs as putative drivers of known disease associations. *Nat Genet* 2013; **45**: 1238–43.

25 Guerreiro R, Wojtas A, Bras J, *et al.* TREM2 variants in Alzheimer’s disease. *N Engl J Med* 2013; **368**: 117–27.

26 Labbé C, Heckman MG, Lorenzo-Betancor O, *et al.* MAPT haplotype H1G is associated with increased risk of dementia with Lewy bodies. *Alzheimers Dement* 2016; published online June 7. DOI:10.1016/j.jalz.2016.05.002.

27 Tsuang D, Leverenz JB, Lopez OL, *et al.* APOE ε4 increases risk for dementia in pure synucleinopathies. *JAMA Neurol* 2013; **70**: 223–8.

28 Peuralinna T, Myllykangas L, Oinas M, *et al.* Genome-wide association study of neocortical Lewy-related pathology. *Ann Clin Transl Neurol* 2015; **2**: 920–31.

29 Nalls MA, Pankratz N, Lill CM, *et al.* Large-scale meta-analysis of genome-wide association data identifies six new risk loci for Parkinson’s disease. *Nat Genet* 2014; **46**: 989–93.

30 International Parkinson’s Disease Genomics Consortium (IPDGC), Wellcome Trust Case Control Consortium 2 (WTCCC2). A two-stage meta-analysis identifies several new loci for Parkinson’s disease. *PLoS Genet* 2011; **7**: e1002142.

31 Smirnova T, Stinnakre J, Mallet J. Characterization of a presynaptic glutamate receptor. *Science* 1993; **262**: 430–3.

32 Schubert J, Siekierska A, Langlois M, *et al.* Mutations in STX1B, encoding a presynaptic protein, cause fever-associated epilepsy syndromes. *Nat Genet* 2014; **46**: 1327–32.

33 Vlaskamp DRM, Rump P, Callenbach PMC, *et al.* Haploinsufficiency of the STX1B gene is associated with myoclonic astatic epilepsy. *Eur J Paediatr Neurol* 2016; **20**: 489–92.

34 Vacic V, Ozelius LJ, Clark LN, *et al.* Genome-wide mapping of IBD segments in an Ashkenazi PD cohort identifies associated haplotypes. *Hum Mol Genet* 2014; **23**: 4693–702.

35 Li QS, Parrado AR, Samtani MN, Narayan VA, Alzheimer's Disease Neuroimaging Initiative. Variations in the FRA10AC1 Fragile Site and 15q21 Are Associated with Cerebrospinal Fluid Aβ1-42 Level. *PLoS One* 2015; **10**: e0134000.

36 Beecham GW, Hamilton K, Naj AC, *et al.* Genome-wide association meta-analysis of neuropathologic features of Alzheimer's disease and related dementias. *PLoS Genet* 2014; **10**: e1004606.

37 Berglund E, Stigbrand T, Carlsson SR. Isolation and characterization of a membrane glycoprotein from human brain with sequence similarities to cell adhesion proteins from chicken and mouse. *Eur J Biochem* 1991; **197**: 549–54.

38 Gennarini G, Bizzoca A, Picocci S, Puzzo D, Corsi P, Furley AJW. The role of Gpi-anchored axonal glycoproteins in neural development and neurological disorders. *Mol Cell Neurosci* 2016; published online Nov 18. DOI:10.1016/j.mcn.2016.11.006.

39 Compton AG, Albrecht DE, Seto JT, *et al.* Mutations in contactin-1, a neural adhesion and neuromuscular junction protein, cause a familial form of lethal congenital myopathy. *Am J Hum Genet* 2008; **83**: 714–24.

40 Derfuss T, Parikh K, Velhin S, *et al.* Contactin-2/TAG-1-directed autoimmunity is identified in multiple sclerosis patients and mediates gray matter pathology in animals. *Proc Natl Acad Sci U S A* 2009; **106**: 8302–7.

41 Keller MF, Saad M, Bras J, *et al.* Using genome-wide complex trait analysis to quantify 'missing heritability' in Parkinson's disease. *Hum Mol Genet* 2012; **21**: 4996–5009.

42 Lek M, Karczewski KJ, Minikel EV, *et al.* Analysis of protein-coding genetic variation in 60,706 humans. *Nature* 2016; **536**: 285–91.

43 Zhang B, Gaiteri C, Bodea L-G, *et al.* Integrated systems approach identifies genetic nodes and networks in late-onset Alzheimer's disease. *Cell* 2013; **153**: 707–20.

Tables

Table 1: Characteristics of the DLB discovery cohort of DLB.

Country of origin	N	N neuropathological diagnosis	M:F	Mean age at onset	Successfully Genotyped	N neuropathological diagnosis
Australia	79	79	1.93	65	72	72
Canada	29	15	2.22	67.5	6	3
Finland	34	34	0.94	94.3 *	24	24
France	18	18	3.5	64.8	16	16
Germany	58	0	2.41	67.8	0	0
The Netherlands	133	133	1.71	78.7 *	132	132
Portugal	13	0	0.63	NA	11	0
Spain	133	16	0.94	73.2	132	15
UK	404	308	2.12	69.7	284	245
USA	786	705	1.93	71.9	539	467
Total	1687	1308	1.83	70.1	1216	974

N: number of samples; M:F: ratio of males to females. * Represents age at death, which was available for these cohorts. These values were not used for calculation of the complete mean age at onset.

Table 2: Characteristics of the replication cohort.

Country of origin	N	N neuropathological diagnosis	M:F	Mean age at onset
USA - cases	527	350	2.01	76.3
USA - controls	663	0	0.75	67.8 a

[a] Denotes age at examination for controls. For cases the age reflects age at onset for the clinical cases and age at death for the path-diagnosed cases.

Table 3: Top signals of association at each locus that passed genome-wide or suggestive thresholds for significance and their replication and meta-analysis p-values.

							Discovery						Replication							Meta-Analysis			
Named Region	**CHR**	**Position**	**Variant**	**R2**	**Eur_AF**	**MA**	**MAF_A**	**MAF_U**	**OR**	**L95**	**U95**	**P-value**	**Power**	**MAF_A**	**MAF_U**	**OR**	**L95**	**U95**	**P-value**	**OR**	**L95**	**U95**	**P-value**
APOE	19	45411941	rs429358	0.949	0.149	C	0.283	0.14	2.41	2.14	2.7	5.31E-50	1	0.247	0.138	2.74	2.15	3.49	4.00E-16	2.46	2.22	2.74	3.31E-64
BCL7C/STX1B	16	30886643	rs897984*	0.984	0.609	T	0.334	0.405	0.73	0.66	0.8	2.64E-10	0.96	0.303	0.31	0.98	0.81	1.19	0.83	0.77	0.71	0.85	1.19E-08
SNCA	4	90756550	rs7681440*	0.996	0.52	C	0.411	0.483	0.74	0.67	0.82	1.45E-09	0.95	0.306	0.357	0.68	0.56	0.82	6.00E-05	0.73	0.67	0.79	9.22E-13
GBA	1	155121143	rs35682329	0.957	0.015	G	0.034	0.014	2.43	1.81	3.27	4.33E-09	0.83	0.043	0.022	1.81	1.05	3.11	0.033	2.27	1.75	2.95	6.57E-10
GABRB3	15	26840998	rs1426210	0.982	0.315	G	0.348	0.293	1.32	1.2	1.46	4.63E-08	0.9	0.24	0.268	0.84	0.68	1.04	0.1	1.22	1.11	1.33	2.05E-05
SOX17	8	55395693	rs144770207	0.937	0.018	G	0.025	0.011	2.44	1.73	3.44	4.02E-07	0.72	0.011	0.021	0.41	0.19	0.86	0.019	1.81	1.32	2.48	2.23E-04
CNTN1	12	41179589	rs79329964	0.993	0.062	A	0.097	0.063	1.54	1.3	1.81	4.35E-07	0.82	0.077	0.052	1.54	1.04	2.28	0.033	1.54	1.32	1.79	3.99E-08

CHR: Chromosome. R2: Imputation R-squared of each specific variant from HRC. OR: Odds ratio. L95: Lower 95% interval. U95: Upper 95% confidence interval. Eur_AF is the alternate allele frequency derived from the European population of gnomAD[42]. * Represents variants for which the gnomAD allele frequency corresponds to the alternate allele and not the effect allele. Power refers to the calculated statistical power to replicate the discovery signal, taking into account the replication sample size, effect and frequency in discovery and an association threshold of p<0.05.

Table 4: Top gene burden results

CHR	BEGIN	END	ID	NS	FRAC_WITH_RARE	NUM_ALL_VARS	NUM_PASS_VARS	NUM_SING_VARS	PVALUE
1	155204797	155210498	GBA	5016	0.05622	8	6	1	1.29E-13
22	39262224	39267761	CBX6	5016	0.010965	6	3	0	1.66E-05
11	130058428	130079477	ST14	5016	0.076754	20	11	2	4.29E-05
10	129347767	129350889	NPS	5016	0.076555	5	3	1	6.74E-05
4	40428010	40434855	RBM47	5016	0.0099681	3	2	1	0.00011289
11	18047141	18057637	TPH1	5016	0.0091707	8	5	0	0.00022217
6	31237124	31239829	HLA-C	5016	0.1262	32	10	1	0.00028923
19	45971941	45976122	FOSB	5016	0.00079745	4	2	1	0.00036517
1	44435905	44438171	DPH2	5016	0.004386	9	6	2	0.00043723
2	238785923	238820379	RAMP1	5016	0.00079745	2	2	1	0.00049746

CHR: Chromosome. NS: Number of samples with non-missing genotypes. FRAC_WITH_RARE : Fraction of individual carrying rare variants below the allele frequency threshold (0.05). NUM_ALL_VARS : Number of all variants defining the gene group. NUM_PASS_VARS : Number of variants passing the frequency and call-rate thresholds. NUM_SING_VARS : Number of singletons among variants in NUM_PASS_VARS.

Legends to Figures

Figure 1:

Manhattan plot showing genome-wide p-values of association. The p-values were obtained by logistic regression analysis using the first 20 principal components as covariates. The y-axis shows −log10 p-values of 8,410,718 SNPs, and the x-axis shows their chromosomal positions. The y-axis was truncated at p-value of $1x10^{-25}$. Horizontal red and green dotted lines represent the thresholds of p= $5x10^{-8}$ for Bonferroni significance and p=$1x10^{-6}$ for selecting SNPs for replication, respectively.

Figure 2:

a) Boxplot showing the association between rs7681440 genotypes and *RP11-67M1.1* expression in the cerebellum in 103 healthy post-mortem samples (p=$2.00E^{-07}$) from the GTEx Consortium. Carriers of the GG genotype (alternative allele) show the lowest levels of expression of the gene. Medians, interquartile ranges and individual data points are indicated. See the GTEx website for details on methods.

b) Boxplot showing the association between rs7681154 and SNCA expression (p=$2.865x10^{-11}$) in brain cerebellum in 468 healthy post-mortem subjects from the Harvard Brain Bank Resource Center (www.brainbank.mclean.org) [43]. Individuals with the alternate allele (C) had increased SNCA expression in the cerebellum, on average, compared to those with the reference allele (G) Sample size for each genotype group is denoted in parentheses. Details on the subjects, experiments, and analytical methods of the eQTL study of the Harvard Brain Bank Resource Center samples are described in Zhang et al. 2013 and www.brainbank.mclean.org. Abbreviations: Homo Ref, homozygous for reference allele; Het, heterozygous; Homo Alt, homozygous for the alternative allele.

Figure 3:

DLB heritability by chromosome. Heritability (y-axis) per chromosome is plotted against chromosome length (x-axis). The red line represents heritability regressed on chromosome length and the shaded grey area represents the 95% confidence interval of the regression model.

Figure 4:

Regional association plot for the *SNCA* locus. Purple represents rs1372517, which is the most associated SNP at the locus also present in the 1000Genomes dataset. The variant rs1372517 is in complete LD with rs7681440. Colours represent LD derived from 1000Genomes between each variant and the most associated SNP.

Figure 5:

Regional association plot for the *BCL7C/STX1B* locus. Purple represents the most associated SNP. Colours represent LD derived from 1000Genomes between each variant and the most associated SNP.


-log10 (p-value)
0
10
20
Chromosome
1
2
3
4
5
6
7
8
9
10
11
12
13
14
15
16
17
19
22

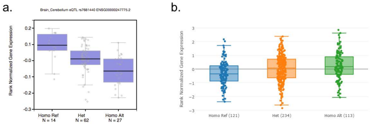
a.
Brain_Cerebellum eQTL rs7681440 ENSG00000247775.2
Rank Normalized Gene Expression
0.2
0.1
-0.0
-0.1
-0.2
-0.3
Homo Ref
N = 14
Het
N = 62
Homo Alt
N = 27
b.
Rank Normalized Gene Expression
3
2
1
0
−1
−2
−3
Homo Ref (121)
Het (234)
Homo Alt (113)


Heritability (h2)
0.05
0.04
0.03
0.02
0.01
Chromosome size (Mb)
50
100
150
200
250
1
2
3
4
5
6
7
8
9
10
11
12
13
14
15
16
17
18
19
20
21
22

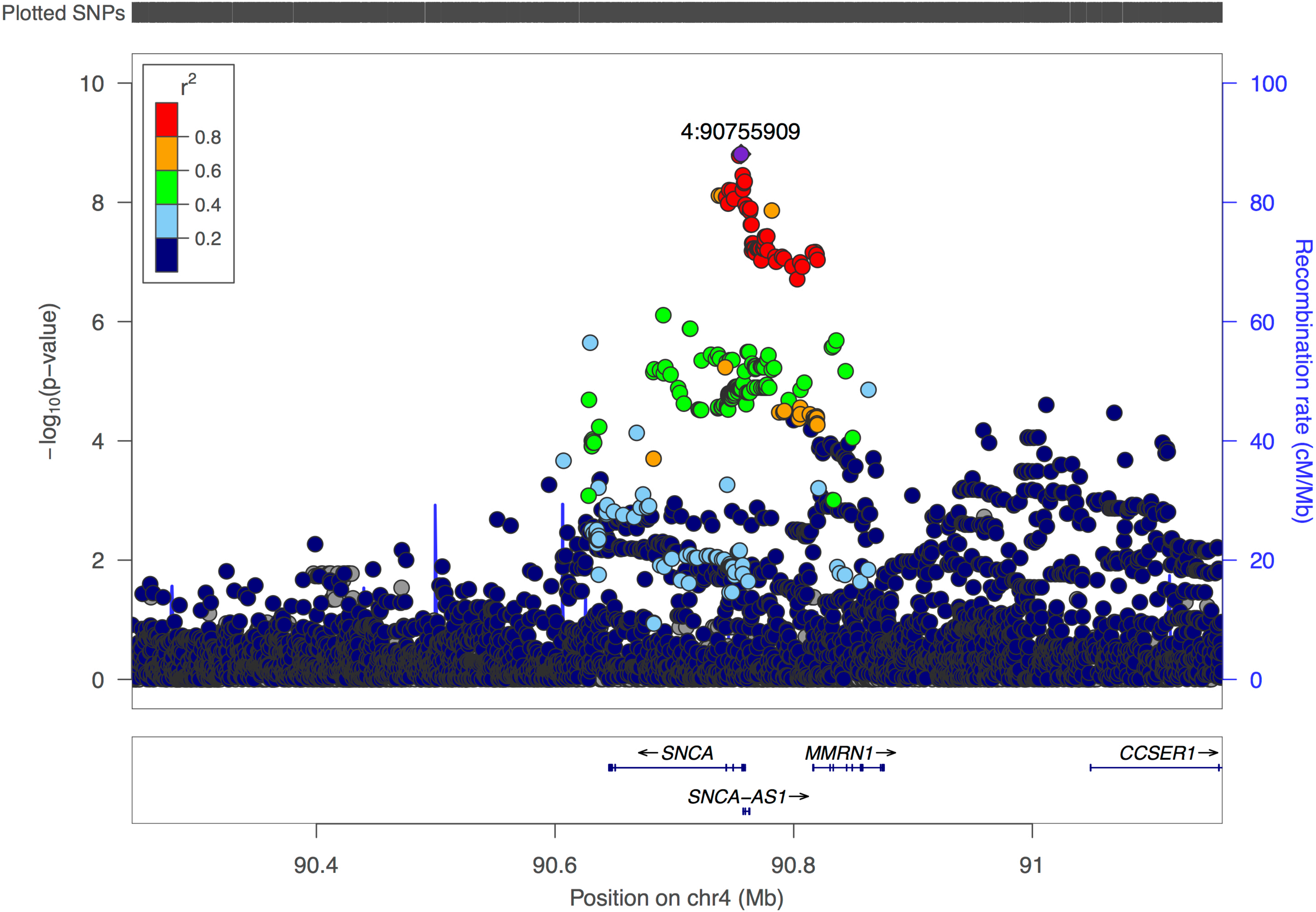
Plotted SNPs
r²
0.8
0.6
0.4
0.2
4:90755909
-log10(p-value)
0
2
4
6
8
10
Recombination rate (cM/Mb)
0
20
40
60
80
100
SNCA
MMRN1
CCSER1
SNCA-AS1
90.4
90.6
90.8
91
Position on chr4 (Mb)

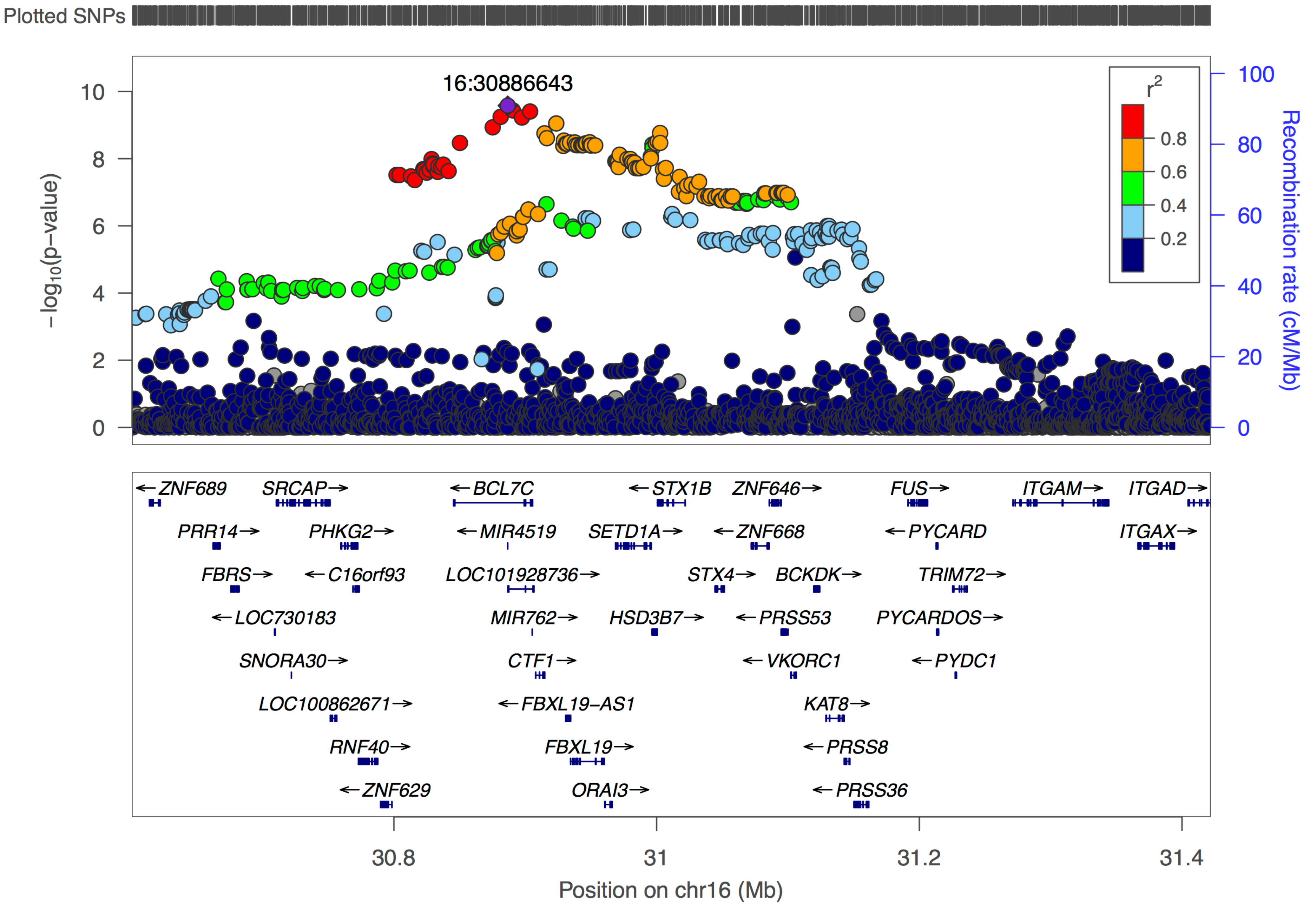
Plotted SNPs
16:30886643
−log10(p−value)
10
8
6
4
2
0
Recombination rate (cM/Mb)
100
80
60
40
20
0
r2
0.8
0.6
0.4
0.2
←ZNF689
SRCAP→
←BCL7C
←STX1B
ZNF646→
FUS→
ITGAM→
ITGAD→
PRR14→
PHKG2→
←MIR4519
SETD1A→
←ZNF668
←PYCARD
ITGAX→
FBRS→
←C16orf93
LOC101928736→
STX4→
BCKDK→
TRIM72→
←LOC730183
MIR762→
HSD3B7→
←PRSS53
PYCARDOS→
SNORA30→
CTF1→
←VKORC1
←PYDC1
LOC100862671→
←FBXL19−AS1
KAT8→
RNF40→
FBXL19→
←PRSS8
←ZNF629
ORAI3→
←PRSS36
30.8
31
31.2
31.4
Position on chr16 (Mb)

Genome-wide association analysis of Dementia with Lewy bodies reveals unique genetic architecture

Rita Guerreiro[1, 2, 3]*, Owen A. Ross[4]*, Celia Kun-Rodrigues[2], Dena Hernandez[5], Tatiana Orme[2], John Eicher[6], Claire Shepherd[7], Laura Parkkinen[8], Lee Darwent[2], Michael G. Heckman[9], Sonja W. Scholz[10], Juan C. Troncoso[11], Olga Pletnikova[11], Olaf Ansorge[8], Jordi Clarimon[12], Alberto Lleo[12], Estrella Morenas-Rodriguez[12], Lorraine Clark[13], Lawrence S Honig[13], Karen Marder[13], Afina Lemstra[14], Ekaterina Rogaeva[15], Peter St. George-Hyslop[15, 16], Elisabet Londos[17], Henrik Zetterberg[18], Imelda Barber[19], Anne Braae[19], Kristelle Brown[19], Kevin Morgan[19], Claire Troakes[20], Safa Al-Sarraj[20], Tammaryn Lashley[21], Janice Holton[21], Yaroslau Compta[22], Vivianna Van Deerlin[23], Geidy E Serrano[24], Thomas G Beach[24], Suzanne Lesage[25], Douglas Galasko[26], Eliezer Masliah[27], Isabel Santana[28], Pau Pastor[29], Monica Diez-Fairen[29], Miquel Aguilar[29], Pentti J. Tienari[30], Liisa Myllykangas[31], Minna Oinas[32], Tamas Revesz[21], Andrew Lees[21], Brad F Boeve[33], Ronald C. Petersen[33], Tanis J Ferman[34], Valentina Escott-Price[35], Neill Graff-Radford[36], Nigel Cairns[37], John C. Morris[37], Stuart Pickering-Brown[38], David Mann[38], Glenda M. Halliday[39, 40], John Hardy[2], John Q. Trojanowski[23], Dennis W. Dickson[4], Andrew Singleton[5], David Stone[6], Jose Bras[1, 2, 3,]†

* - Denotes equally contributing authors

† - Corresponding author. Email: j.bras@ucl.ac.uk

1 - UK Dementia Research Institute (UK DRI) at UCL, London, UK

2 - Department of Molecular Neuroscience, UCL Institute of Neurology, London, UK

3 - Department of Medical Sciences and Institute of Biomedicine, iBiMED, University of Aveiro, 3810-193 Aveiro, Portugal

4 - Department of Neuroscience, Mayo Clinic, Jacksonville, FL, USA

5 - Laboratory of Neurogenetics, National Institutes on Aging, NIH, Bethesda, MD, USA

6 - Genetics and Pharmacogenomics, Merck Research Laboratories, West Point, Pennsylvania, USA

7 - Neuroscience Research Australia, Sydney, Australia and School of Medical Sciences, Faculty of Medicine, University of New South Wales, Sydney, Australia

8 - Nuffield Department of Clinical Neurosciences, Oxford Parkinson's Disease Centre, University of Oxford, Oxford, UK

9 - Division of Biomedical Statistics and Informatics, Mayo Clinic, Jacksonville, FL, USA
10 - Neurodegenerative Diseases Research Unit, National Institute of Neurological Disorders and Stroke, National Institutes of Health, Bethesda, Maryland, USA
11 - Department of Pathology (Neuropathology), Johns Hopkins University School of Medicine, Baltimore, MD, USA
12 - Memory Unit, Department of Neurology, IIB Sant Pau, Hospital de la Santa Creu i Sant Pau, Universitat Autonoma de Barcelona, Barcelona, Spain; Centro de Investigacion Biomedica en Red en Enfermedades Neurodegenerativas (CIBERNED), Instituto de Salud Carlos III, Madrid, Spain
13 - Taub Institute for Alzheimer Disease and the Aging Brain and Department of Pathology and Cell Biology, Columbia University, New York, NY, USA
14 - Department of Neurology and Alzheimer Center, Neuroscience Campus Amsterdam, VU University Medical Center, Amsterdam, the Netherlands
15 - Tanz Centre for Research in Neurodegenerative Diseases and department of Medicine, University of Toronto, Ontario, Canada
16 - Department of Clinical Neurosciences, Cambridge Institute for Medical Research, University of Cambridge, Cambridge, UK
17 - Clinical Memory Research Unit, Institution of Clinical Sciences Malmo, Lund University, Sweden
18 - UK Dementia Research Institute at UCL, London UK, Department of Molecular Neuroscience, UCL Institute of Neurology, London, UK and Clinical Neurochemistry Laboratory, Institute of Neuroscience and Physiology, Sahlgrenska Academy at the University of Gothenburg, Molndal, Sweden
19 - Human Genetics, School of Life Sciences, Queen’s Medical Centre, University of Nottingham, Nottingham, UK
20 - Department of Basic and Clinical Neuroscience and Institute of Psychiatry, Psychology and Neuroscience, King’s College London, London, UK
21 - Queen Square Brain Bank, Department of Molecular Neuroscience, UCL Institute of Neurology, London, UK
22 - Queen Square Brain Bank, Department of Molecular Neuroscience, UCL Institute of Neurology, London, UK and Movement Disorders Unit, Neurology Service, Clinical Neuroscience Institute (ICN), Hospital Clinic, University of Barcelona, IDIBAPS, Barcelona, Spain
23 - Department of Pathology and Laboratory Medicine, Center for Neurodegenerative Disease Research, Perelman School of Medicine at the University of Pennsylvania, 3600 Spruce Street, Philadelphia, USA

24 - Banner Sun Health Research Institute, 10515 W Santa Fe Drive, Sun City, AZ 85351, USA
25 - Inserm U1127, CNRS UMR7225, Sorbonne Universites, UPMC Univ Paris 06, UMR and S1127, Institut du Cerveau et de la Moelle epiniere, Paris, France
26 - Department of Neurosciences, University of California, San Diego, La Jolla, CA, United States; Veterans Affairs San Diego Healthcare System, La Jolla, CA, United States
27 - Department of Neurosciences, University of California, San Diego, La Jolla, CA, United States; Department of Pathology, University of California, San Diego, La Jolla, CA, United States
28 - Neurology Service, University of Coimbra Hospital, Coimbra, Portugal
29 - Memory Unit, Department of Neurology, University Hospital Mutua de Terrassa, University of Barcelona, and Fundacio de Docencia I Recerca Mutua de Terrassa, Terrassa, Barcelona, Spain. Centro de Investigacion Biomedica en Red Enfermedades Neurdegenerativas (CIBERNED), Madrid, Spain
30 - Molecular Neurology, Research Programs Unit, University of Helsinki, Department of Neurology, Helsinki University Hospital, Helsinki, Finland
31 - Department of Pathology, Haartman Institute, University of Helsinki and HUSLAB
32 - Department of Neuropathology and Neurosurgery, Helsinki University Hospital and University of Helsinki, Helsinki, Finland
33 - Neurology Department, Mayo Clinic, Rochester, MN, USA
34 - Department of Psychiatry and Department of Psychology, Mayo Clinic, Jacksonville, FL, USA
35 - MRC Centre for Neuropsychiatric Genetics and Genomics, School of Medicine, Cardiff University, Cardiff, UK
36 - Department of Neurology, Mayo Clinic, Jacksonville, FL, USA
37 - Knight Alzheimer’s Disease Research Center, Department of Neurology, Washington University School of Medicine, Saint Louis, MO, USA
38 - Institute of Brain, Behaviour and Mental Health, Faculty of Medical and Human Sciences, University of Manchester, Manchester, UK
39 - Neuroscience Research Australia, Sydney, Australia and School of Medical Sciences, Faculty of Medicine, University of New South Wales,Sydney, Australia
40 - Brain and Mind Centre, Sydney Medical School, The University of Sydney, Sydney, Australia

Supplementary Table 1: Replication stage associations

		Clinical DLB patients vs. controls				High likelihood DLB Lewy body disease patients vs. controls			Combined disease group vs. controls		
Variant	MA	MAF in controls (N=663)	MAF in DLB (N=177)	OR (95% CI)	P-value	MAF in high likelihood DLB (N=350)	OR (95% CI)	P-value	MAF in combined disease group	OR (95% CI)	P-value
rs10177808	C	9.8%	10.8%	0.99 (0.67, 1.46)	0.96	7.8%	0.76 (0.53, 1.09)	0.13	8.8%	0.86 (0.64, 1.17)	0.34
rs10900950	C	47.5%	50.3%	1.06 (0.83, 1.36)	0.65	45.1%	0.81 (0.65, 1.00)	0.052	46.9%	0.92 (0.77, 1.11)	0.39
rs12695305	C	7.3%	9.0%	1.47 (0.96, 2.25)	0.075	7.6%	1.21 (0.81, 1.80)	0.36	8.1%	1.32 (0.94, 1.85)	0.11
rs13010219	G	2.1%	2.6%	1.22 (0.54, 2.78)	0.63	3.3%	1.79 (0.92, 3.49)	0.089	3.1%	1.48 (0.82, 2.67)	0.20
rs13237830	G	11.1%	11.0%	1.00 (0.67, 1.48)	0.98	10.3%	1.03 (0.73, 1.45)	0.87	10.5%	1.00 (0.75, 1.35)	1.00
rs1426210	G	30.7%	30.1%	0.93 (0.71, 1.24)	0.63	27%	0.82 (0.65, 1.05)	0.11	28.1%	0.84 (0.68, 1.04)	0.10
rs144770207	G	2.1%	1.1%	0.40 (0.13, 1.21)	0.10	1.3%	0.35 (0.14, 0.83)	0.020	1.2%	0.41 (0.19, 0.86)	0.019
rs1958800	A	15.2%	16.6%	1.14 (0.80, 1.61)	0.47	19.8%	1.36 (1.02, 1.82)	0.038	18.7%	1.29 (1.00, 1.66)	0.050
rs2301134	A	48.6%	40.3%	0.71 (0.55, 0.92)	0.009	38.6%	0.65 (0.52, 0.81)	0.0001	39.2%	0.67 (0.55, 0.81)	3 x 10^{-5}
rs2498957	A	3.2%	1.4%	0.40 (0.15, 1.05)	0.061	1.7%	0.61 (0.30, 1.22)	0.16	1.6%	0.58 (0.32, 1.07)	0.082
rs25907	A	2.5%	1.1%	0.36 (0.12, 1.09)	0.070	2.9%	0.89 (0.45, 1.77)	0.74	2.3%	0.73 (0.39, 1.36)	0.32
rs2722033	C	7.2%	8.7%	1.43 (0.92, 2.22)	0.11	7.4%	1.21 (0.80, 1.82)	0.37	7.8%	1.29 (0.91, 1.84)	0.15
rs2834213	G	24.4%	26.8%	1.19 (0.89, 1.58)	0.24	22.7%	0.96 (0.74, 1.25)	0.76	24.1%	1.06 (0.85, 1.32)	0.62
rs34811744	A	2.0%	2.5%	1.32 (0.57, 3.01)	0.52	3.0%	1.79 (0.89, 3.59)	0.10	2.8%	1.52 (0.82, 2.80)	0.18
rs35407583	A	7.7%	8.8%	0.98 (0.62, 1.55)	0.94	7.5%	0.80 (0.53, 1.21)	0.30	7.9%	0.87 (0.61, 1.23)	0.42
rs35682329	G	2.2%	4.0%	1.48 (0.73, 3.02)	0.28	4.6%	1.83 (1.00, 3.36)	0.051	4.4%	1.81 (1.05, 3.11)	0.033
rs35989721	C	4.8%	4.2%	0.89 (0.48, 1.64)	0.70	5.3%	1.01 (0.61, 1.66)	0.98	4.9%	1.00 (0.64, 1.54)	0.98
rs429358	C	14.8%	29.4%	2.74 (2.00, 3.74)	2 x 10^{-10}	27.5%	2.85 (2.15, 3.78)	3 x 10^{-13}	28.2%	2.74 (2.15, 3.49)	4 x 10^{-16}
rs55864141	C	48.9%	55.6%	1.35 (1.05, 1.74)	0.020	47.4%	0.95 (0.77, 1.17)	0.62	50.2%	1.08 (0.90, 1.30)	0.42
rs56162468	A	7.1%	8.0%	1.09 (0.70, 1.71)	0.70	8.3%	1.21 (0.82, 1.78)	0.34	8.2%	1.18 (0.85, 1.65)	0.32
rs61454308	DEL	2.1%	0.9%	0.33 (0.09, 1.16)	0.084	2.2%	0.71 (0.32, 1.57)	0.39	1.7%	0.61 (0.30, 1.25)	0.18
rs62227703	G	23.8%	24.6%	1.10 (0.82, 1.47)	0.53	22.0%	0.97 (0.75, 1.27)	0.84	22.9%	1.02 (0.82, 1.28)	0.86
rs6964466	A	40.7%	40.6%	0.92 (0.72, 1.18)	0.51	42.8%	0.97 (0.79, 1.21)	0.80	42.0%	0.99 (0.82, 1.19)	0.88
rs71326956	T	23.8%	24.7%	1.11 (0.82, 1.48)	0.51	22.0%	1.00 (0.76, 1.30)	0.97	22.9%	1.04 (0.83, 1.31)	0.74
rs71427040	A	2.0%	2.6%	1.31 (0.57, 3.00)	0.52	3.2%	1.86 (0.94, 3.69)	0.077	3.0%	1.55 (0.84, 2.85)	0.16
rs72987470	C	10.8%	11.1%	0.91 (0.63, 1.33)	0.63	8.3%	0.75 (0.53, 1.06)	0.11	9.3%	0.83 (0.62, 1.11)	0.22
rs7681440	C	47.0%	39.5%	0.73 (0.57, 0.95)	0.016	37.3%	0.66 (0.53, 0.82)	0.0002	38.0%	0.68 (0.56, 0.82)	6 x 10^{-5}
rs78478169	C	23.7%	24.7%	1.11 (0.83, 1.49)	0.49	22.0%	0.99 (0.76, 1.29)	0.92	22.9%	1.03 (0.82, 1.30)	0.78
rs79329964	A	5.2%	7.4%	1.37 (0.81, 2.31)	0.23	7.9%	1.54 (0.98, 2.42)	0.060	7.7%	1.54 (1.04, 2.28)	0.033
rs8129184	A	34.0%	35.8%	1.01 (0.77, 1.32)	0.95	36.0%	1.02 (0.81, 1.27)	0.87	36.0%	1.02 (0.84, 1.24)	0.85
rs897984	T	38.8%	36.9%	0.95 (0.74, 1.23)	0.72	36.7%	0.97 (0.77, 1.21)	0.78	36.8%	0.98 (0.81, 1.19)	0.83
rs928779	C	23.8%	25.9%	1.17 (0.88, 1.56)	0.29	22.6%	1.02 (0.79, 1.33)	0.86	23.7%	1.08 (0.87, 1.35)	0.49

MA=minor allele; MAF=minor allele frequency; OR=odds ratio; CI=confidence interval. ORs, 95% CIs, and p-values result from logistic regression models adjusted for age (age at DLB diagnosis for the clinically diagnosed DLB patients, age at death for the high likelihood DLB Lewy body disease patients, and age at study for controls) and gender. Variants were examined under an additive model, and therefore ORs correspond to each additional minor allele. P-values ≤ 0.0015 are considered as statistically significant after applying a Bonferroni correction for multiple testing.

Supplementary Table 2: Association p-values in DLB for variants showing the most significant association at each locus in PD, AD and LB-related pathology

DISEASE	CHR	POS	REPORTED GENE(S)	SNP	P-VALUE	OR	95% CI	DLB p-value	DLB OR	95% CI
PD	4	90626111	SNCA	rs356182	4.00E-73	1.32	[1.29-1.35]	0.1831	0.9341	[0.84-1.03]
PD	17	43994648	MAPT	rs17649553	2.00E-48	1.3	[1.27-1.34]	0.0126	0.8606	[0.76-0.97]
AD	2	127892810	BIN1	rs6733839	7.00E-44	1.22	[1.18-1.25]	0.0275	1.114	[1.01-1.23]
PD	4	951947	TMEM175, GAK, DGKQ	rs34311866	1.00E-43	1.27	[1.24-1.30]	0.01025	1.167	[1.04-1.31]
PD	1	155135036	GBA, SYT11	rs35749011	1.00E-29	1.824	[1.72-1.93]	1.772E-09	2.533	[1.87-3.43]
AD	11	85867875	PICALM	rs10792832	9.00E-26	1.1494	[1.12-1.18]	0.3379	0.953	[0.86-1.05]
AD	8	27467686	CLU	rs9331896	3.00E-25	1.1628	[1.12-1.19]	0.5654	0.9724	[0.88-1.07]
AD	1	207692049	CR1	rs6656401	6.00E-24	1.18	[1.14-1.22]	0.1224	1.1	[0.97-1.24]
PD	3	182762437	MCCC1	rs12637471	2.00E-21	1.1876	[1.15-1.22]	0.9495	1.004	[0.89-1.13]
PD	2	169110394	STK39	rs1474055	1.00E-20	1.214	[1.17-1.26]	0.5102	0.9539	[0.83-1.1]
PD	2	135539967	ACMSD, TMEM163	rs6430538	9.00E-20	1.1429	[1.11-1.17]	0.6149	0.9756	[0.89-1.07]
PD	4	15737101	BST1	rs11724635	9.00E-18	1.126	[1.1-1.15]	0.1021	0.9247	[0.84-1.02]
PD	1	205723572	NUCKS1, RAB7L1	rs823118	2.00E-16	1.122	[1.09-1.15]	0.08666	0.9209	[0.84-1.01]
AD	11	59923508	MS4A6A	rs983392	6.00E-16	1.1111	[1.09-1.15]	0.9336	1.004	[0.91-1.1]
AD	19	1063443	ABCA7	rs4147929	1.00E-15	1.15	[1.11-1.19]	0.9324	0.9946	[0.88-1.13]
AD	11	121435587	SORL1	rs11218343	1.00E-14	1.2987	[1.22-1.39]	0.6151	0.9374	[0.73-1.21]
PD	12	40614434	LRRK2	rs76904798	5.00E-14	1.155	[1.12-1.19]	0.7628	1.021	[0.89-1.17]
AD	8	27195121	PTK2B	rs28834970	7.00E-14	1.1	[1.08-1.13]	0.06481	1.097	[0.99-1.21]
PD	14	67984370	TMEM229B	rs1555399	7.00E-14	1.1148	[1.09-1.14]	0.5962	0.9747	[0.89-1.07]
AD	7	143110762	EPHA1	rs11771145	1.00E-13	1.1111	[1.08-1.14]	0.3838	1.045	[0.95-1.15]
PD	10	121536327	INPP5F	rs117896735	4.00E-13	1.624	[1.49-1.76]	0.2254	0.7705	[0.51-1.17]
PD	6	32666660	HLA-DQB	rs9275326	1.00E-12	1.21	[1.16-1.26]	0.02004	0.8273	[0.71-0.97]
PD	7	23293746	GPNMB	rs199347	1.00E-12	1.11	[1.08-1.14]	0.531	0.9697	[0.88-1.07]
PD	16	31121793	BCKDK, STX1B	rs14235	2.00E-12	1.103	[1.08-1.13]	0.000001369	1.268	[1.15-1.4]
AD	6	32578530	HLA-DRB5, HLA-DRB1	rs9271192	3.00E-12	1.11	[1.08-1.18]	0.5224	1.035	[0.93-1.15]
PD	12	123303586	CCDC62	rs11060180	6.00E-12	1.105	[1.08-1.13]	0.4567	0.9649	[0.88-1.06]
PD	18	40673380	RIT2	rs12456492	8.00E-12	1.11	[1.08-1.14]	0.2923	1.056	[0.95-1.17]
PD	11	133765367	MIR4697	rs329648	1.00E-11	1.105	[1.08-1.13]	0.4612	1.038	[0.94-1.15]
PD	15	61994134	VPS13C	rs2414739	1.00E-11	1.113	[1.08-1.14]	0.3731	1.049	[0.94-1.17]
PD	4	77198986	SCARB2, FAM47E	rs6812193	3.00E-11	1.1	[1.07-1.13]	0.2897	0.9484	[0.86-1.05]
PD	20	3168166	DDRGK1	rs8118008	3.00E-11	1.111	[1.08-1.14]	NA	NA	NA
AD	6	47487762	CD2AP	rs10948363	5.00E-11	1.1	[1.07-1.13]	0.03905	1.114	[1.01-1.24]
PD	14	55348869	GCH1	rs11158026	6.00E-11	1.11	[1.08-1.14]	0.8457	0.9902	[0.9-1.09]

PD	1	232664611	SIPA1L2	rs10797576	5.00E-10	1.131	[1.09-1.17]	0.6302	1.034	[0.9-1.19]
AD	7	100004446	ZCWPW1	rs1476679	6.00E-10	1.0989	[1.06-1.12]	0.1552	1.077	[0.97-1.19]
AD	7	37841534	NME8	rs2718058	5.00E-09	1.0753	[1.05-1.11]	0.1563	0.9312	[0.84-1.03]
AD	14	92926952	SLC24A4, RIN3	rs10498633	6.00E-09	1.0989	[1.06-1.14]	0.2435	0.9353	[0.84-1.05]
AD	14	53400629	FERMT2	rs17125944	8.00E-09	1.14	[1.09-1.19]	0.4939	0.9427	[0.8-1.12]
AD	11	47557871	CELF1	rs10838725	1.00E-08	1.08	[1.05-1.11]	0.874	1.008	[0.91-1.12]
AD	2	234068476	INPP5D	rs35349669	3.00E-08	1.08	[1.05-1.11]	0.02416	1.116	[1.01-1.23]
AD	5	88223420	MEF2C	rs190982	3.00E-08	1.0753	[1.05-1.11]	0.1497	0.9319	[0.85-1.03]
AD	20	55018260	CASS4	rs7274581	3.00E-08	1.1364	[1.09-1.19]	0.1953	0.8969	[0.76-1.06]
AD	4	11630049	HS3ST1	rs6448799	7.00E-08	1.08	[1.05-1.11]	0.3626	0.9525	[0.86-1.06]
PD	8	16697091	FGF20	rs591323	7.00E-08	1.09	[1.06-1.12]	0.1252	0.9206	[0.83-1.02]
AD	8	96054000	NDUFAF6	rs7818382	8.00E-08	1.07	[1.04-1.10]	0.2664	1.055	[0.96-1.16]
LB	6	33030112	HLA-DPB1	rs9277685	0.000000129	5.31	[2.59-10.91]	0.3643	1.065	[0.93-1.22]
AD	1	193625233	intergenic	rs6678275	3.00E-07	1.09	[1.05-1.13]	0.5663	0.9649	[0.85-1.09]
AD	10	11720308	ECHDC3	rs7920721	3.00E-07	1.07	[1.04-1.10]	0.01155	1.131	[1.03-1.24]
AD	12	43967677	ADAMTS20	rs7295246	3.00E-07	1.07	[1.04-1.10]	0.05886	0.9129	[0.83-1]
AD	14	107180574	IGH	rs2337406	3.00E-07	1.1494	[1.09-1.2]	NA	NA	NA
AD	15	51040798	SPPL2A	rs8035452	3.00E-07	1.0753	[1.04-1.1]	0.1213	0.9242	[0.84-1.02]
AD	17	59615509	ACE	rs138190086	3.00E-07	1.34	[1.20-1.50]	NA	NA	NA
AD	15	64725490	TRIP4	rs74615166	4.00E-07	1.29	[1.17-1.42]	0.5352	0.8994	[0.64-1.26]
AD	17	5137047	SCIMP	rs7225151	4.00E-07	1.1	[1.06-1.15]	0.009792	0.8198	[0.71-0.95]
PD	11	83544472	DLG2	rs3793947	4.00E-07	1.0764	[1.05-1.11]	0.4757	0.966	[0.88-1.06]
AD	6	41154650	TREML2	rs9381040	6.00E-07	1.0753	[1.04-1.1]	0.5929	0.9721	[0.88-1.08]
AD	11	941941	AP2A2	rs10751667	6.00E-07	1.0753	[1.04-1.1]	0.06146	1.098	[1-1.21]
PD	19	2363319	SPPL2B	rs62120679	6.00E-07	1.097	[1.06-1.13]	0.07867	1.095	[0.99-1.21]
AD	5	179238261	SQSTM1	rs72807343	7.00E-07	1.35	[1.20-1.52]	0.5932	0.9021	[0.62-1.32]
LB	6	33034596	HLA-DPA1	rs9277334	0.000000965	5.27	[2.56-10.81]	0.301	1.074	[0.94-1.23]
LB	6	33043520	HLA-DPA1	rs2301226	0.00000116	3.75	[2.15-6.54]	0.4627	1.052	[0.92-1.20]
LB	15	33083134	Intergenic	rs8041665	0.00000139	7.41	[2.92-18.81]	0.67	0.975	[0.87-1.09]
LB	15	33084148	Intergenic	rs8037309	0.00000139	7.41	[2.92-18.81]	0.6585	0.9741	[0.87-1.09]
LB	6	33087684	HLA-DPB1	rs4713610	0.00000151	3.51	[2.02-6.11]	0.6805	0.9759	[0.87-1.09]
LB	6	33088084	HLA-DPB1	rs2071349	0.00000208	3.63	[2.08-6.32]	0.5024	0.9567	[0.84-1.08]
LB	6	33107955	HLA-DPB1	rs9277656	0.0000025	3.41	[2.01-5.79]	0.5514	0.9615	[0.85-1.09]
AD	19	51727962	CD33	rs3865444	3.00E-06	1.06	[1.04-1.1]	0.7582	1.016	[0.92-1.12]
LB	2	38150179	SPTBN1	rs7595929	0.00000386	3.23	[1.93-5.39]	0.2597	1.11	[0.93-1.33]
LB	2	38150438	SPTBN1	rs4315567	0.00000486	3.21	[1.92-5.38]	0.2597	1.11	[0.93-1.33]
LB	2	54626240	MAP10	rs3796058	0.00000497	3.23	[1.92-5.44]	0.8225	0.9889	[0.90-1.09]
LB	6	54655944	HLA-DPB1	rs2395349	0.00000501	3.27	[1.93-5.52]	0.233	0.9417	[0.85-1.03]

LB	6	172942448	HLA-DPB1	rs9277682	0.00000501	3.27	[1.93-5.52]	0.4574	0.955	[0.85-1.08]
LB	18	1210675	Intergenic	rs1472194	0.00000519	8.06	[2.84-22.87]	0.957	0.9944	[0.81-1.22]
LB	5	116388579	Intergenic	rs6872138	0.0000064	3.82	[2.07-7.45]	0.2241	0.9151	[0.79-1.05]
LB	5	116419511	Intergenic	rs1459086	0.00000715	3.54	[1.99-6.30]	0.1367	0.8823	[0.74-1.04]

CHR: Chromosome. POS: Position according to hg19. PD refers to variants from Nalls M et al, Nat Genet, 2014. AD refers to Lambert JC, et al, Nat Genet, 2013. LB refers to Peraulinna T, et al. Ann Clin Transl Neurol 2015.

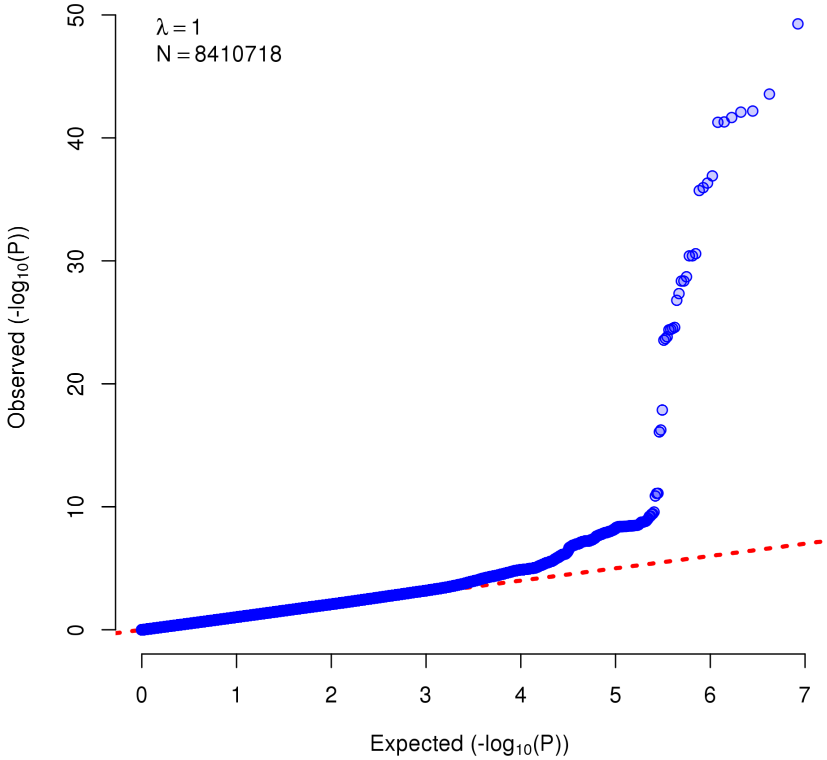

Supplementary Figure 1: Quantile-quantile (Q-Q) plot of observed versus expected P values of the GWAS results following imputation. The straight dotted line in the Q-Q plot indicates the distribution of SNPs under the null hypothesis.

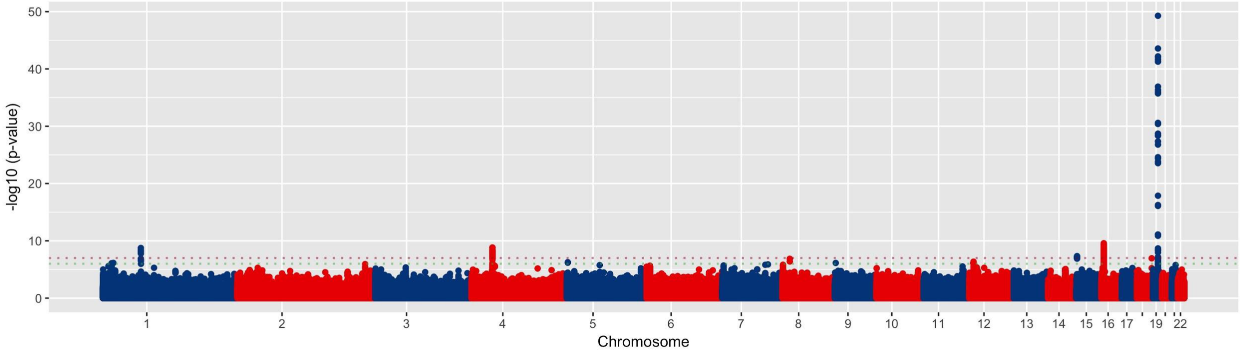

Supplementary Figure 2: Non-truncated Manhattan plot showing genome-wide p-values of association. The p-values were obtained by logistic regression analysis using the first 20 principal components as covariates. The y-axis shows −log10 p-values of 8,410,718 SNPs, and the x axis shows their chromosomal positions. Horizontal red and green dotted lines represent the thresholds of p= $5x10^{-8}$ for Bonferroni significance and p=$1x10^{-6}$ for selecting SNPs for replication, respectively.

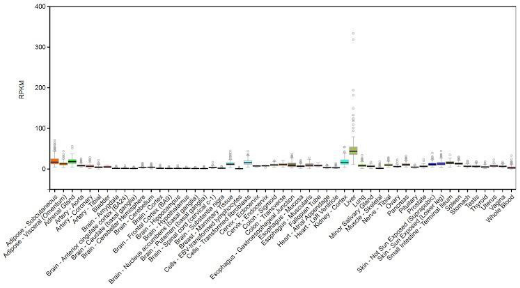
HSD3B7

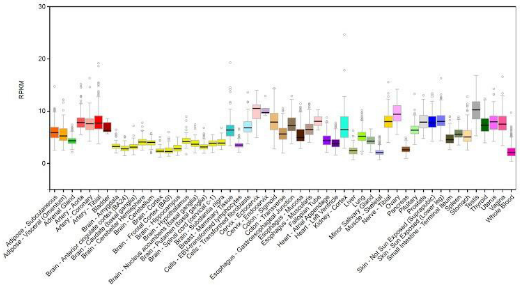
BCL7C

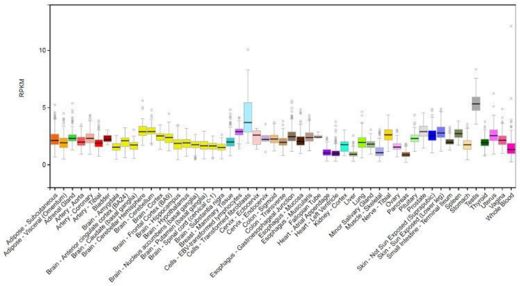
ZNF668

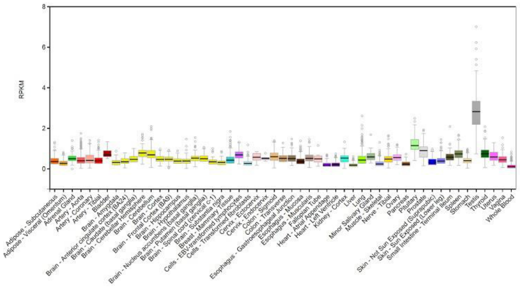
MIR4519

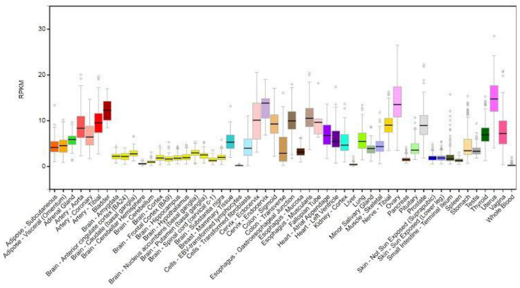
CTF1

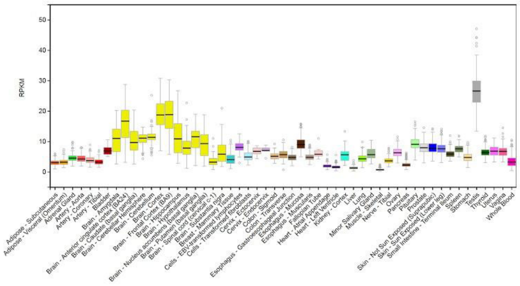
FBXL19

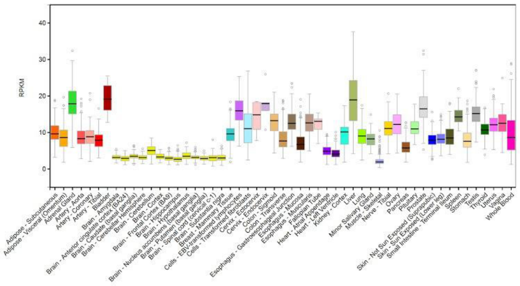
ORAI3

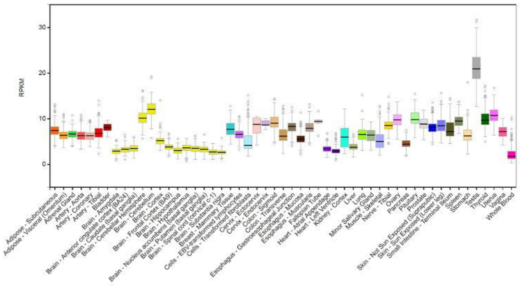
SETD1A

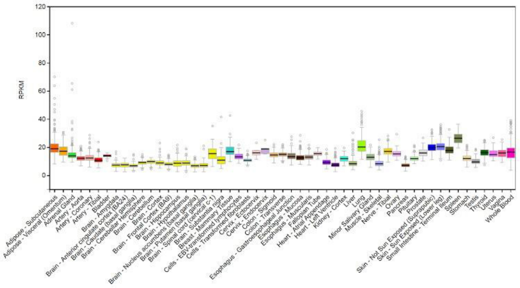
STX4

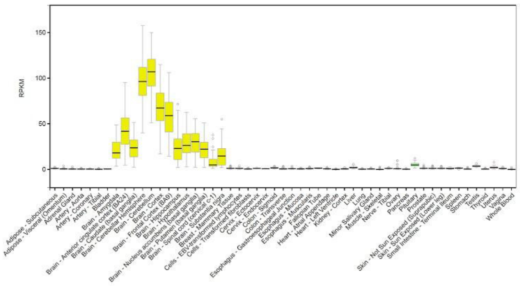
STX1B

Supplementary Figure 3: Tissue expression profiles for the genes located in the *BCL7C*/*STX1B* locus. Data from the GTEx portal. *STX1B* shows much higher expression in brain tissues when compared with other tissues and other genes in the locus.

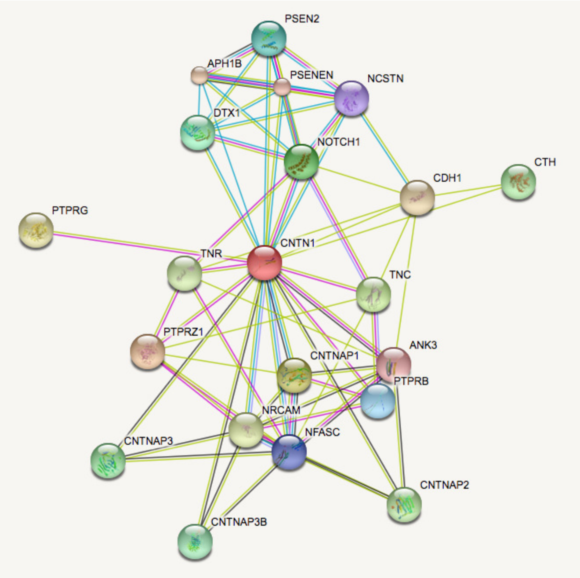

Supplementary Figure 4: Protein interaction network of *CNTN1* using STRING. Network created with a maximum number of 20 interactors and minimum required interaction score of 0.4.

Supplementary Figures 5 to 64: Co-localization of GWAS signals between DLB and either PD or AD. Data for PD is derived from Nalls et al 2014, while for AD it is derived from Lambert JC et al 2013.

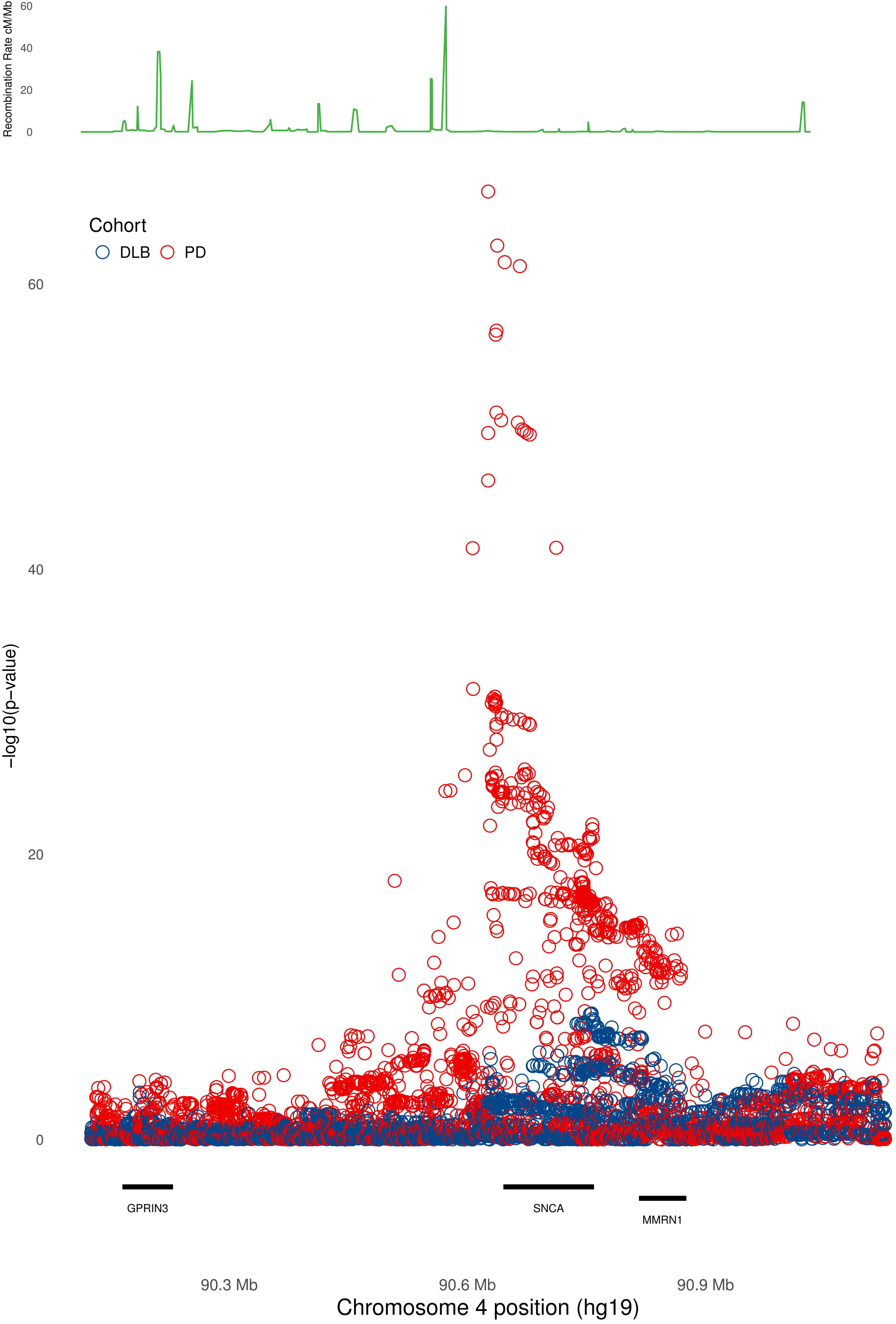
Recombination Rate cM/Mb
60
40
20
0
Cohort
DLB
PD
60
40
20
0
−log10(p−value)
GPRIN3
SNCA
MMRN1
90.3 Mb
90.6 Mb
90.9 Mb
Chromosome 4 position (hg19)

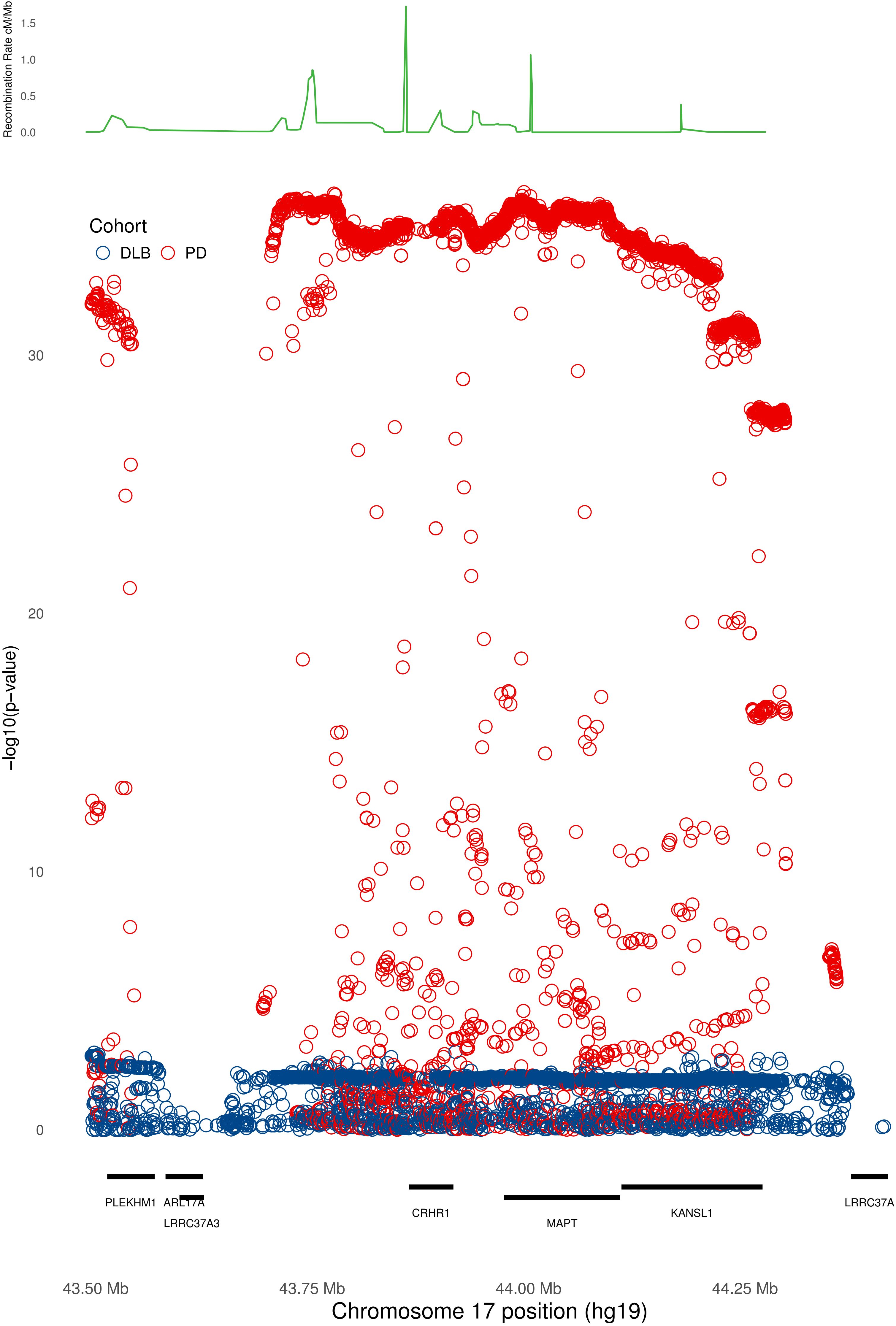
Recombination Rate cM/Mb
1.5
1.0
0.5
0.0
Cohort
DLB
PD
30
20
10
0
-log10(p-value)
PLEKHM1
ARL17A
LRRC37A3
CRHR1
MAPT
KANSL1
LRRC37A
43.50 Mb
43.75 Mb
44.00 Mb
44.25 Mb
Chromosome 17 position (hg19)

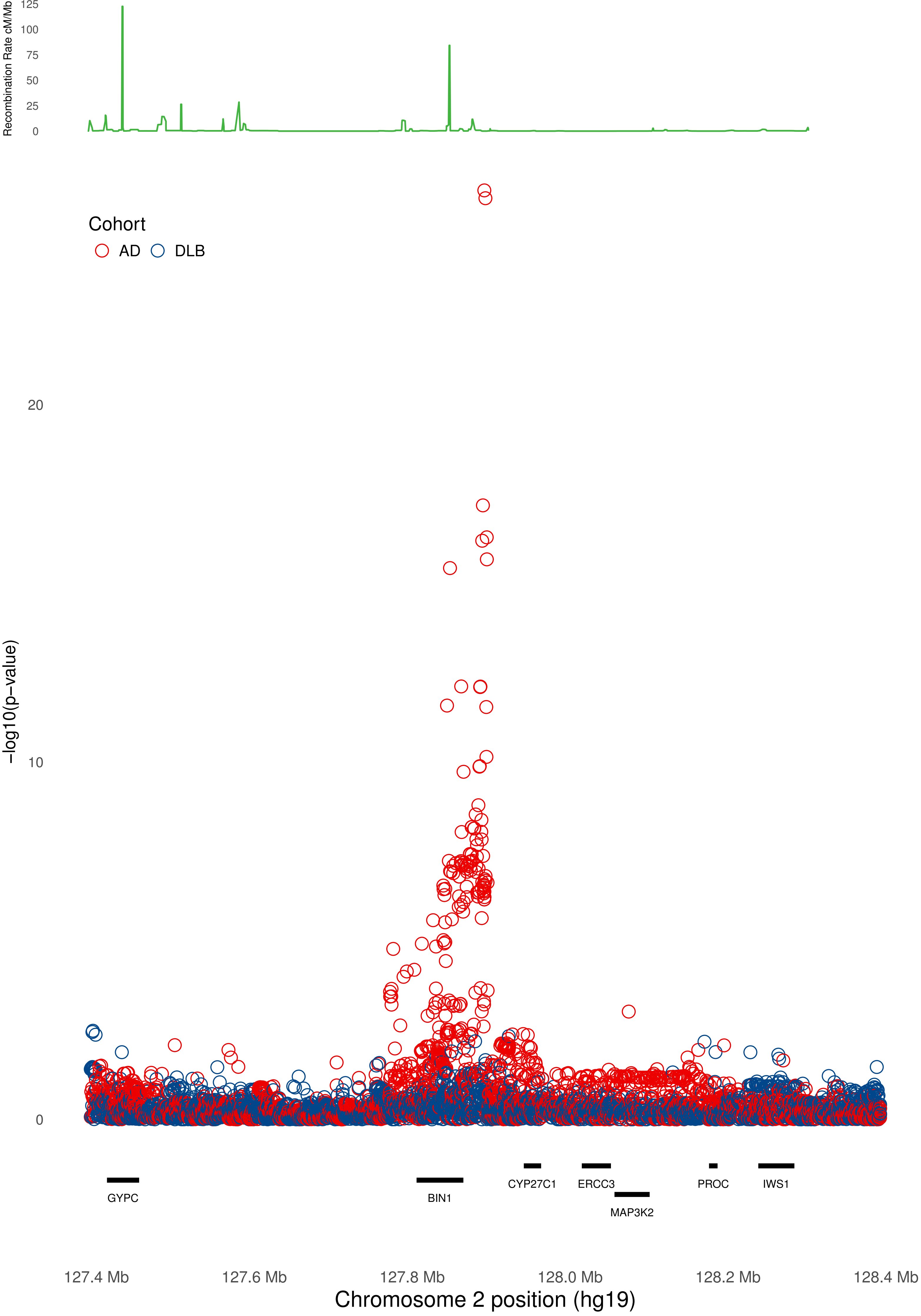
Recombination Rate cM/Mb
125
100
75
50
25
0
Cohort
○ AD ○ DLB
20
10
0
-log10(p-value)
GYPC
BIN1
CYP27C1
ERCC3
MAP3K2
PROC
IWS1
127.4 Mb
127.6 Mb
127.8 Mb
128.0 Mb
128.2 Mb
128.4 Mb
Chromosome 2 position (hg19)

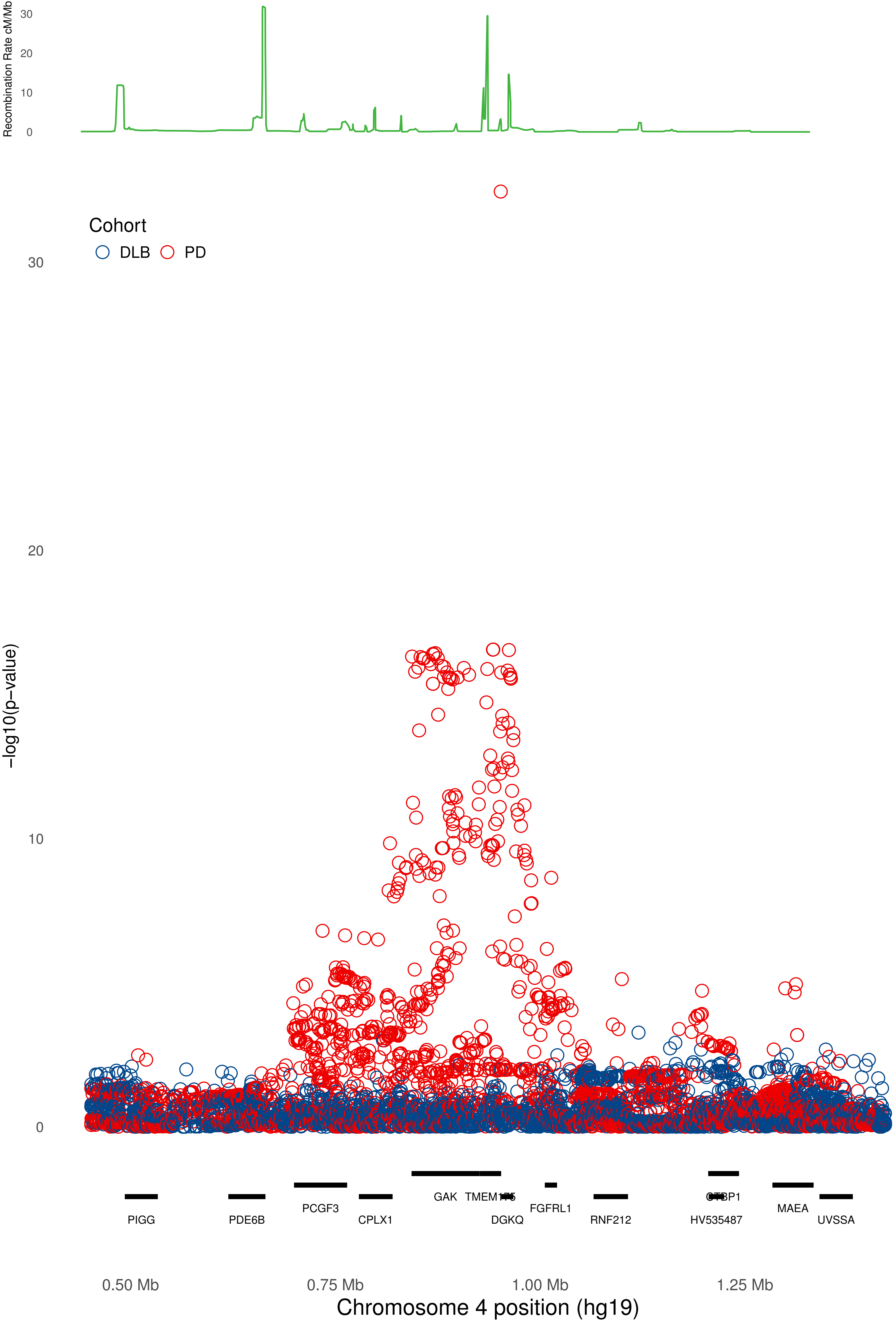
Recombination Rate cM/Mb
30
20
10
0
Cohort
○ DLB ○ PD
30
20
10
0
−log10(p−value)
PIGG
PDE6B
PCGF3
CPLX1
GAK
TMEM175
DGKQ
FGFRL1
RNF212
CTBP1
HV535487
MAEA
UVSSA
0.50 Mb
0.75 Mb
1.00 Mb
1.25 Mb
Chromosome 4 position (hg19)

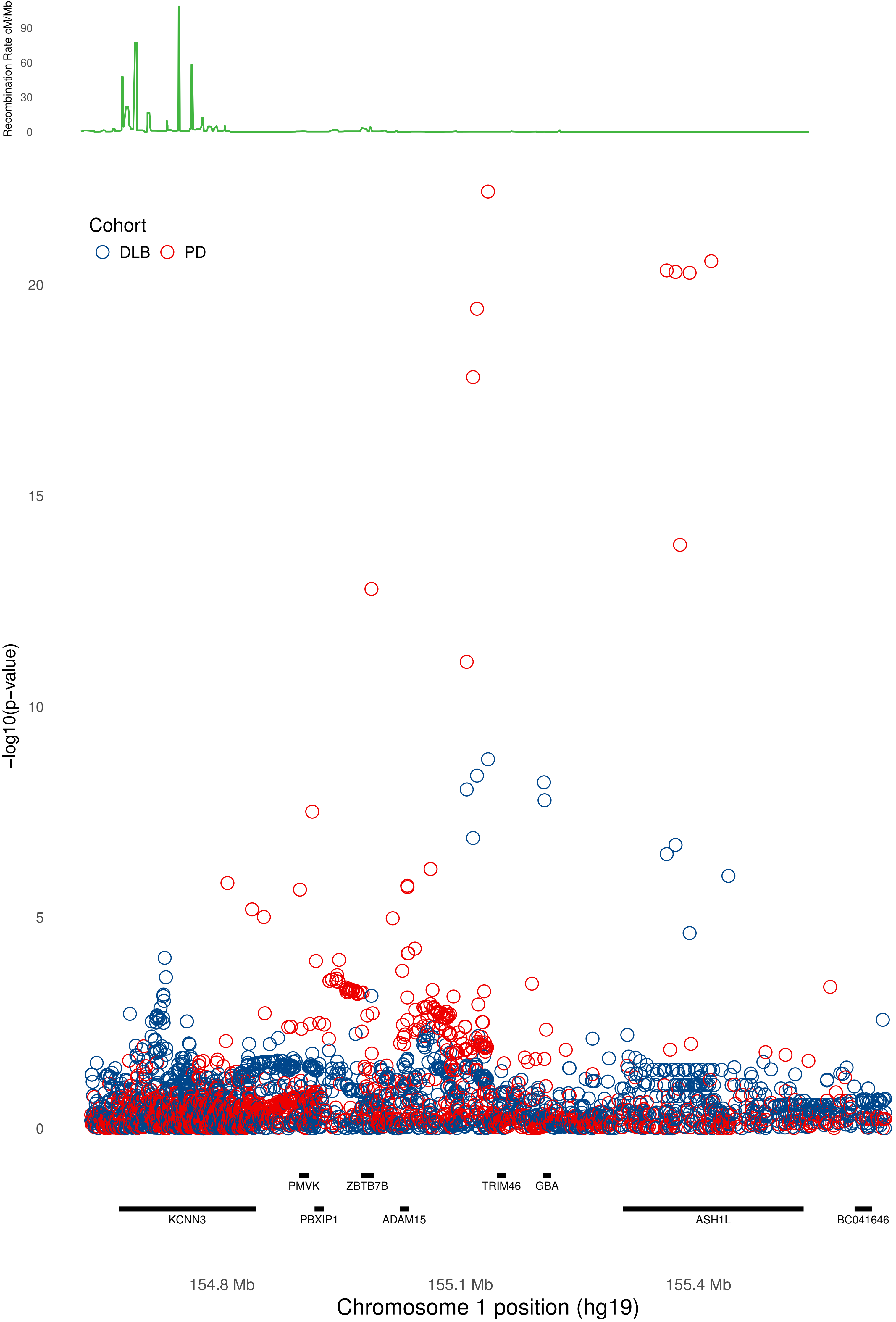
Recombination Rate cM/Mb
90
60
30
0
Cohort
DLB
PD
-log10(p-value)
20
15
10
5
0
PMVK
ZBTB7B
TRIM46
GBA
KCNN3
PBXIP1
ADAM15
ASH1L
BC041646
154.8 Mb
155.1 Mb
155.4 Mb
Chromosome 1 position (hg19)

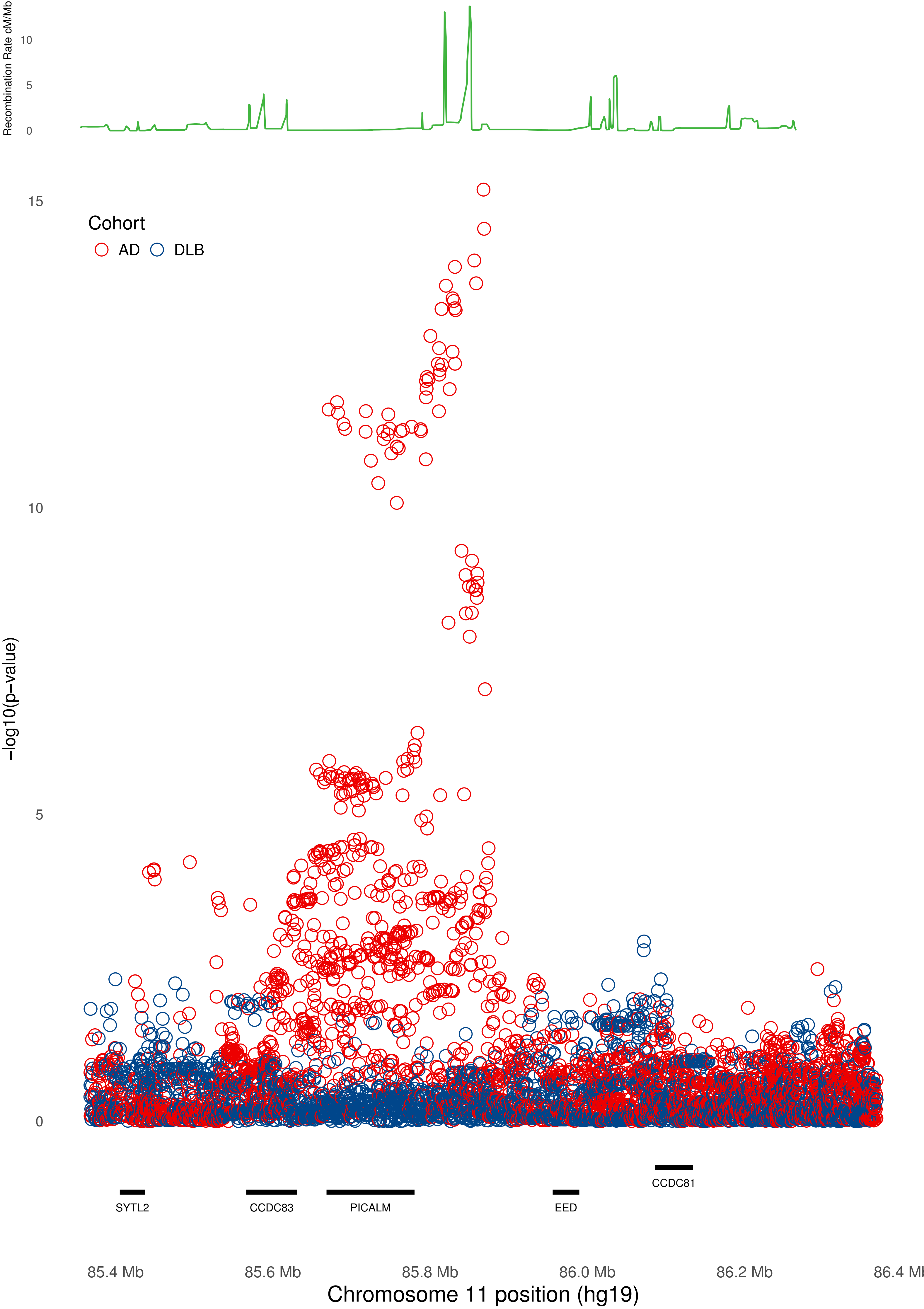
Recombination Rate cM/Mb
10
5
0
15
10
5
0
-log10(p-value)
Cohort
AD
DLB
SYTL2
CCDC83
PICALM
EED
CCDC81
85.4 Mb
85.6 Mb
85.8 Mb
86.0 Mb
86.2 Mb
86.4 Mb
Chromosome 11 position (hg19)

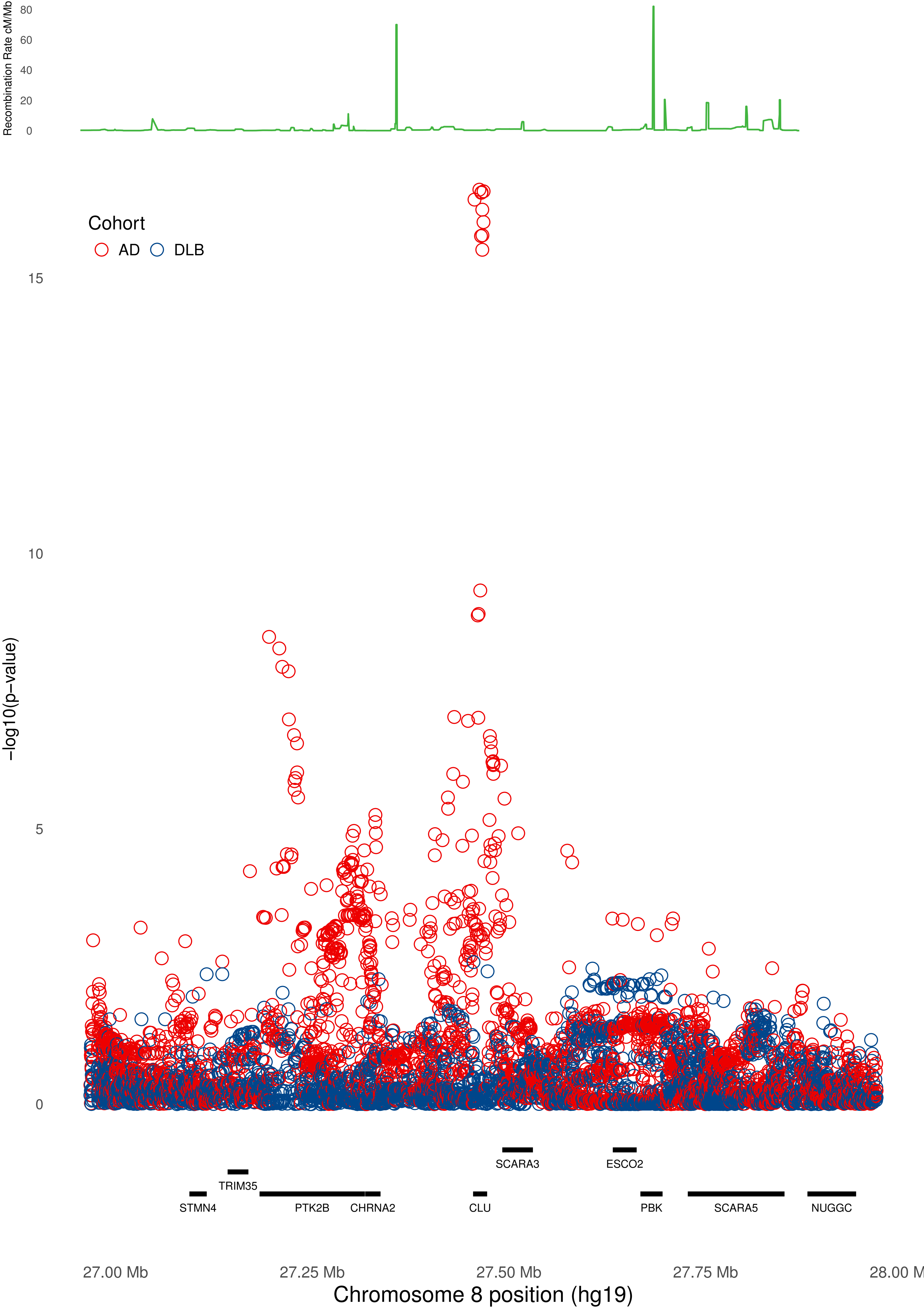
Recombination Rate cM/Mb
80
60
40
20
0
Cohort
AD
DLB
−log10(p−value)
15
10
5
0
SCARA3
ESCO2
TRIM35
STMN4
PTK2B
CHRNA2
CLU
PBK
SCARA5
NUGGC
27.00 Mb
27.25 Mb
27.50 Mb
27.75 Mb
28.00 M
Chromosome 8 position (hg19)

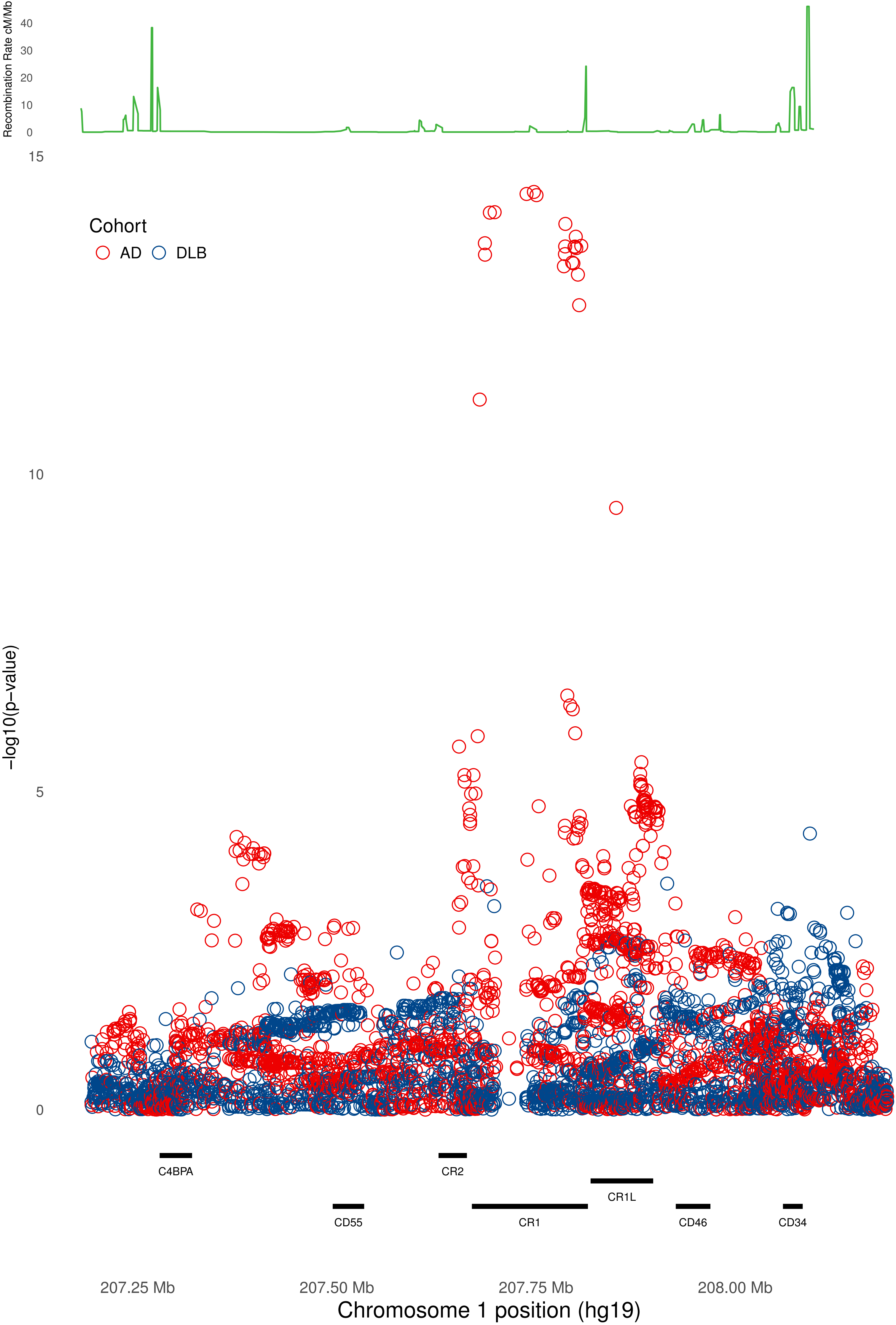
Recombination Rate cM/Mb
40
30
20
10
0
15
Cohort
AD
DLB
10
−log10(p−value)
5
0
C4BPA
CR2
CR1L
CD55
CR1
CD46
CD34
207.25 Mb
207.50 Mb
207.75 Mb
208.00 Mb
Chromosome 1 position (hg19)

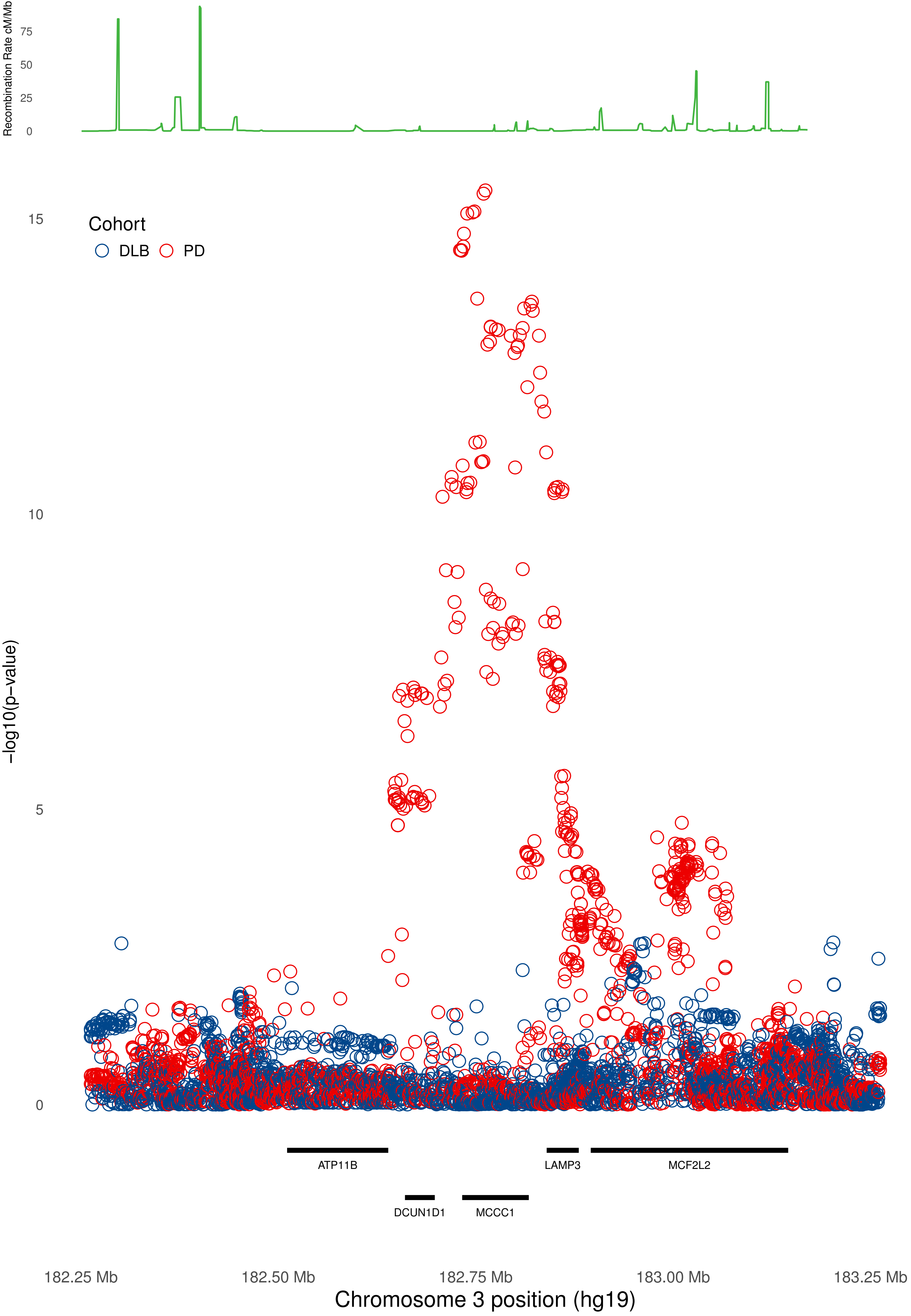
Recombination Rate cM/Mb
75
50
25
0
Cohort
DLB
PD
15
10
5
0
-log10(p-value)
ATP11B
LAMP3
MCF2L2
DCUN1D1
MCCC1
182.25 Mb
182.50 Mb
182.75 Mb
183.00 Mb
183.25 Mb
Chromosome 3 position (hg19)

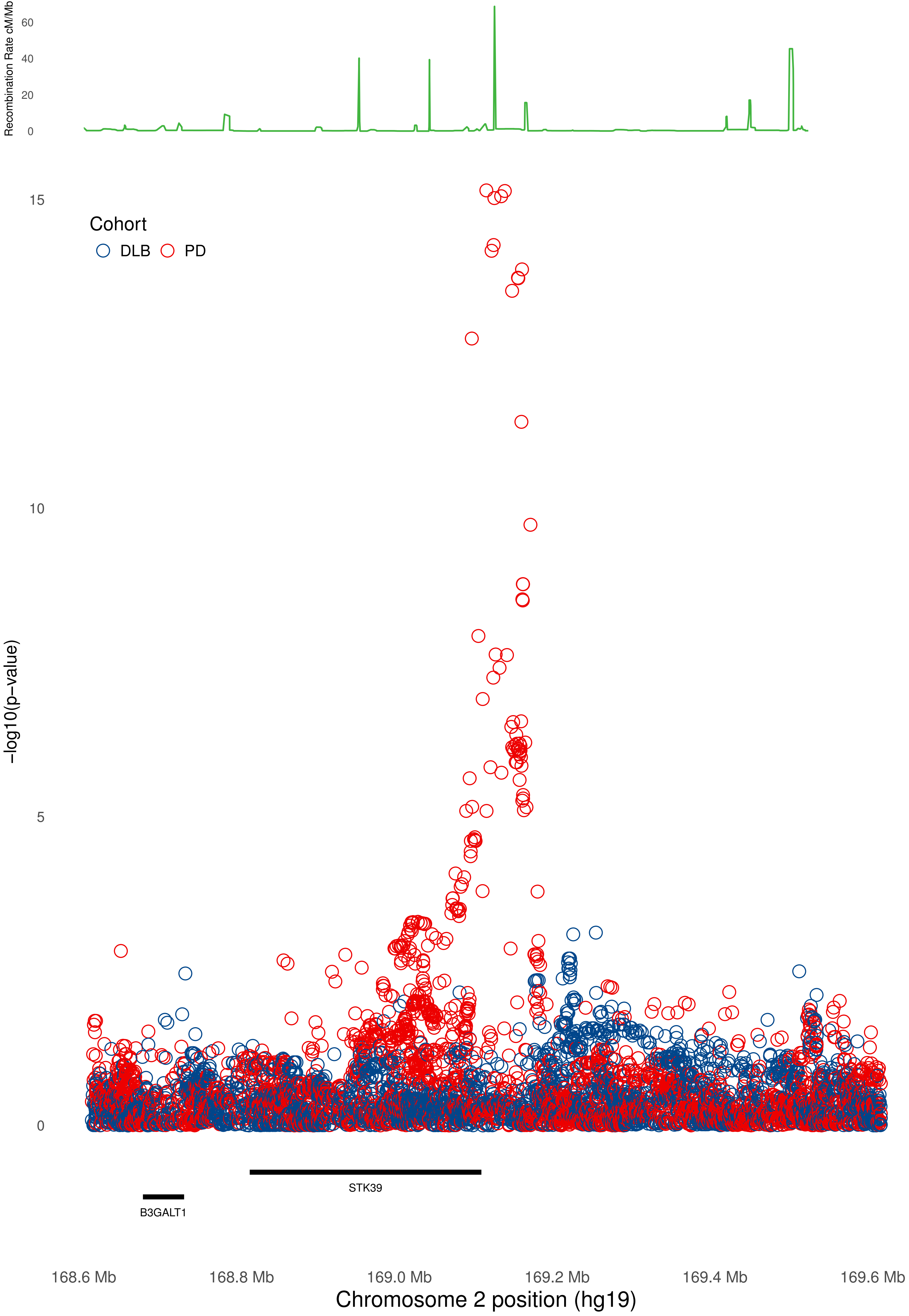Recombination Rate cM/Mb
60
40
20
0
15
Cohort
DLB
PD
10
5
0
−log10(p−value)
STK39
B3GALT1
168.6 Mb
168.8 Mb
169.0 Mb
169.2 Mb
169.4 Mb
169.6 Mb
Chromosome 2 position (hg19)

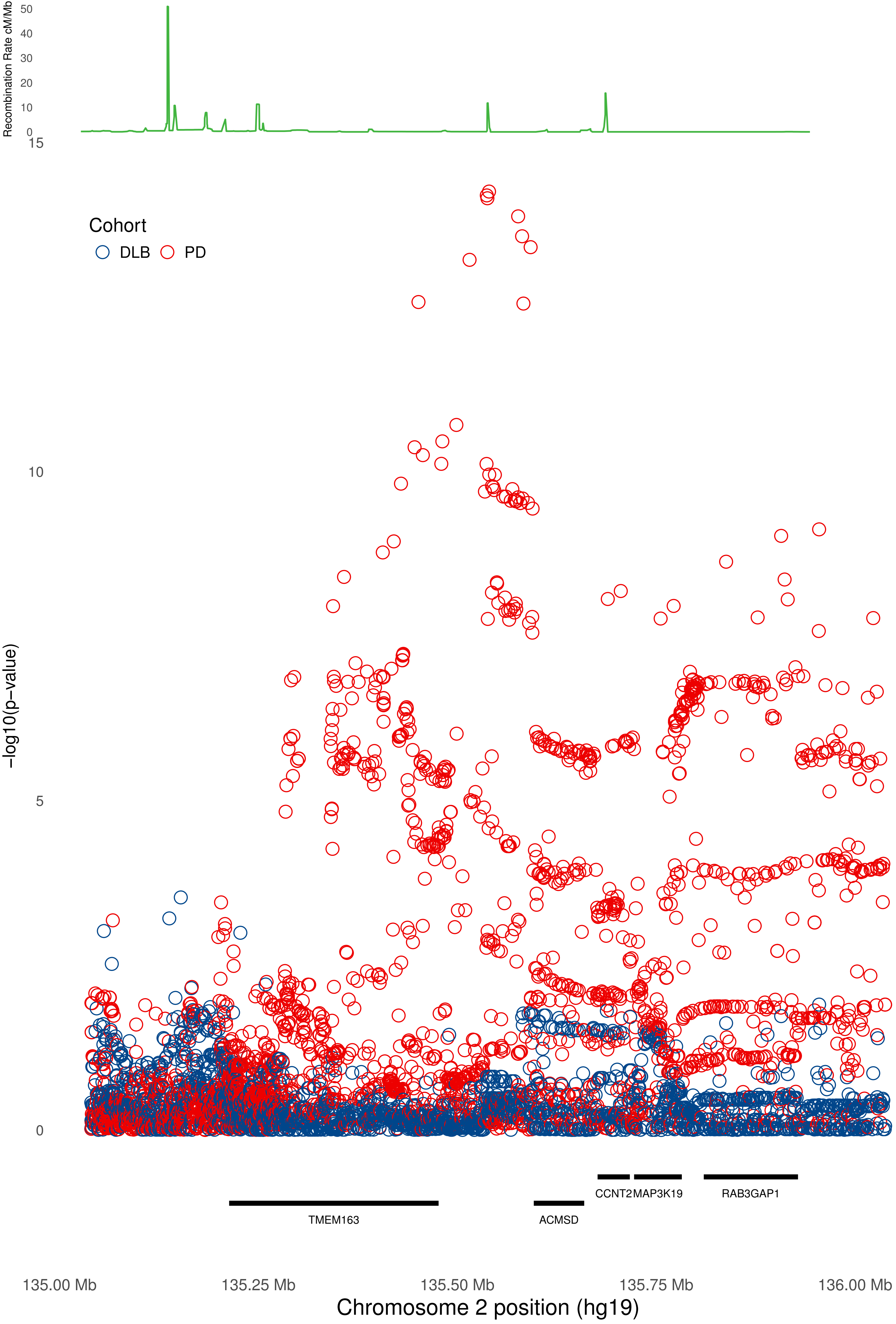
Recombination Rate cM/Mb
50
40
30
20
10
0
15
Cohort
DLB
PD
10
5
0
−log10(p−value)
CCNT2
MAP3K19
RAB3GAP1
TMEM163
ACMSD
135.00 Mb
135.25 Mb
135.50 Mb
135.75 Mb
136.00 Mb
Chromosome 2 position (hg19)

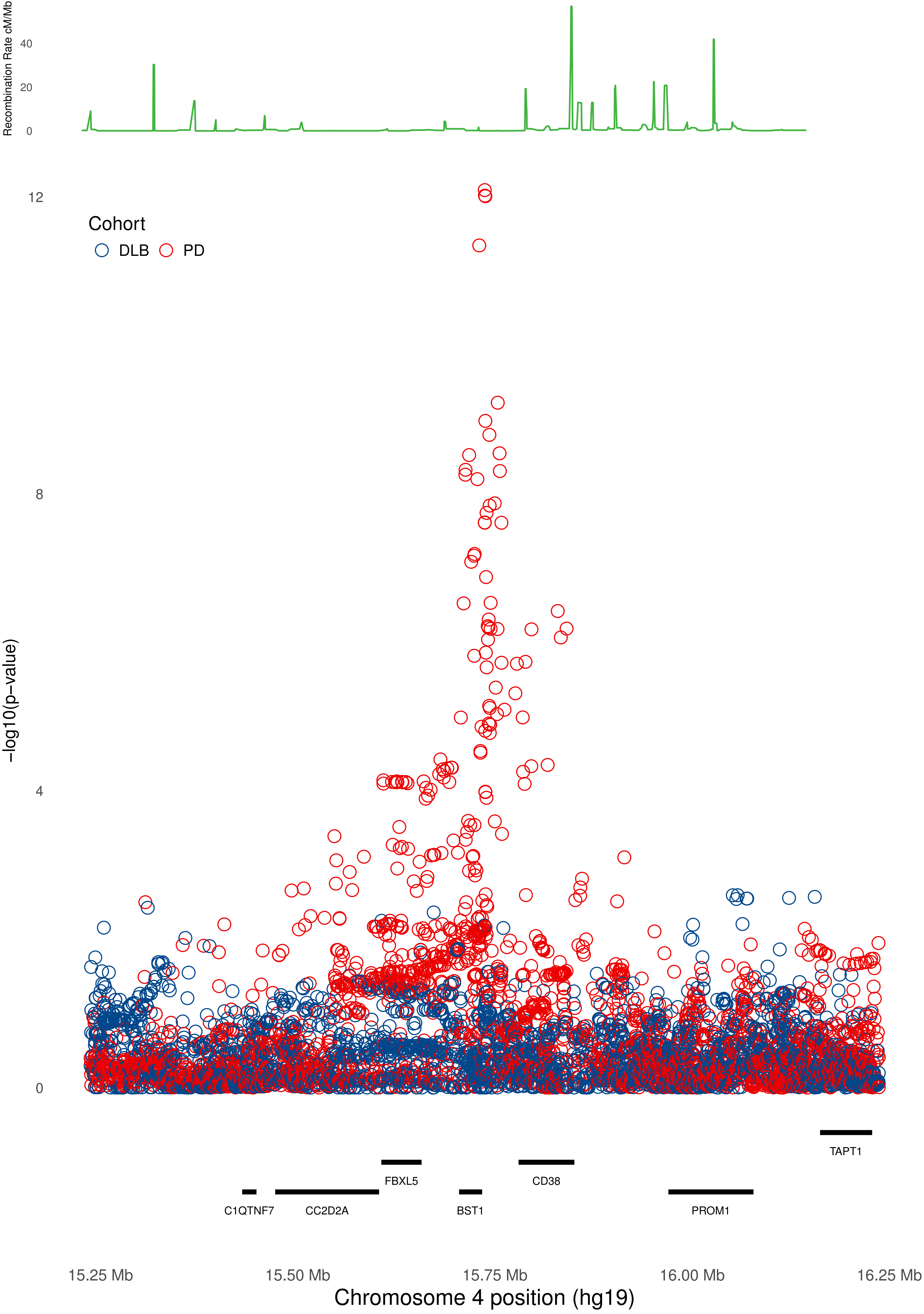
Recombination Rate cM/Mb
40
20
0
12
8
4
0
-log10(p-value)
Cohort
DLB
PD
TAPT1
FBXL5
CD38
C1QTNF7
CC2D2A
BST1
PROM1
15.25 Mb
15.50 Mb
15.75 Mb
16.00 Mb
16.25 Mb
Chromosome 4 position (hg19)

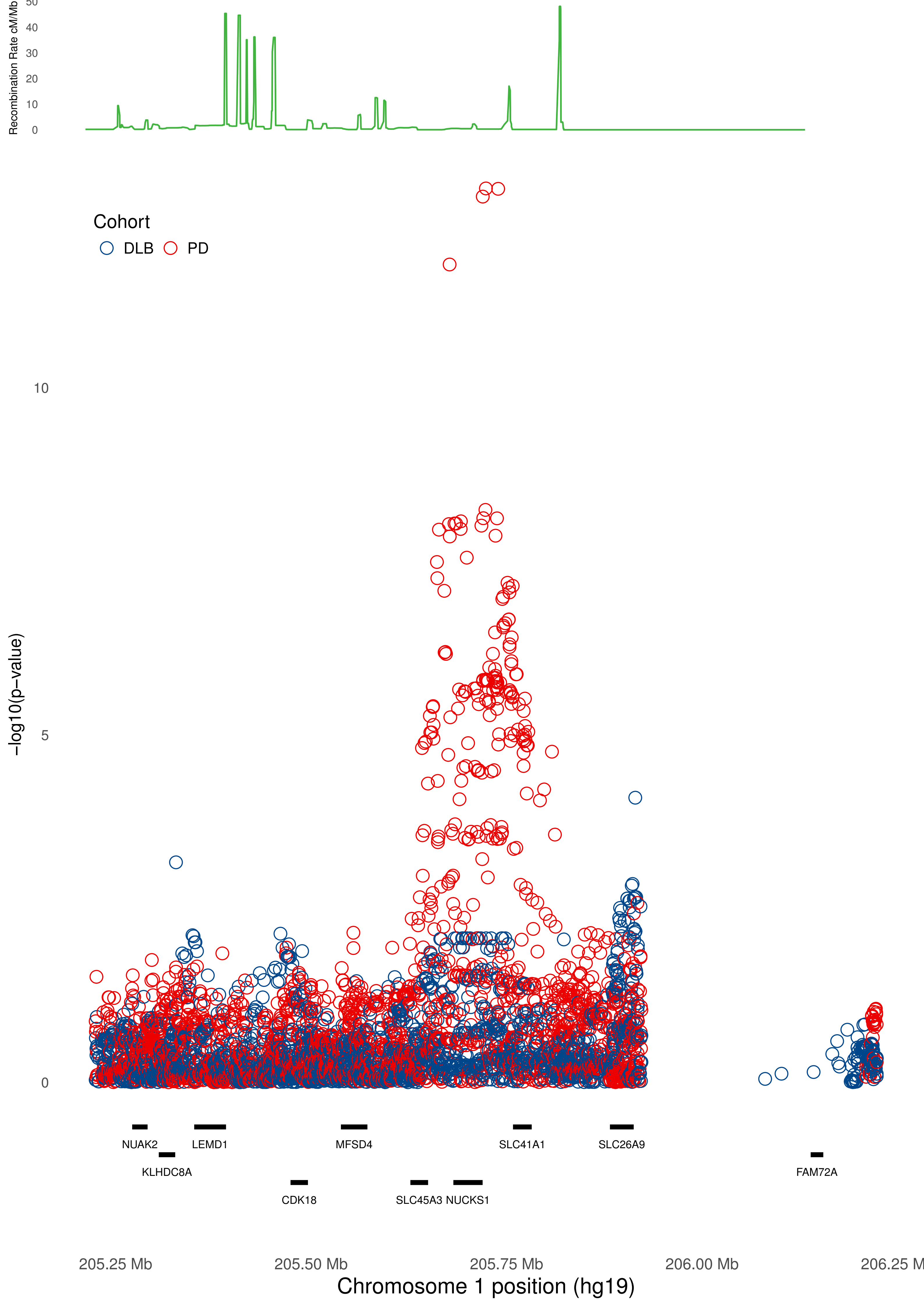
Recombination Rate cM/Mb
50
40
30
20
10
0
Cohort
○ DLB ○ PD
−log10(p−value)
10
5
0
NUAK2
LEMD1
MFSD4
SLC41A1
SLC26A9
KLHDC8A
FAM72A
CDK18
SLC45A3
NUCKS1
205.25 Mb
205.50 Mb
205.75 Mb
206.00 Mb
206.25 M
Chromosome 1 position (hg19)

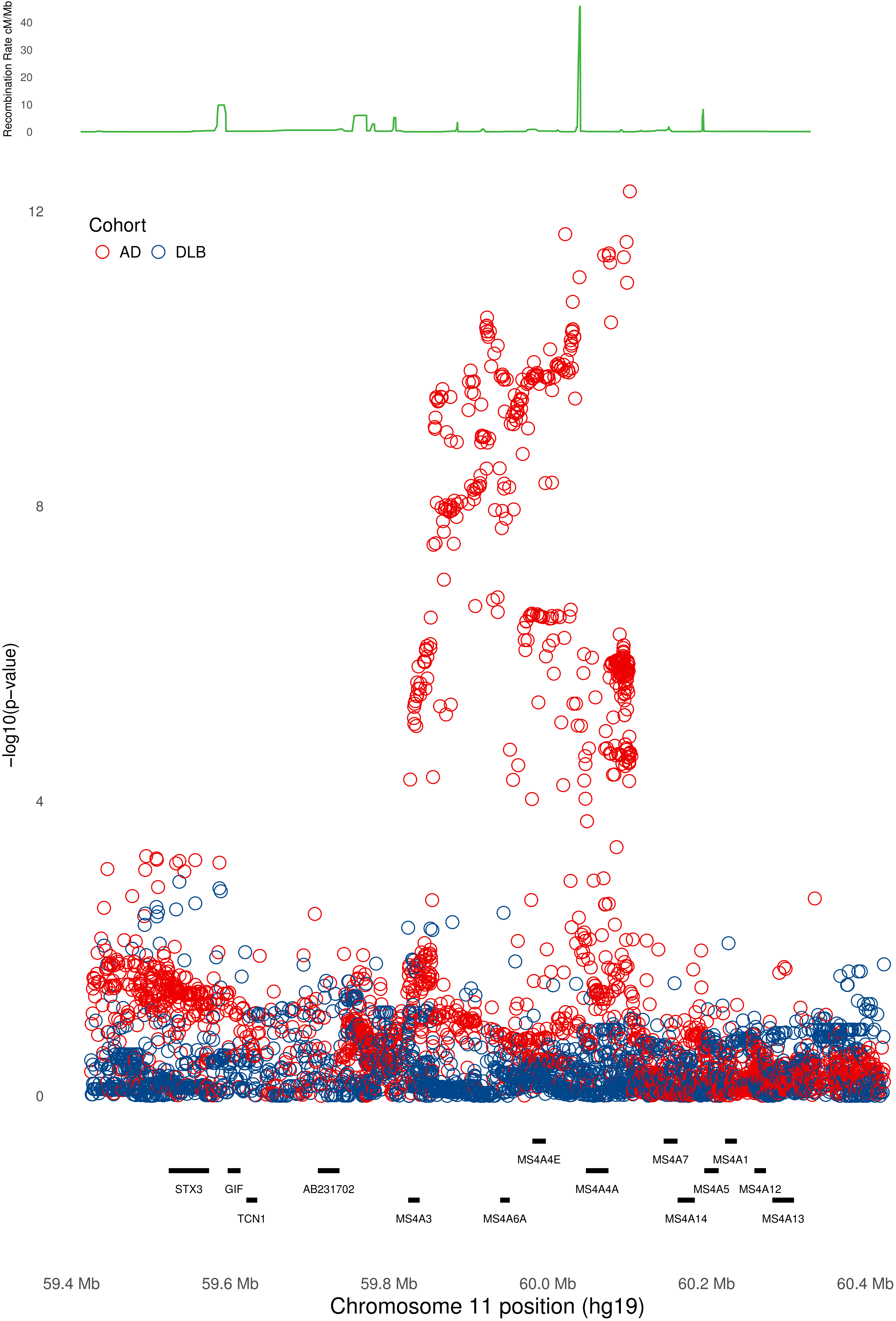
Recombination Rate cM/Mb
40
30
20
10
0
12
8
4
0
-log10(p-value)
Cohort
AD
DLB
MS4A4E
MS4A7
MS4A1
STX3
GIF
AB231702
MS4A4A
MS4A5
MS4A12
TCN1
MS4A3
MS4A6A
MS4A14
MS4A13
59.4 Mb
59.6 Mb
59.8 Mb
60.0 Mb
60.2 Mb
60.4 Mb
Chromosome 11 position (hg19)

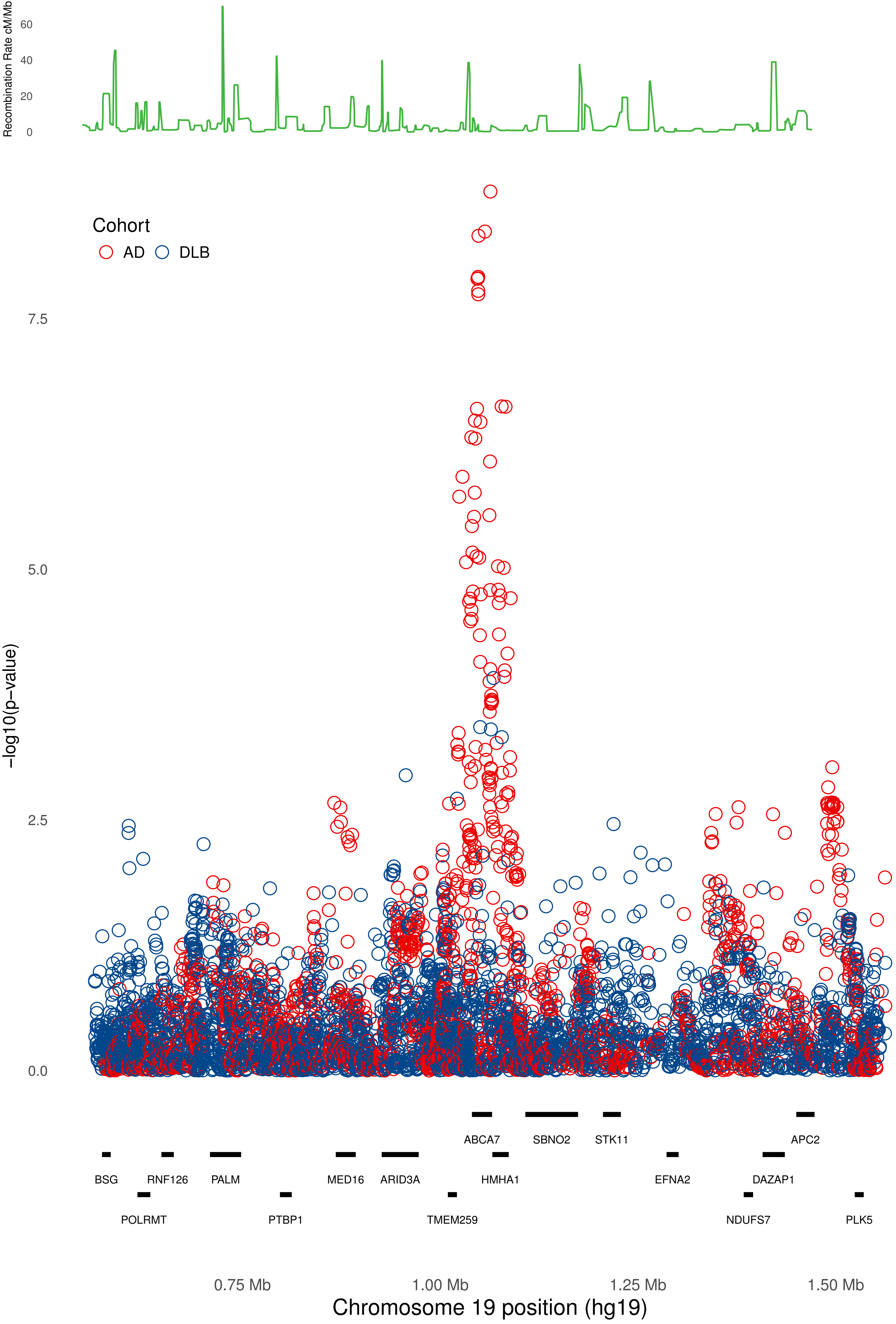
Recombination Rate cM/Mb
60
40
20
0
Cohort
AD
DLB
-log10(p-value)
7.5
5.0
2.5
0.0
ABCA7
SBNO2
STK11
APC2
BSG
RNF126
PALM
MED16
ARID3A
HMHA1
EFNA2
DAZAP1
POLRMT
PTBP1
TMEM259
NDUFS7
PLK5
0.75 Mb
1.00 Mb
1.25 Mb
1.50 Mb
Chromosome 19 position (hg19)

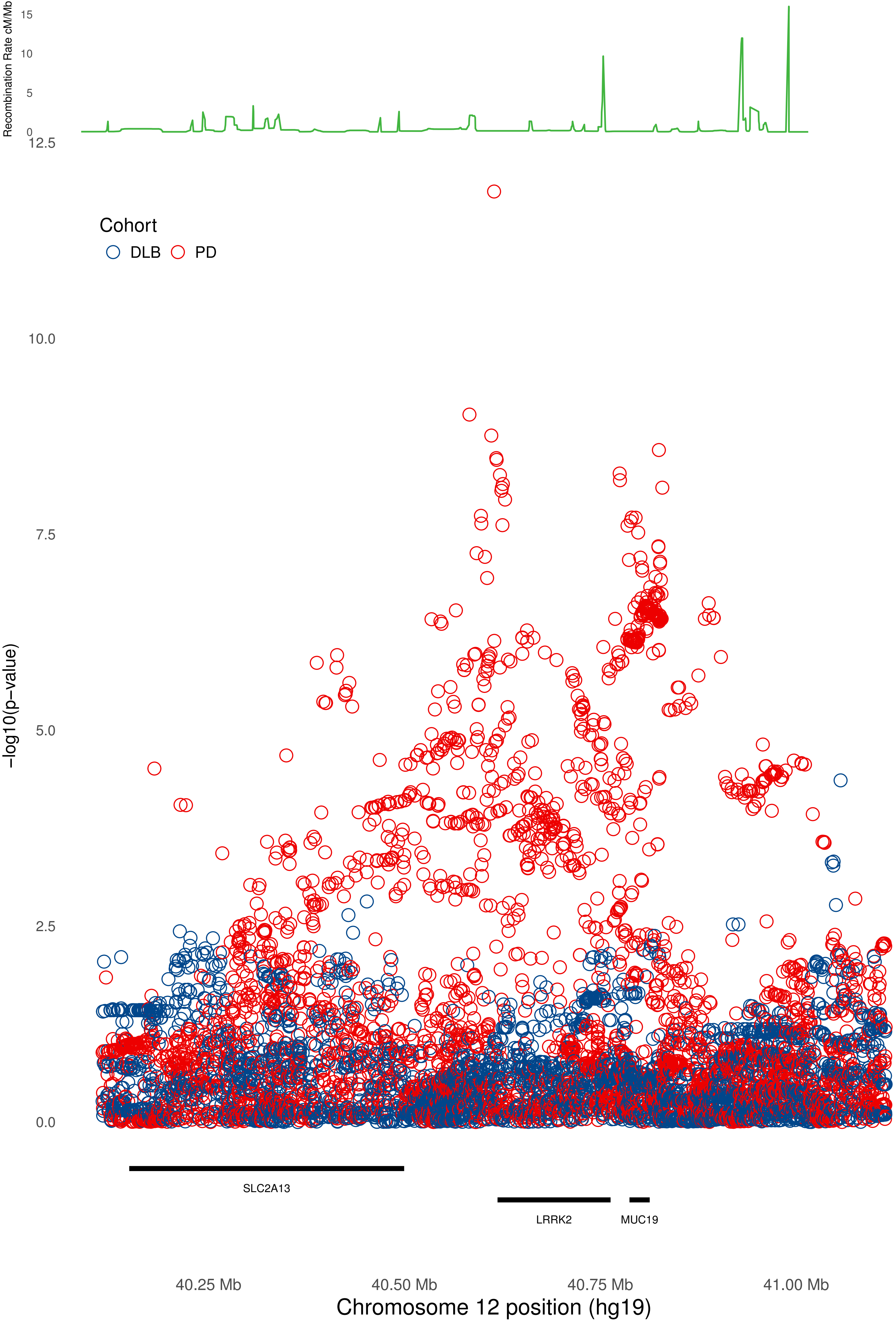
Recombination Rate cM/Mb
15
10
5
0
12.5
Cohort
DLB
PD
10.0
7.5
5.0
2.5
0.0
-log10(p-value)
SLC2A13
LRRK2
MUC19
40.25 Mb
40.50 Mb
40.75 Mb
41.00 Mb
Chromosome 12 position (hg19)

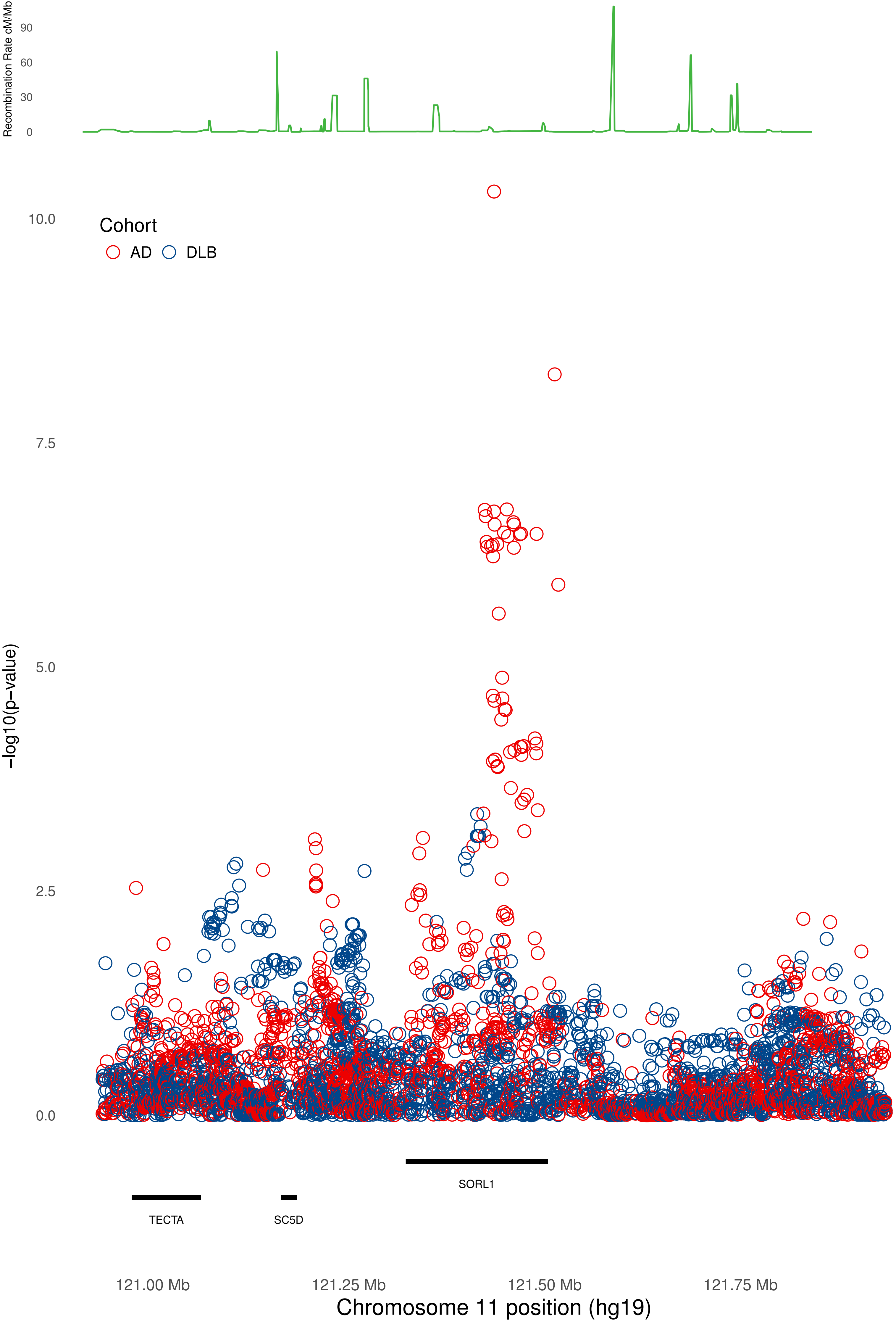
Recombination Rate cM/Mb
90
60
30
0
Cohort
AD
DLB
10.0
7.5
5.0
2.5
0.0
−log10(p−value)
SORL1
TECTA
SC5D
121.00 Mb
121.25 Mb
121.50 Mb
121.75 Mb
Chromosome 11 position (hg19)

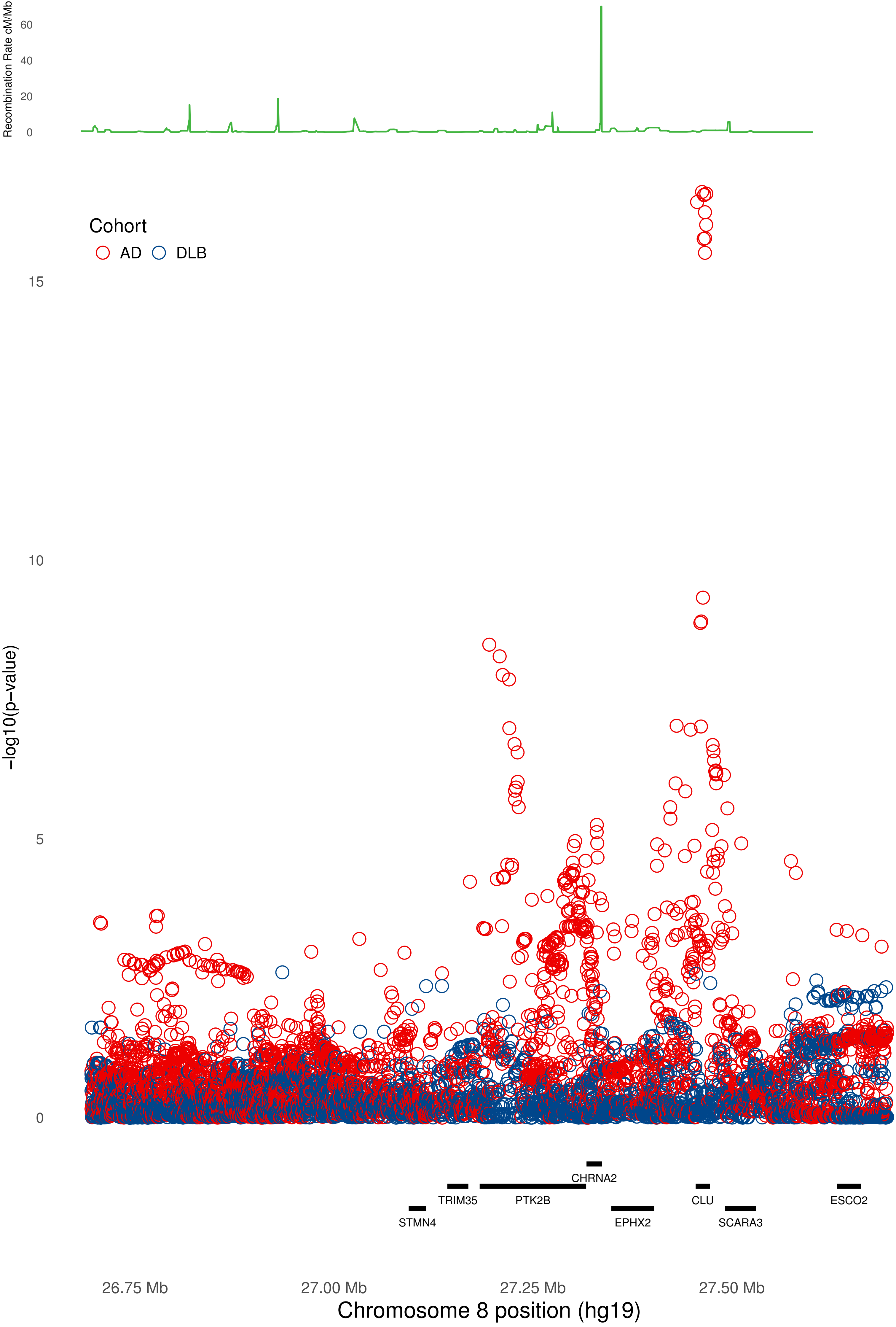
Recombination Rate cM/Mb
60
40
20
0
Cohort
AD
DLB
15
10
5
0
-log10(p-value)
CHRNA2
TRIM35
PTK2B
CLU
ESCO2
STMN4
EPHX2
SCARA3
26.75 Mb
27.00 Mb
27.25 Mb
27.50 Mb
Chromosome 8 position (hg19)

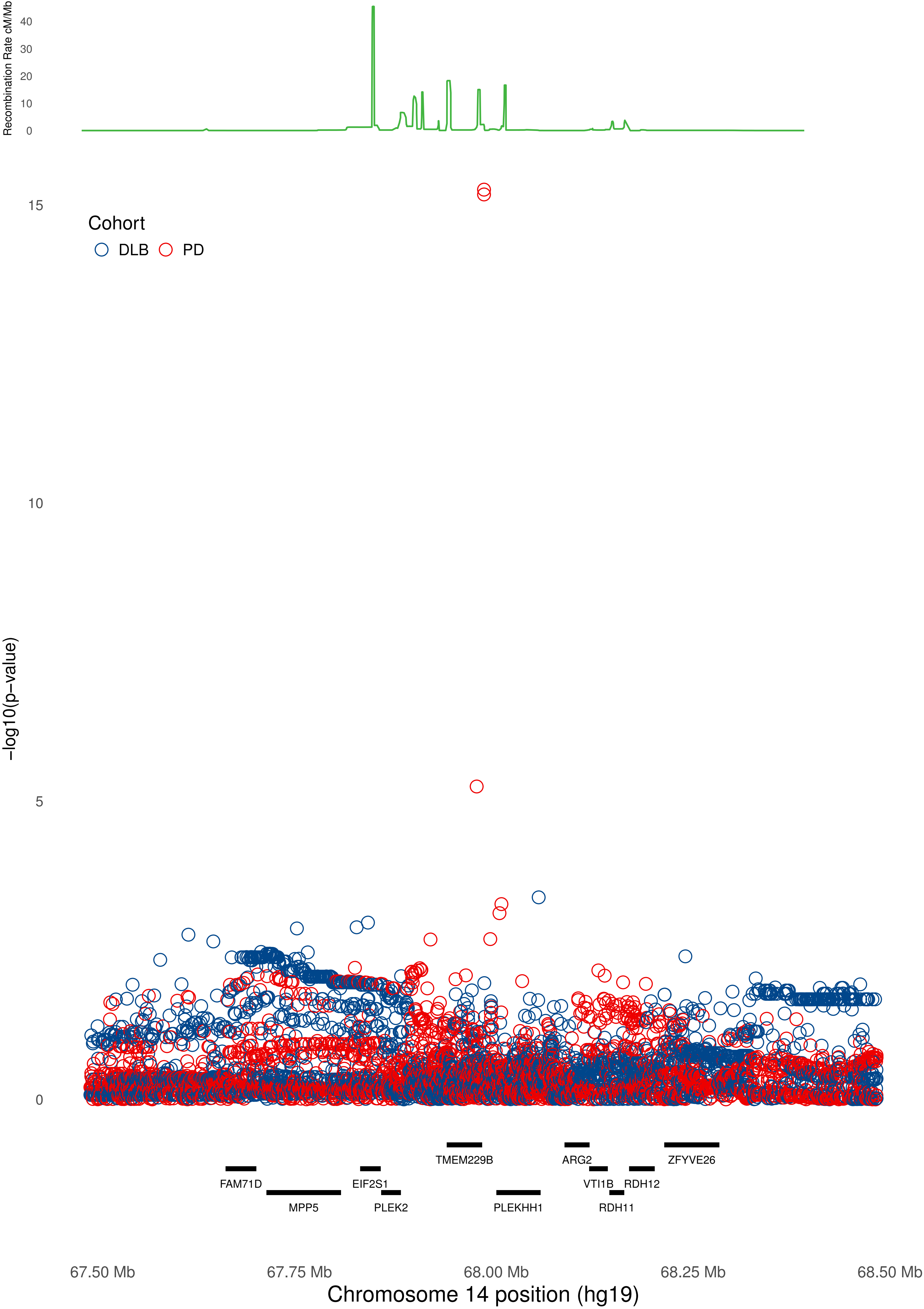
Recombination Rate cM/Mb
40
30
20
10
0
Cohort
DLB
PD
15
10
5
0
-log10(p-value)
TMEM229B
ARG2
ZFYVE26
FAM71D
EIF2S1
VTI1B
RDH12
MPP5
PLEK2
PLEKHH1
RDH11
67.50 Mb
67.75 Mb
68.00 Mb
68.25 Mb
68.50 Mb
Chromosome 14 position (hg19)

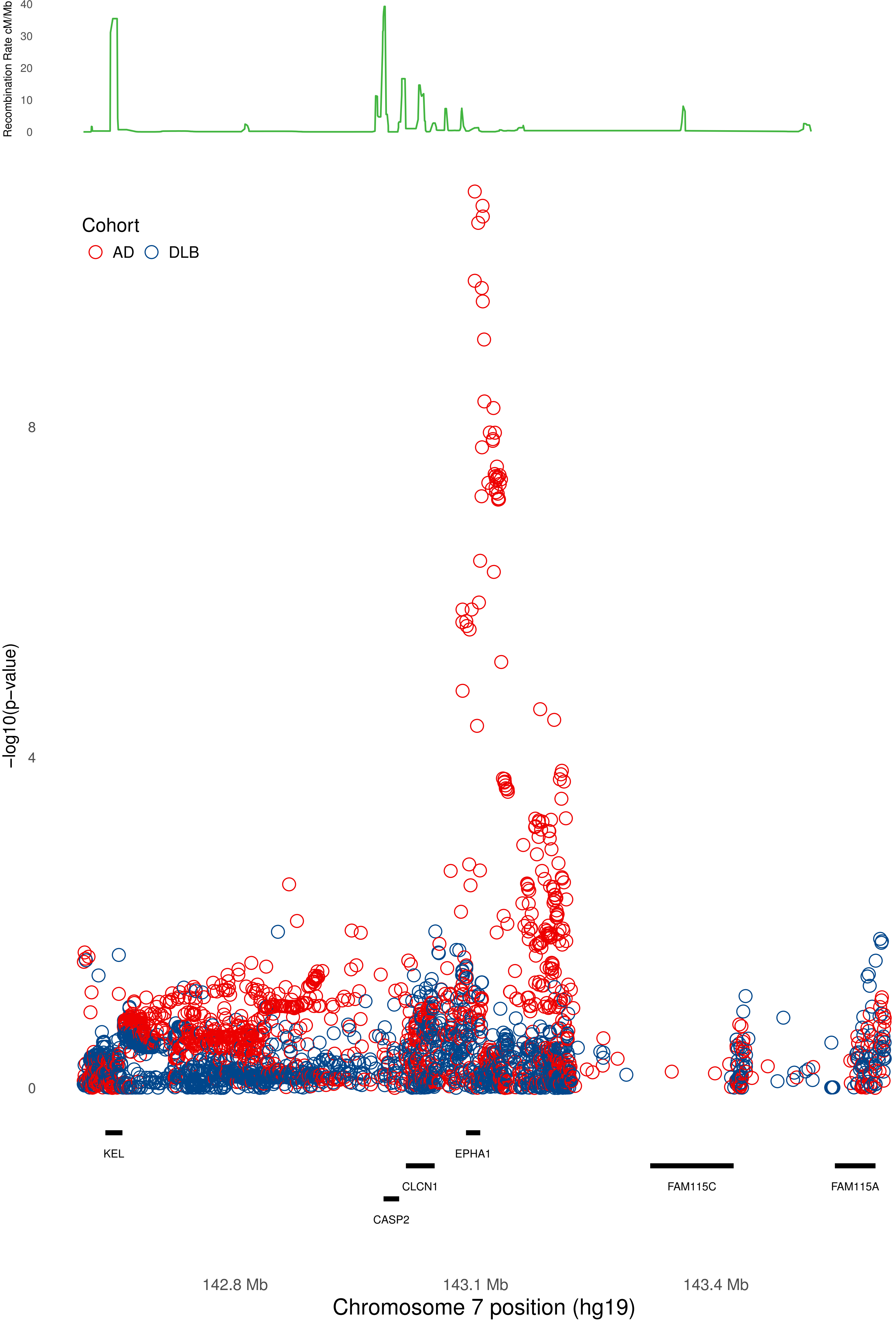
Recombination Rate cM/Mb
40
30
20
10
0
Cohort
AD
DLB
−log10(p−value)
8
4
0
KEL
EPHA1
CLCN1
CASP2
FAM115C
FAM115A
142.8 Mb
143.1 Mb
143.4 Mb
Chromosome 7 position (hg19)

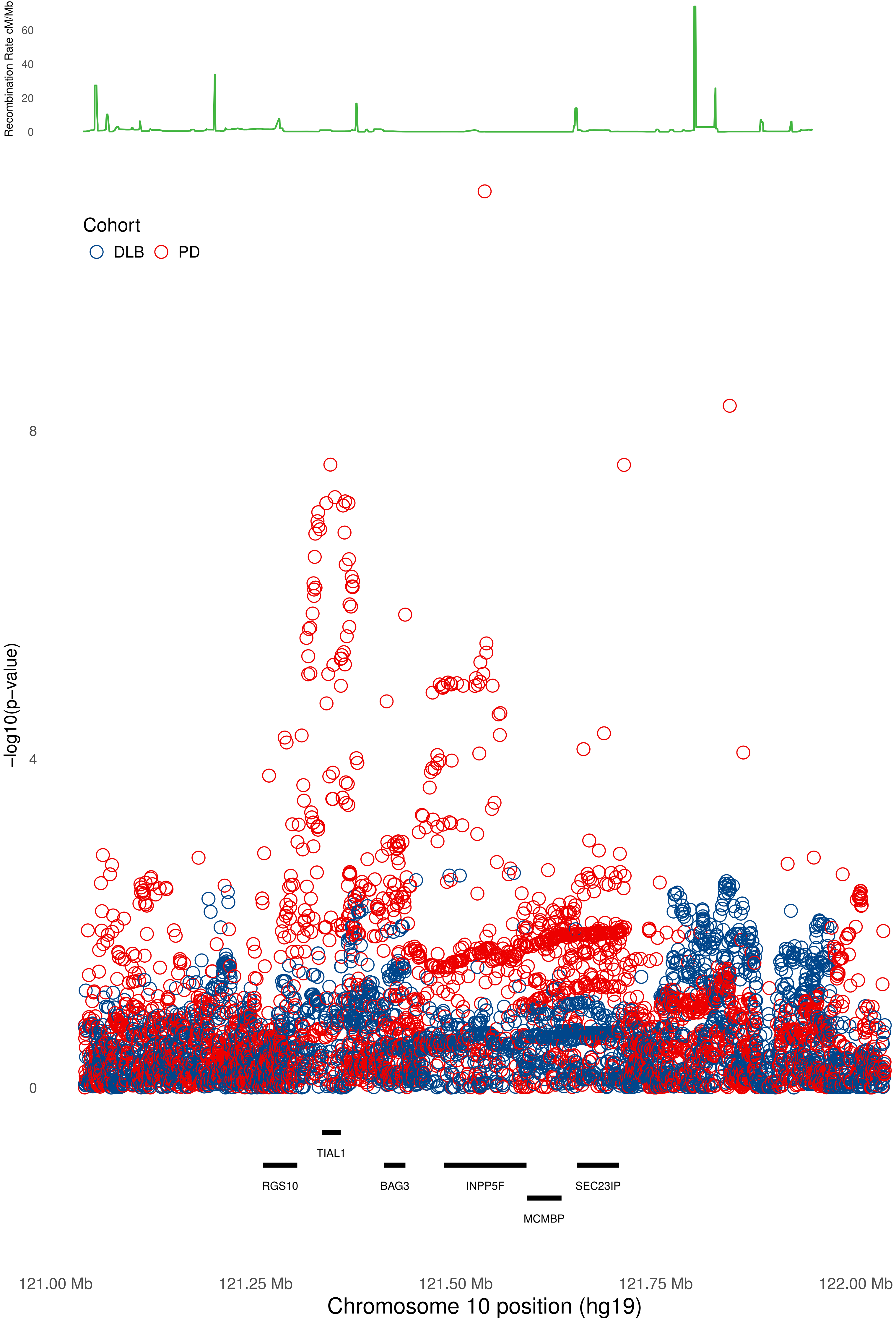
Recombination Rate cM/Mb
60
40
20
0
Cohort
DLB
PD
−log10(p−value)
8
4
0
TIAL1
RGS10
BAG3
INPP5F
SEC23IP
MCMBP
121.00 Mb
121.25 Mb
121.50 Mb
121.75 Mb
122.00 Mb
Chromosome 10 position (hg19)

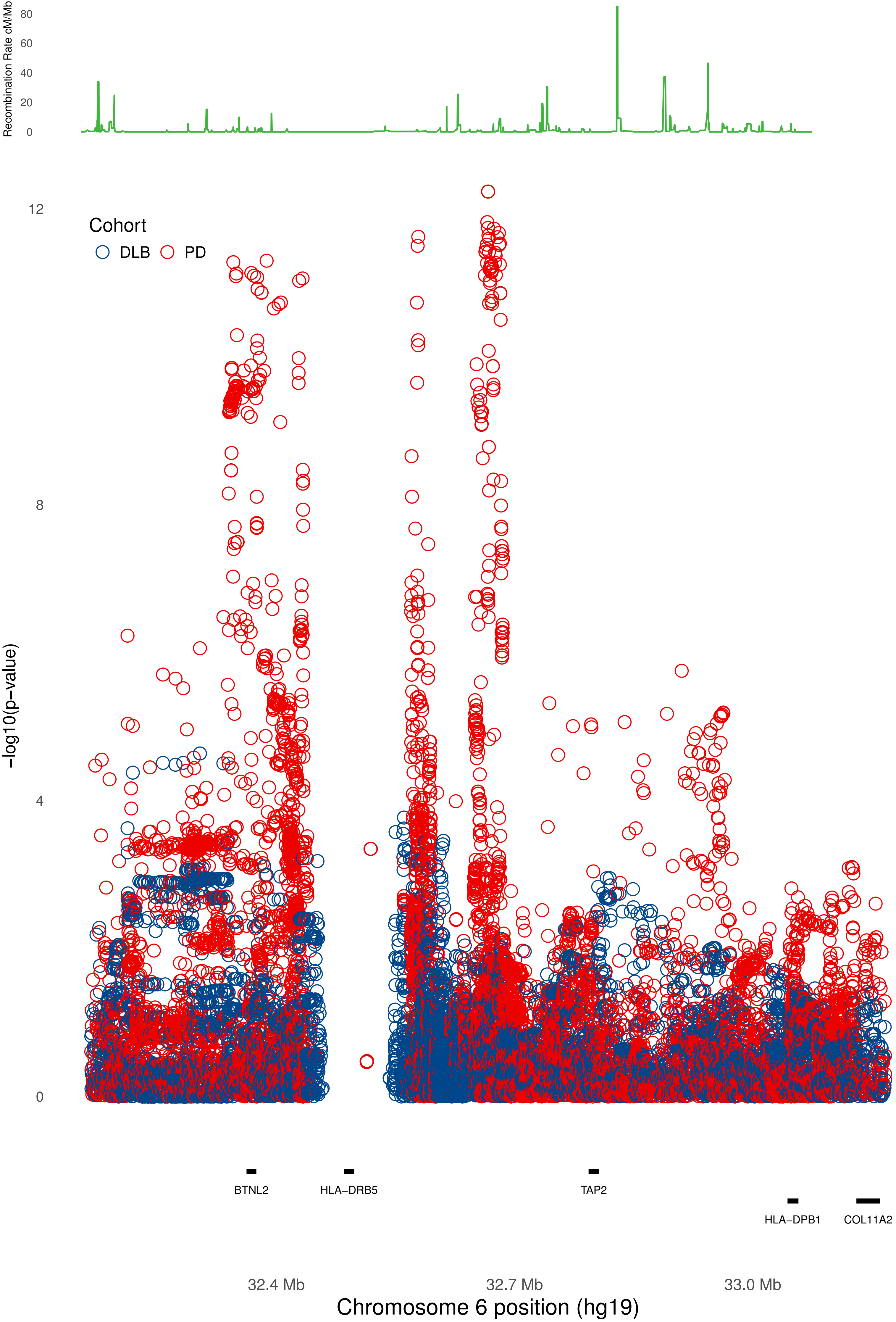
Recombination Rate cM/Mb
80
60
40
20
0
Cohort
DLB
PD
−log10(p−value)
12
8
4
0
BTNL2
HLA−DRB5
TAP2
HLA−DPB1
COL11A2
32.4 Mb
32.7 Mb
33.0 Mb
Chromosome 6 position (hg19)

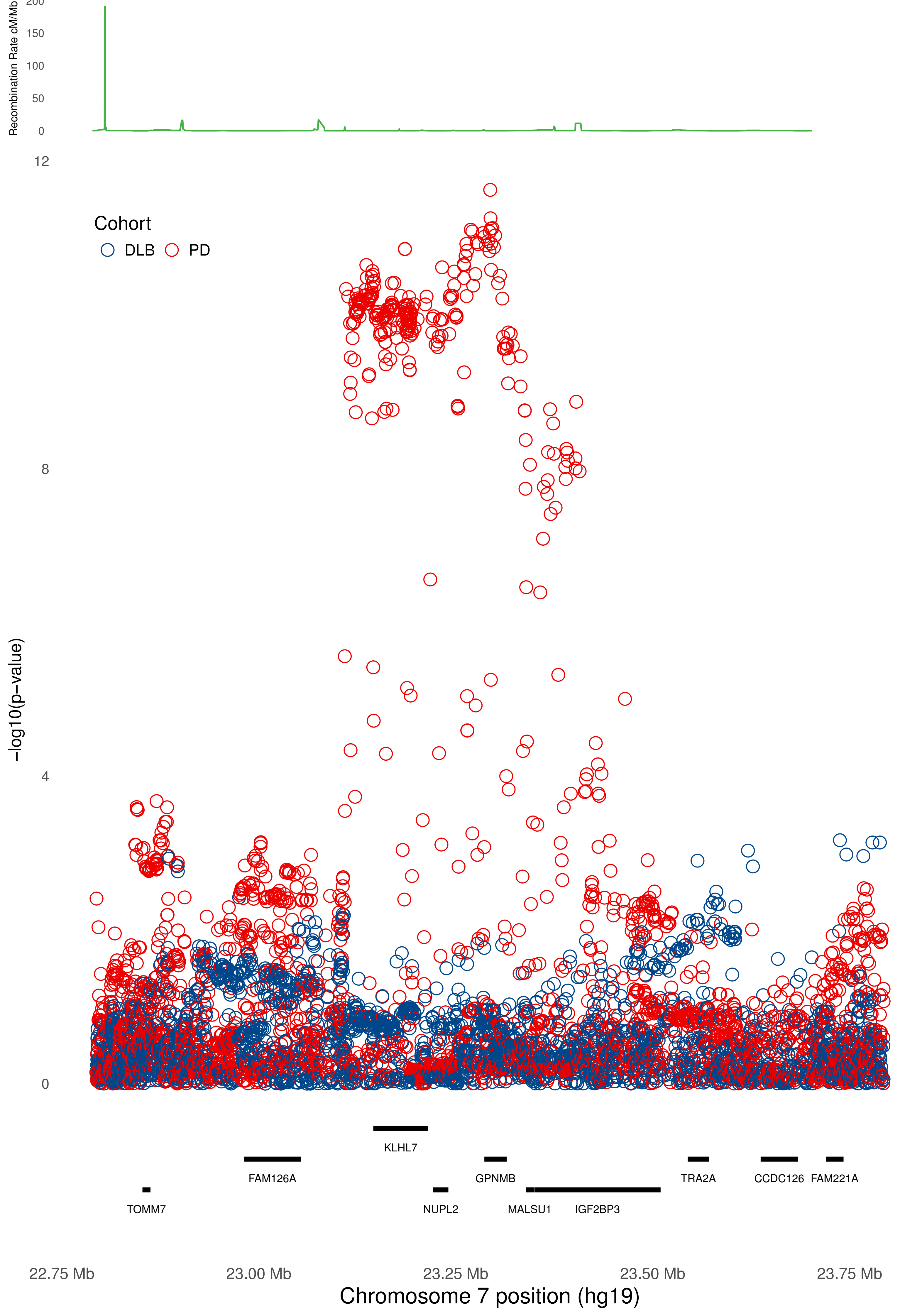
Recombination Rate cM/Mb
200
150
100
50
0
12
Cohort
DLB
PD
8
4
0
−log10(p−value)
KLHL7
FAM126A
GPNMB
TRA2A
CCDC126
FAM221A
TOMM7
NUPL2
MALSU1
IGF2BP3
22.75 Mb
23.00 Mb
23.25 Mb
23.50 Mb
23.75 Mb
Chromosome 7 position (hg19)

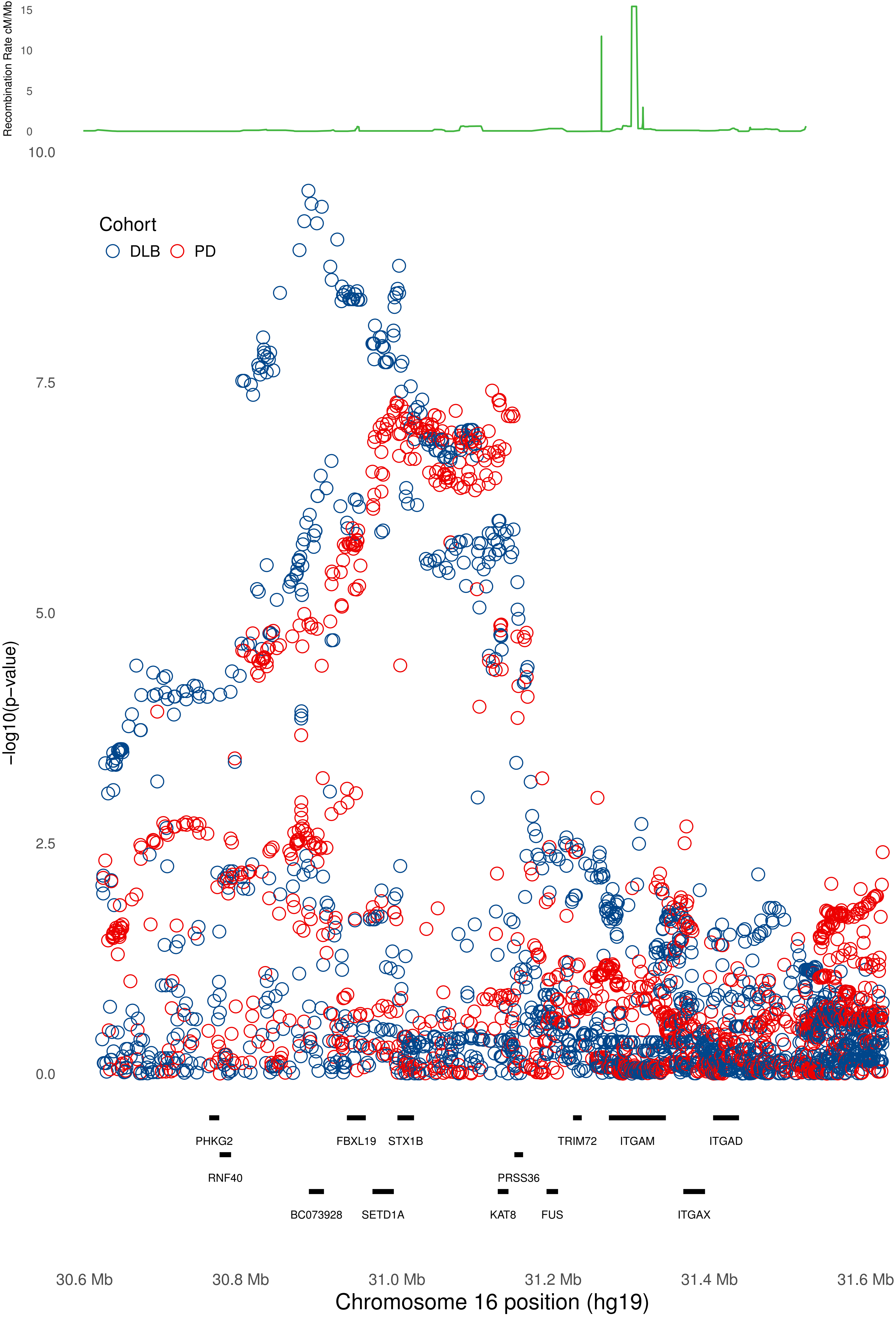
Recombination Rate cM/Mb
15
10
5
0
10.0
7.5
5.0
2.5
0.0
-log10(p-value)
Cohort
DLB
PD
PHKG2
RNF40
BC073928
FBXL19
SETD1A
STX1B
KAT8
PRSS36
FUS
TRIM72
ITGAM
ITGAX
ITGAD
30.6 Mb
30.8 Mb
31.0 Mb
31.2 Mb
31.4 Mb
31.6 Mb
Chromosome 16 position (hg19)

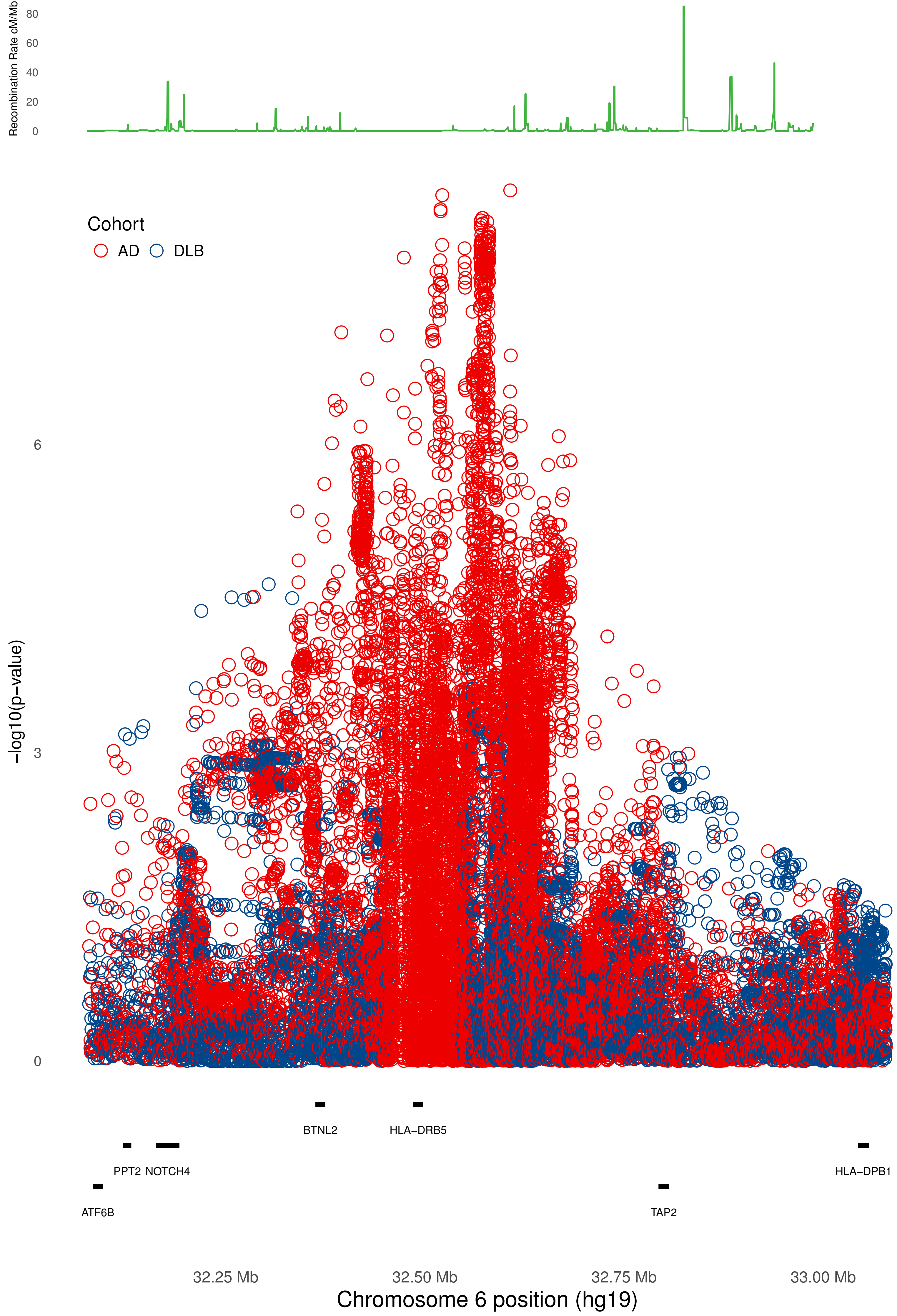

Recombination Rate cM/Mb
80
60
40
20
0
Cohort
AD
DLB
−log10(p−value)
6
3
0
BTNL2
HLA−DRB5
PPT2
NOTCH4
HLA−DPB1
ATF6B
TAP2
32.25 Mb
32.50 Mb
32.75 Mb
33.00 Mb
Chromosome 6 position (hg19)

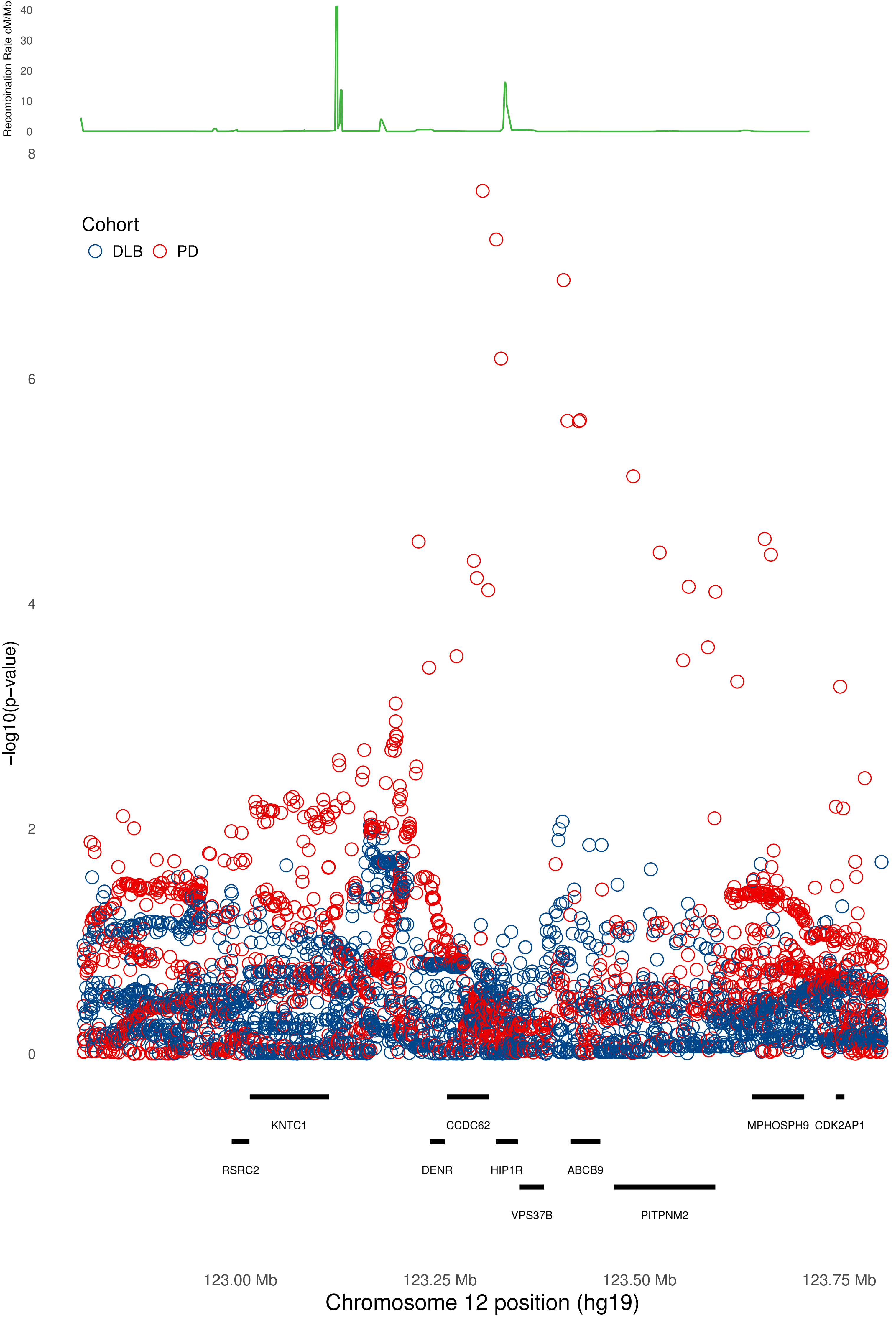
Recombination Rate cM/Mb
40
30
20
10
0
8
6
4
2
0
-log10(p-value)
Cohort
DLB
PD
KNTC1
CCDC62
MPHOSPH9
CDK2AP1
RSRC2
DENR
HIP1R
ABCB9
VPS37B
PITPNM2
123.00 Mb
123.25 Mb
123.50 Mb
123.75 Mb
Chromosome 12 position (hg19)

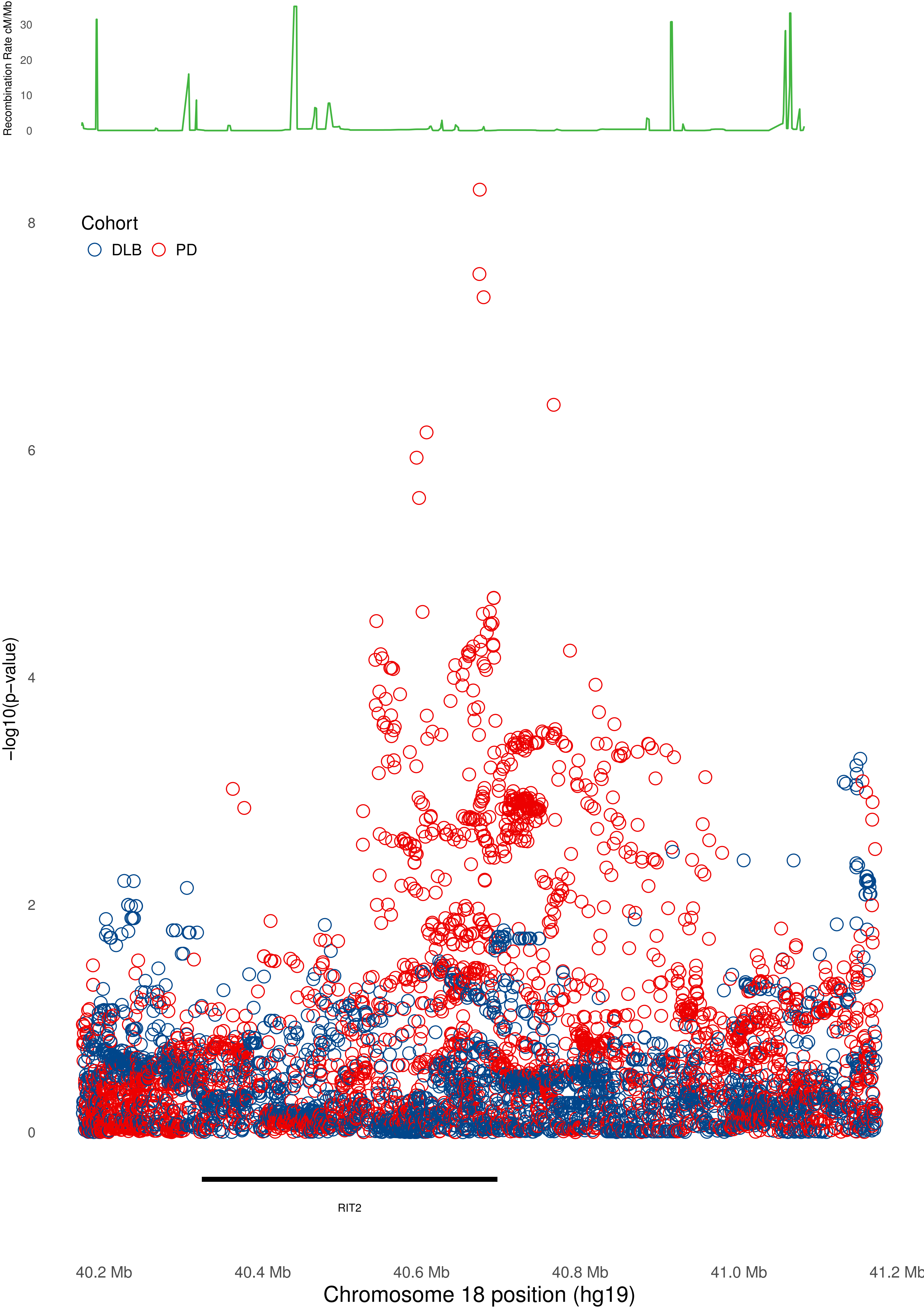
Recombination Rate cM/Mb
30
20
10
0
Cohort
DLB
PD
8
6
4
2
0
-log10(p-value)
RIT2
40.2 Mb
40.4 Mb
40.6 Mb
40.8 Mb
41.0 Mb
41.2 Mb
Chromosome 18 position (hg19)

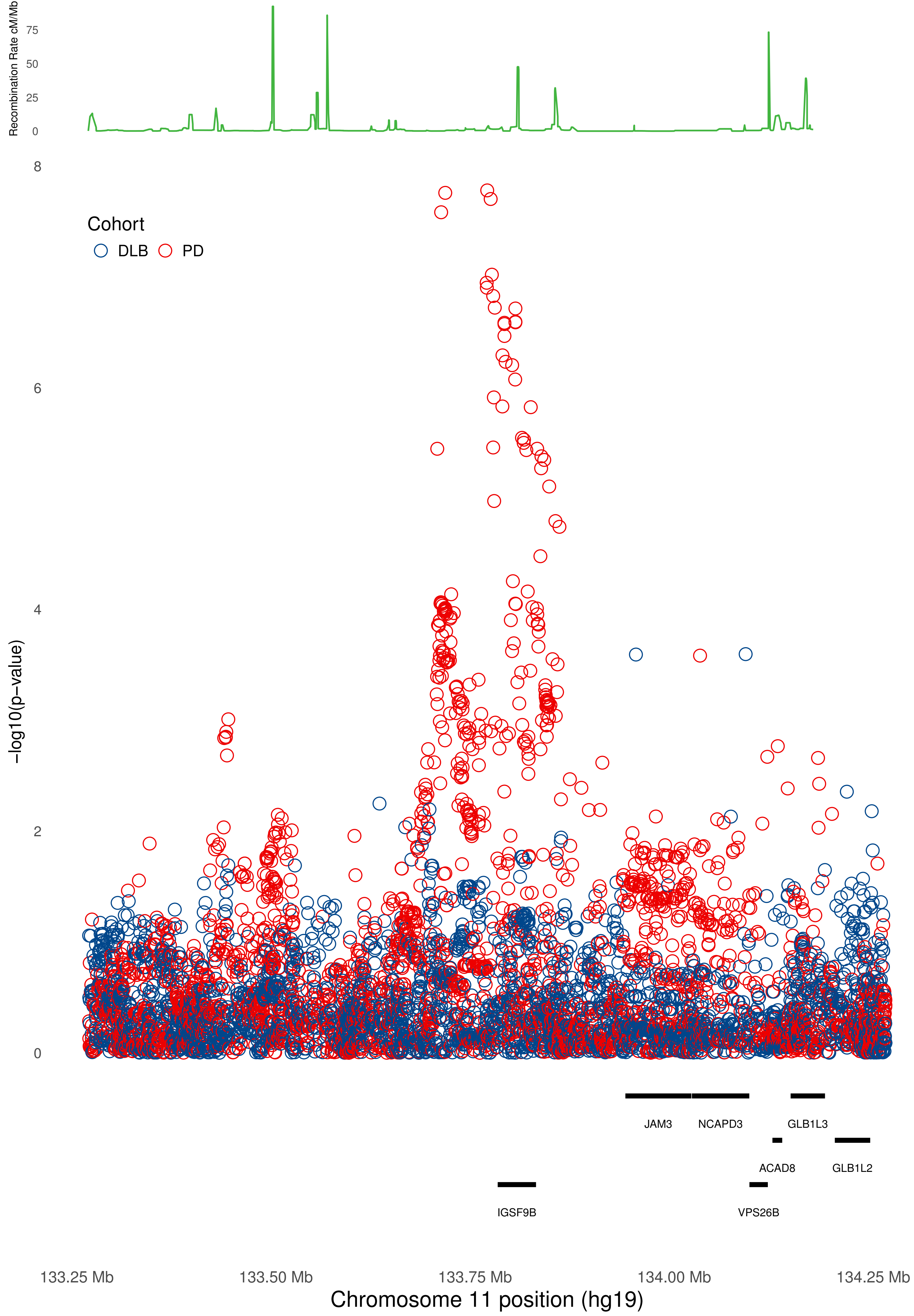
Recombination Rate cM/Mb
75
50
25
0
Cohort
○ DLB ○ PD
-log10(p-value)
8
6
4
2
0
JAM3
NCAPD3
GLB1L3
ACAD8
GLB1L2
IGSF9B
VPS26B
133.25 Mb
133.50 Mb
133.75 Mb
134.00 Mb
134.25 Mb
Chromosome 11 position (hg19)

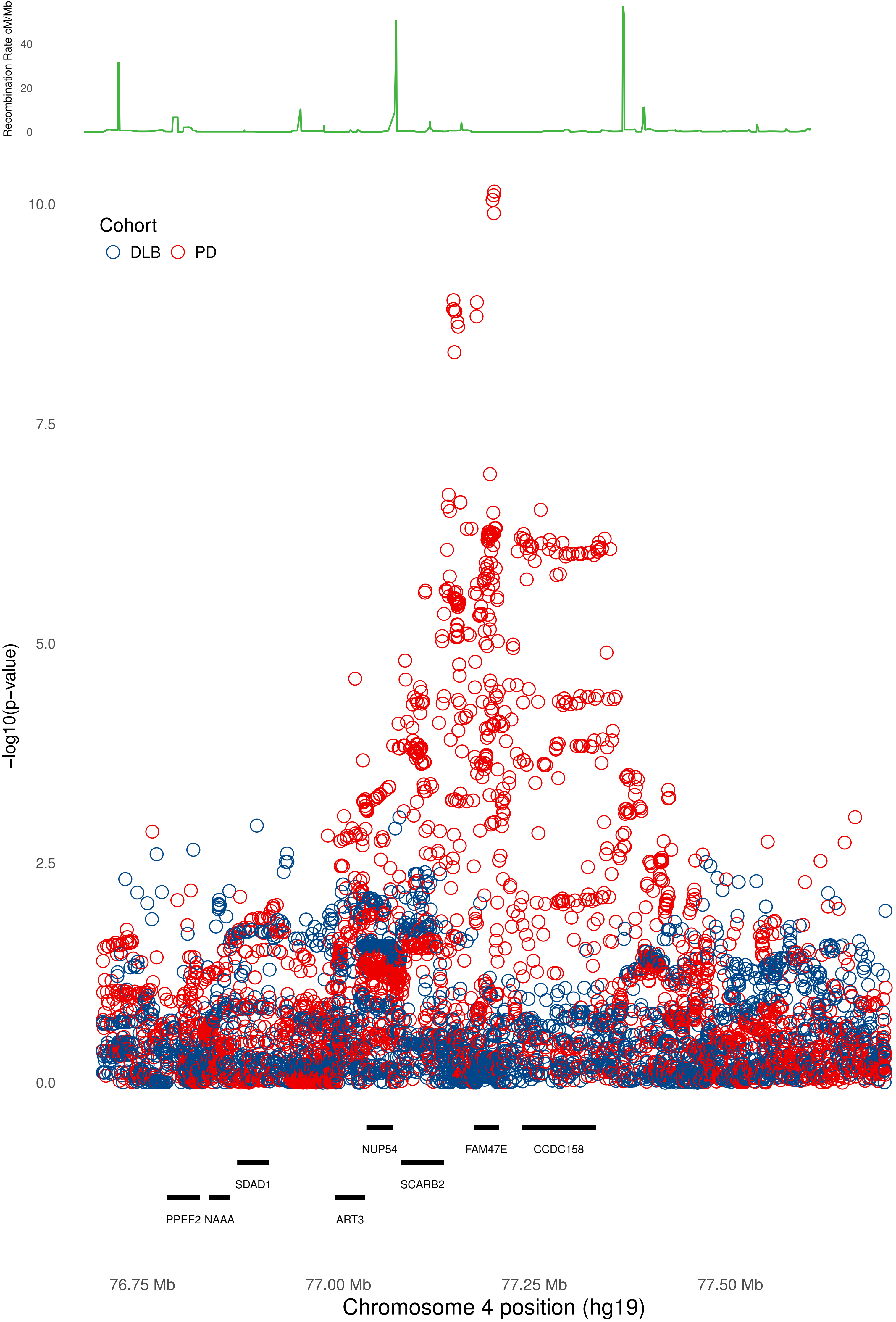
Recombination Rate cM/Mb
40
20
0
10.0
7.5
5.0
2.5
0.0
−log10(p−value)
Cohort
DLB
PD
NUP54
FAM47E
CCDC158
SDAD1
SCARB2
PPEF2
NAAA
ART3
76.75 Mb
77.00 Mb
77.25 Mb
77.50 Mb
Chromosome 4 position (hg19)

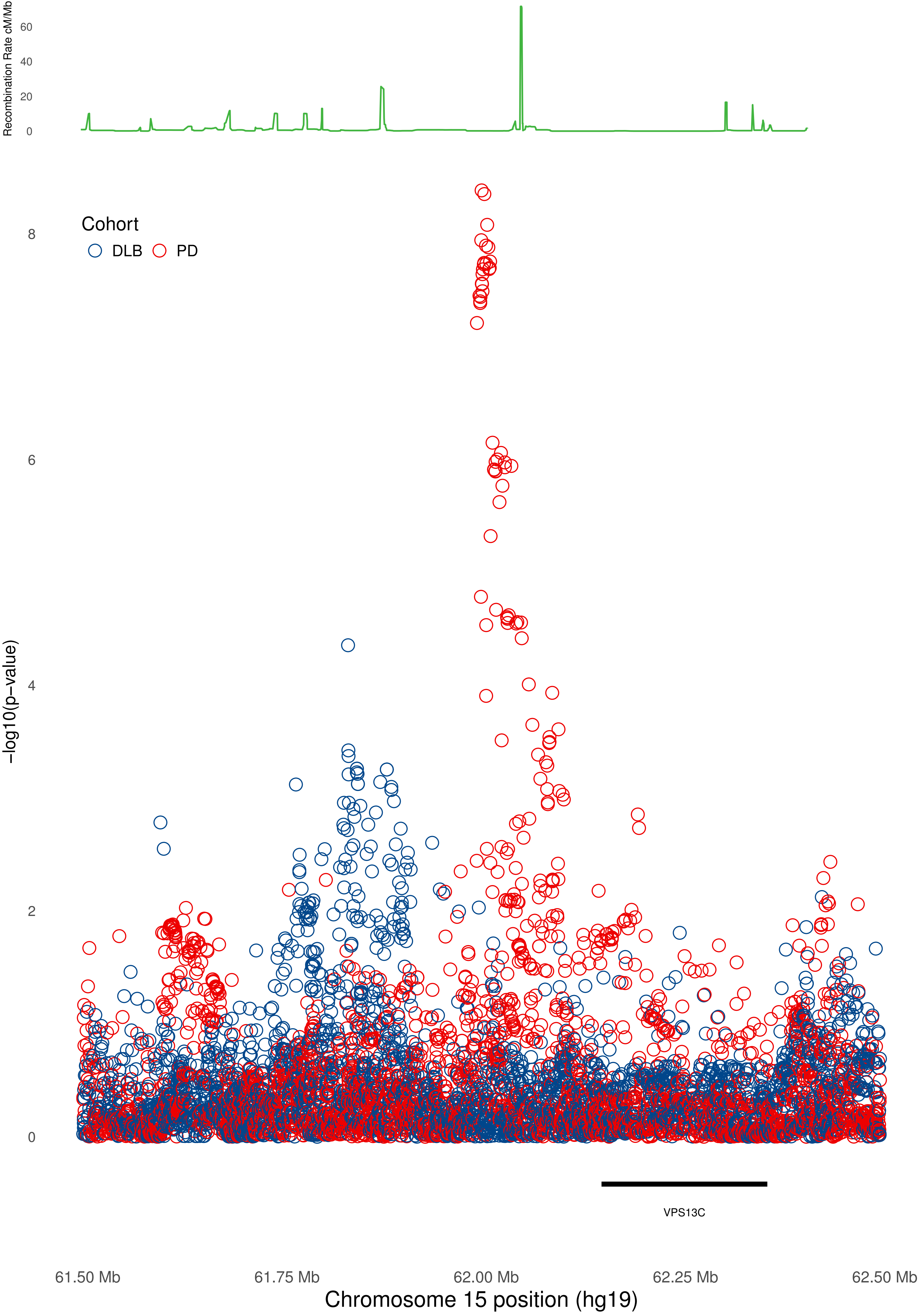
Recombination Rate cM/Mb
60
40
20
0
Cohort
DLB
PD
8
6
4
2
0
−log10(p−value)
VPS13C
61.50 Mb
61.75 Mb
62.00 Mb
62.25 Mb
62.50 Mb
Chromosome 15 position (hg19)

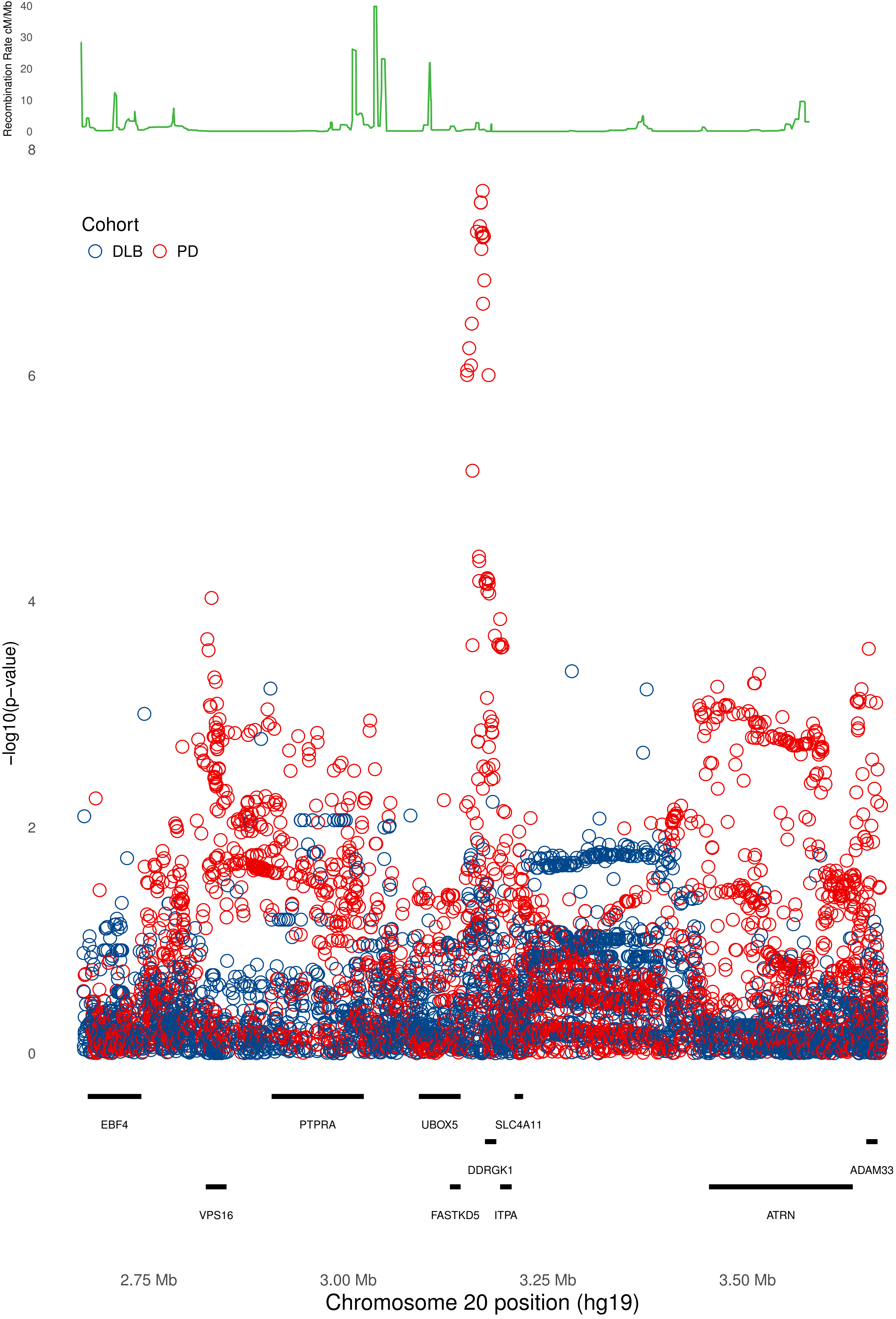
Recombination Rate cM/Mb
40
30
20
10
0
8
6
4
2
0
-log10(p-value)
Cohort
DLB
PD
EBF4
PTPRA
UBOX5
SLC4A11
DDRGK1
ADAM33
VPS16
FASTKD5
ITPA
ATRN
2.75 Mb
3.00 Mb
3.25 Mb
3.50 Mb
Chromosome 20 position (hg19)

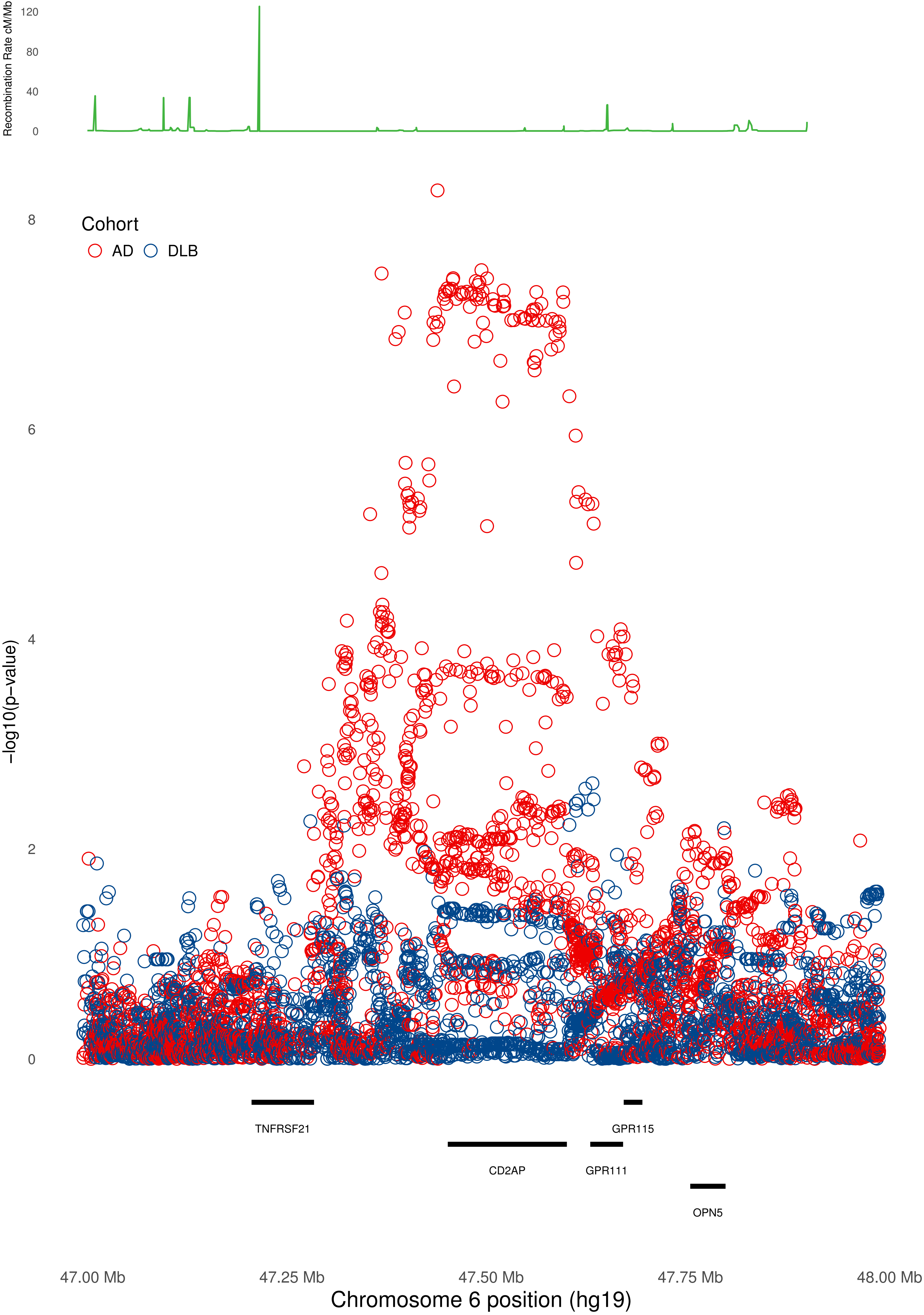
Recombination Rate cM/Mb
120
80
40
0
Cohort
AD
DLB
-log10(p-value)
8
6
4
2
0
TNFRSF21
GPR115
CD2AP
GPR111
OPN5
47.00 Mb
47.25 Mb
47.50 Mb
47.75 Mb
48.00 Mb
Chromosome 6 position (hg19)

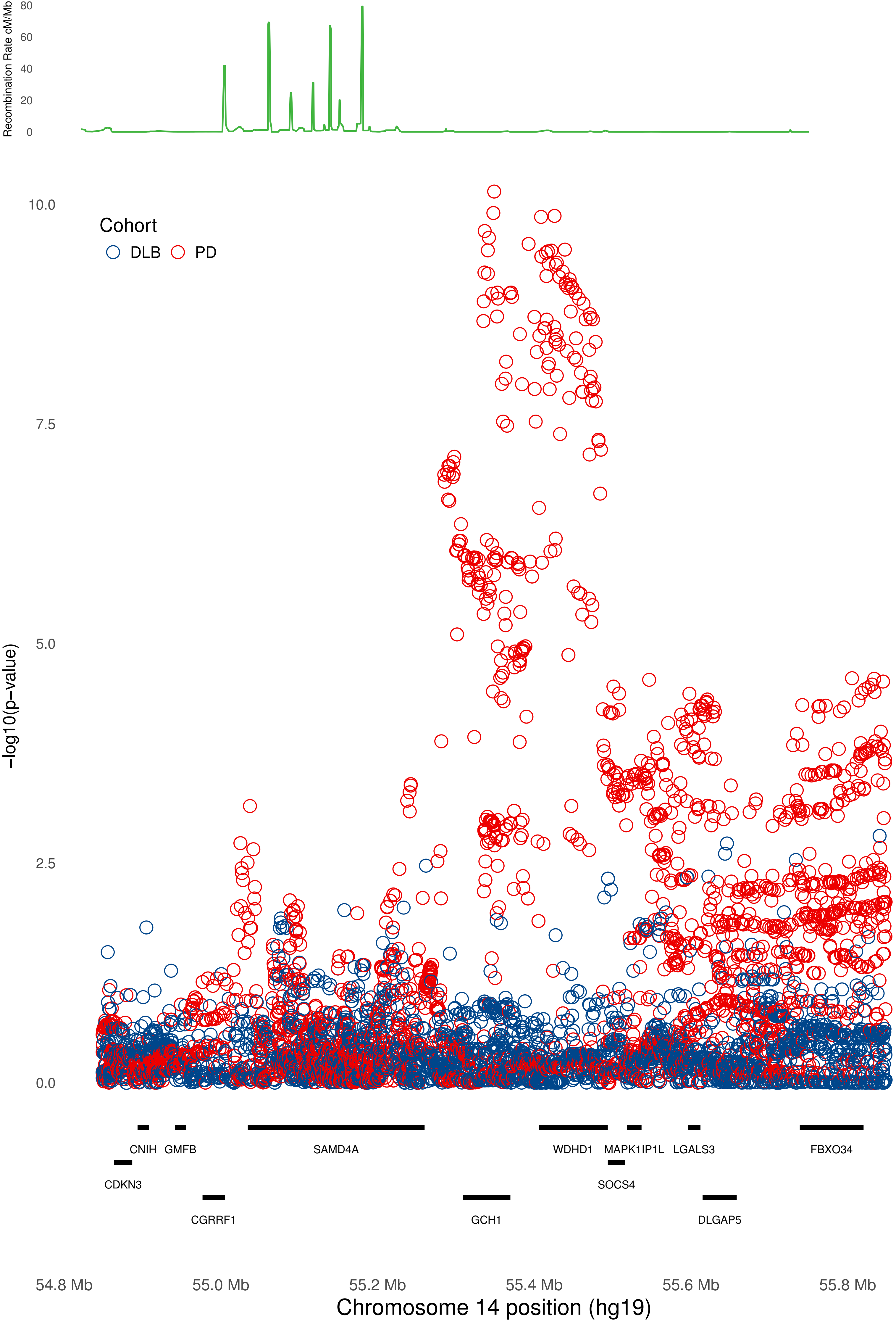
Recombination Rate cM/Mb
80
60
40
20
0
10.0
7.5
5.0
2.5
0.0
-log10(p-value)
Cohort
DLB
PD
CNIH
GMFB
SAMD4A
WDHD1
MAPK1IP1L
LGALS3
FBXO34
CDKN3
SOCS4
CGRRF1
GCH1
DLGAP5
54.8 Mb
55.0 Mb
55.2 Mb
55.4 Mb
55.6 Mb
55.8 Mb
Chromosome 14 position (hg19)

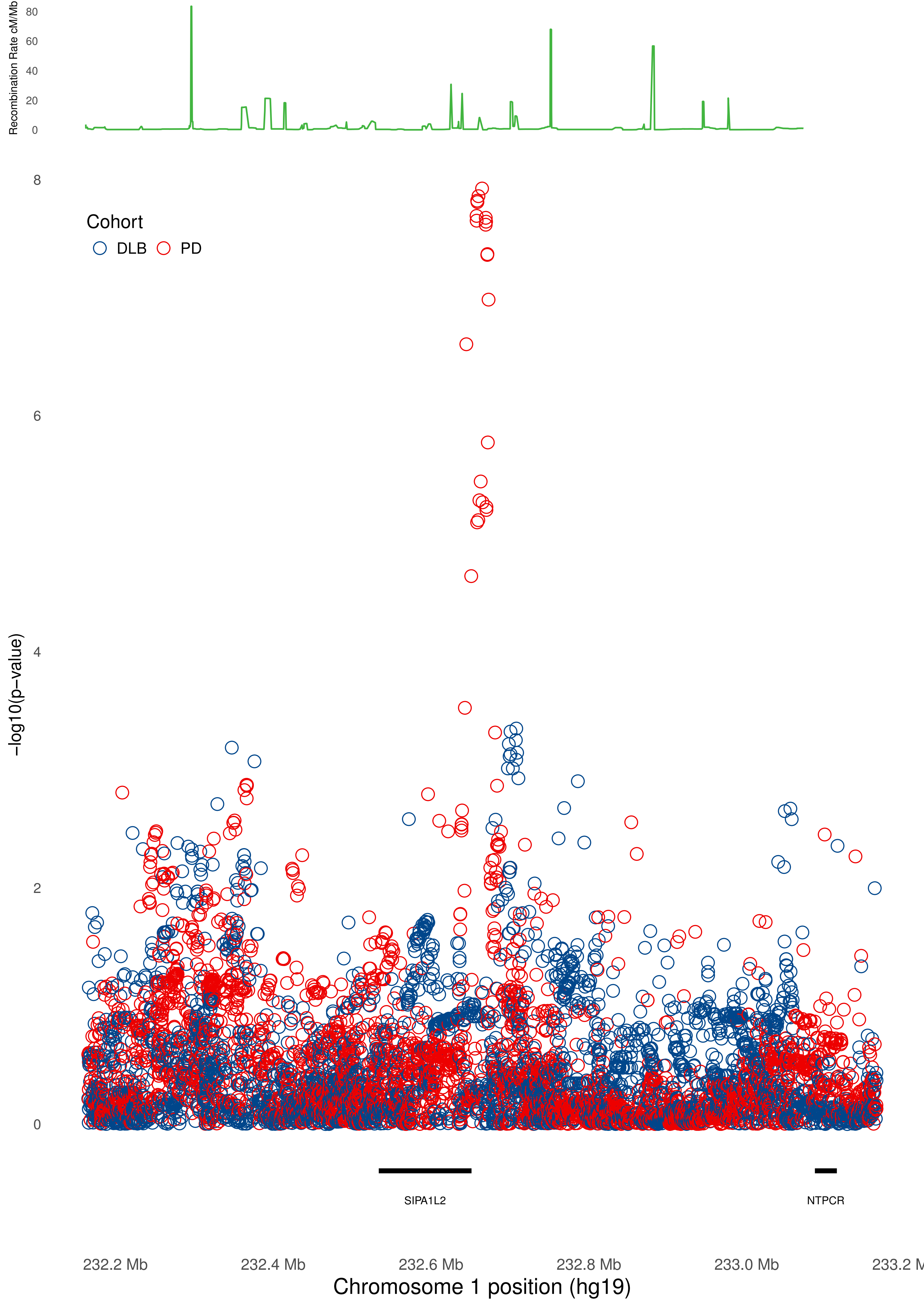
Recombination Rate cM/Mb
80
60
40
20
0
8
6
4
2
0
Cohort
DLB
PD
-log10(p-value)
SIPA1L2
NTPCR
232.2 Mb
232.4 Mb
232.6 Mb
232.8 Mb
233.0 Mb
233.2 M
Chromosome 1 position (hg19)

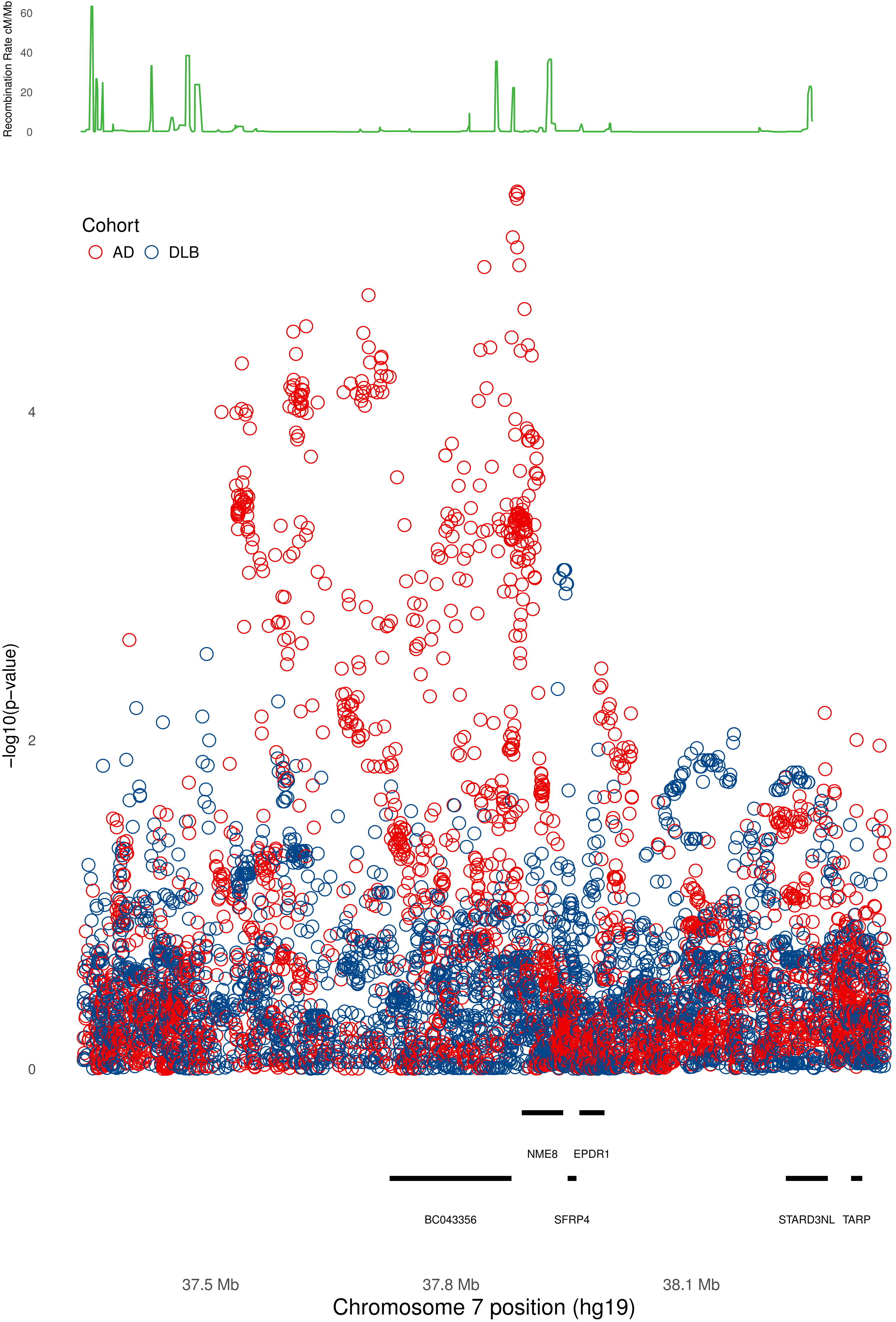
Recombination Rate cM/Mb
60
40
20
0
Cohort
AD
DLB
4
2
0
−log10(p−value)
NME8
EPDR1
BC043356
SFRP4
STARD3NL
TARP
37.5 Mb
37.8 Mb
38.1 Mb
Chromosome 7 position (hg19)

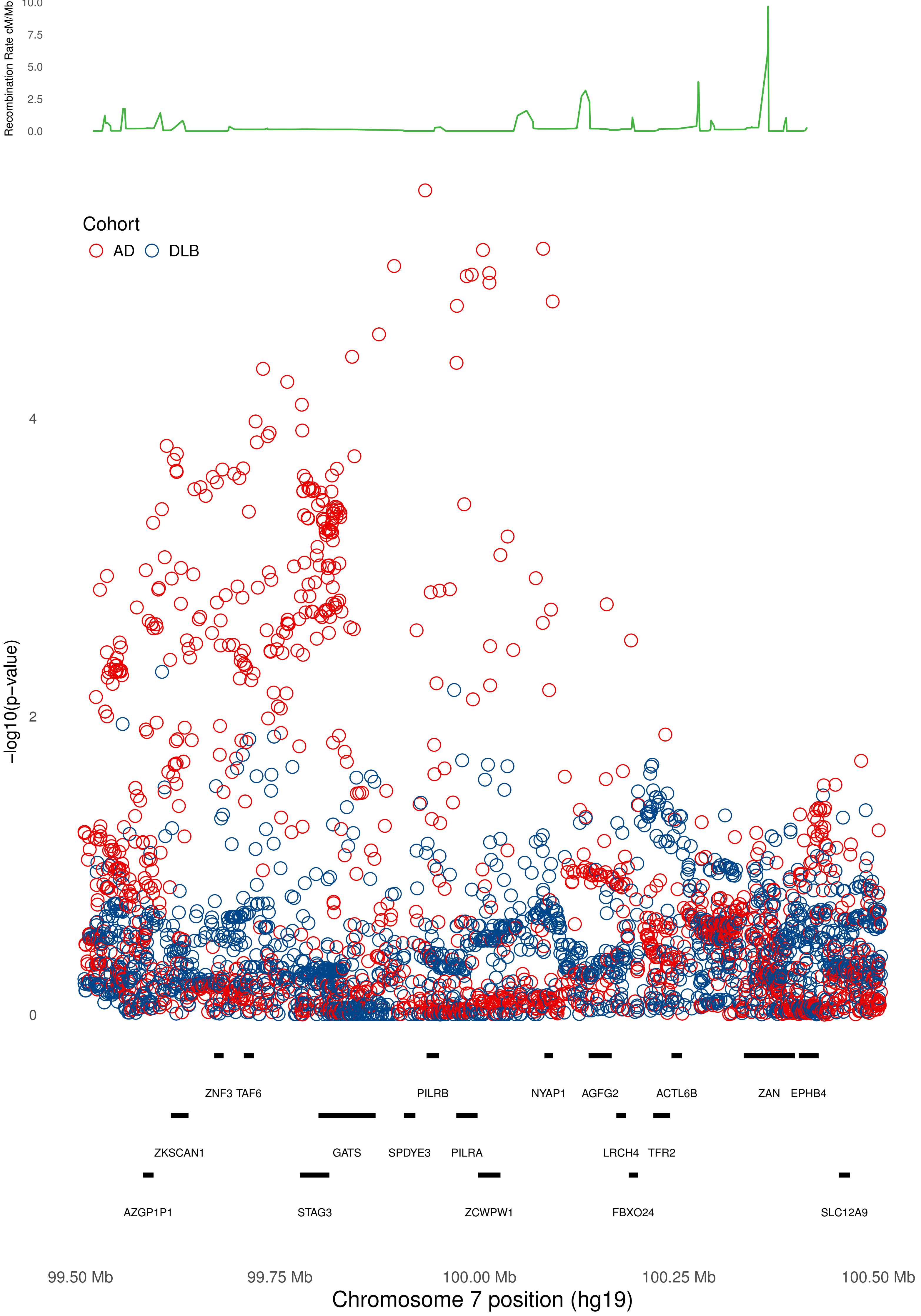
Recombination Rate cM/Mb
10.0
7.5
5.0
2.5
0.0
Cohort
AD
DLB
−log10(p−value)
4
2
0
ZNF3
TAF6
PILRB
NYAP1
AGFG2
ACTL6B
ZAN
EPHB4
ZKSCAN1
GATS
SPDYE3
PILRA
LRCH4
TFR2
AZGP1P1
STAG3
ZCWPW1
FBXO24
SLC12A9
99.50 Mb
99.75 Mb
100.00 Mb
100.25 Mb
100.50 Mb
Chromosome 7 position (hg19)

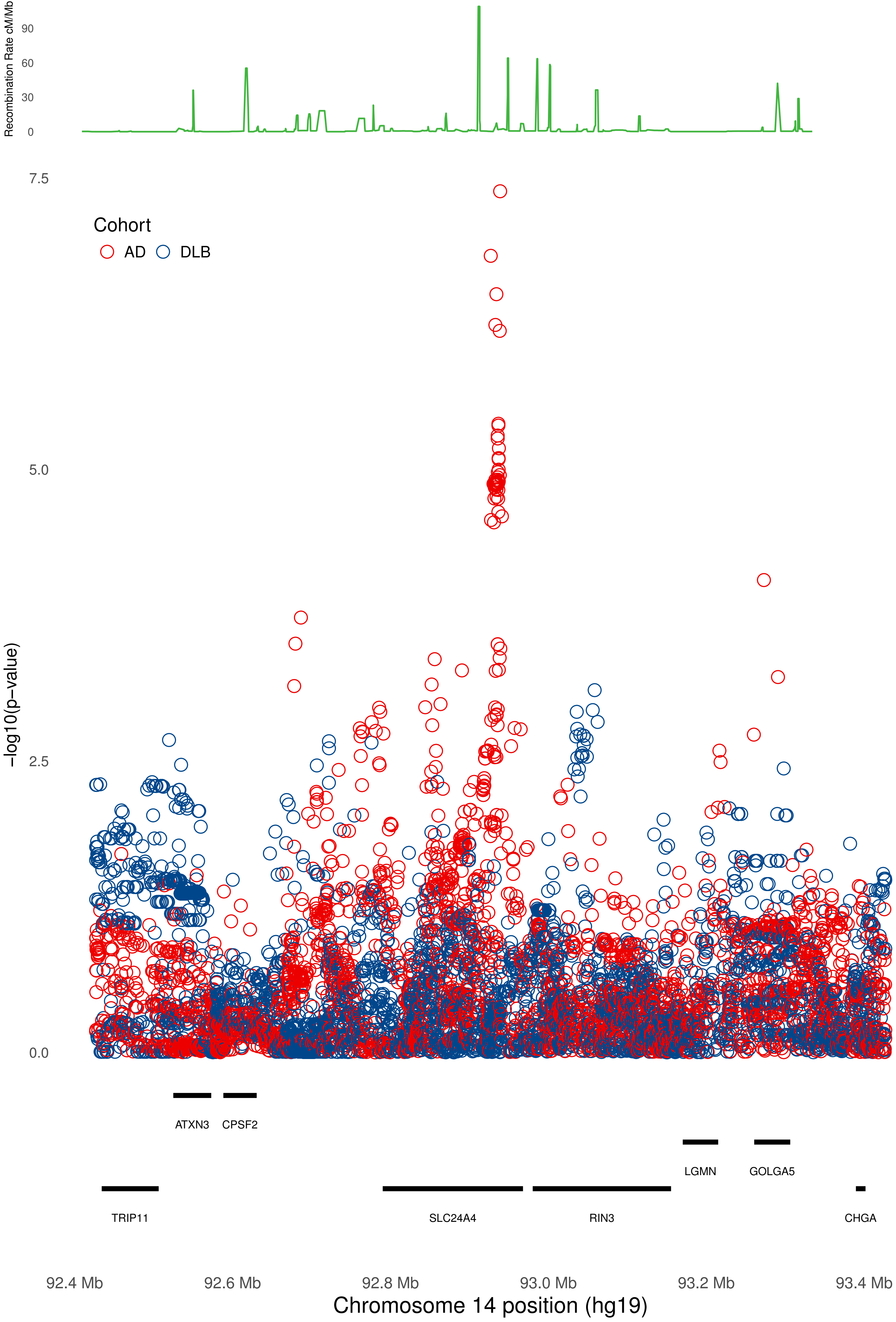
Recombination Rate cM/Mb
90
60
30
0
7.5
5.0
2.5
0.0
-log10(p-value)
Cohort
AD
DLB
ATXN3
CPSF2
LGMN
GOLGA5
TRIP11
SLC24A4
RIN3
CHGA
92.4 Mb
92.6 Mb
92.8 Mb
93.0 Mb
93.2 Mb
93.4 Mb
Chromosome 14 position (hg19)

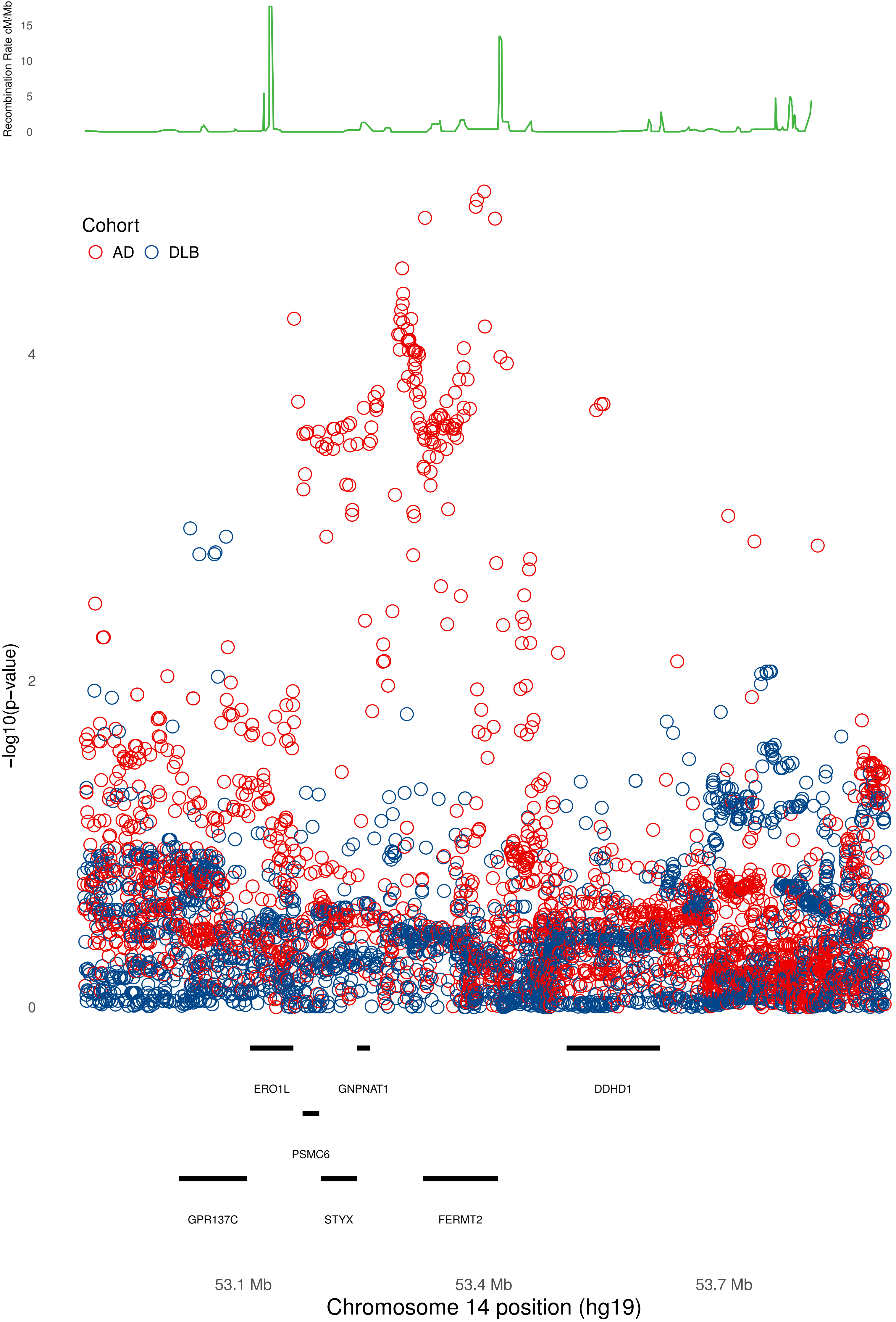

Recombination Rate cM/Mb
15
10
5
0
Cohort
AD
DLB
−log10(p−value)
4
2
0
ERO1L
GNPNAT1
DDHD1
PSMC6
GPR137C
STYX
FERMT2
53.1 Mb
53.4 Mb
53.7 Mb
Chromosome 14 position (hg19)

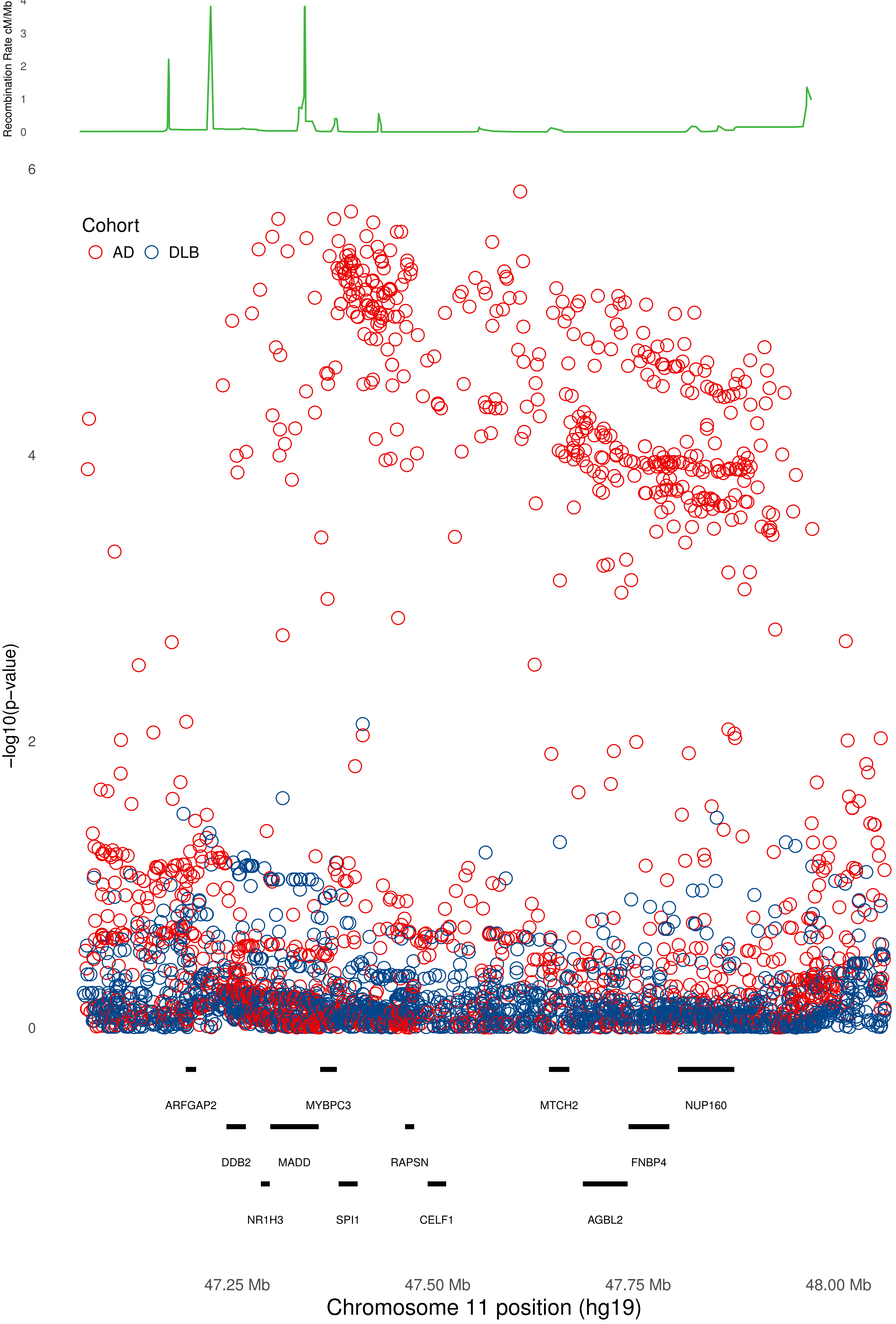
Recombination Rate cM/Mb
4
3
2
1
0
6
Cohort
AD
DLB
4
2
0
-log10(p-value)
ARFGAP2
MYBPC3
MTCH2
NUP160
DDB2
MADD
RAPSN
FNBP4
NR1H3
SPI1
CELF1
AGBL2
47.25 Mb
47.50 Mb
47.75 Mb
48.00 Mb
Chromosome 11 position (hg19)

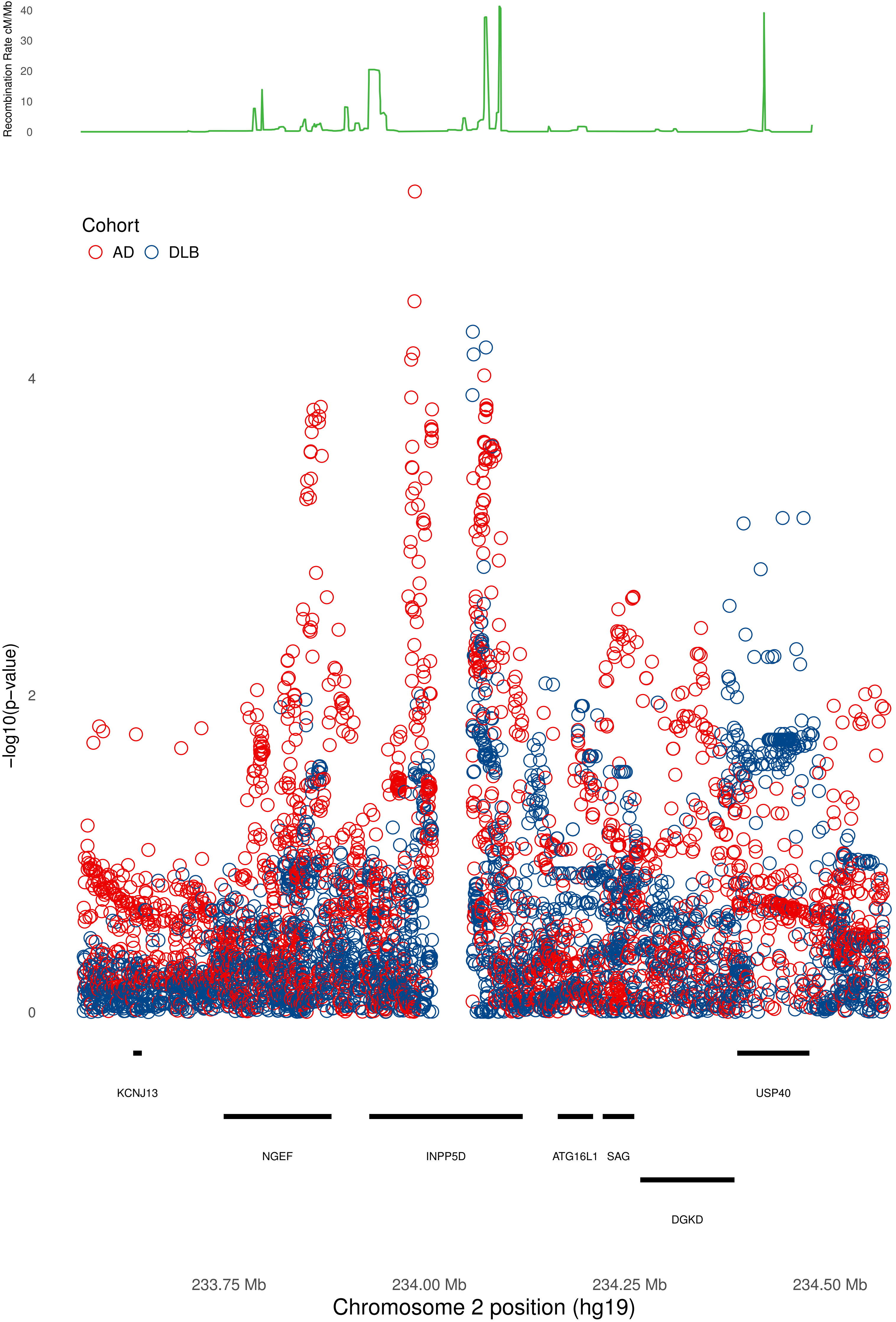
Recombination Rate cM/Mb
40
30
20
10
0
Cohort
AD
DLB
4
2
0
-log10(p-value)
KCNJ13
USP40
NGEF
INPP5D
ATG16L1
SAG
DGKD
233.75 Mb
234.00 Mb
234.25 Mb
234.50 Mb
Chromosome 2 position (hg19)

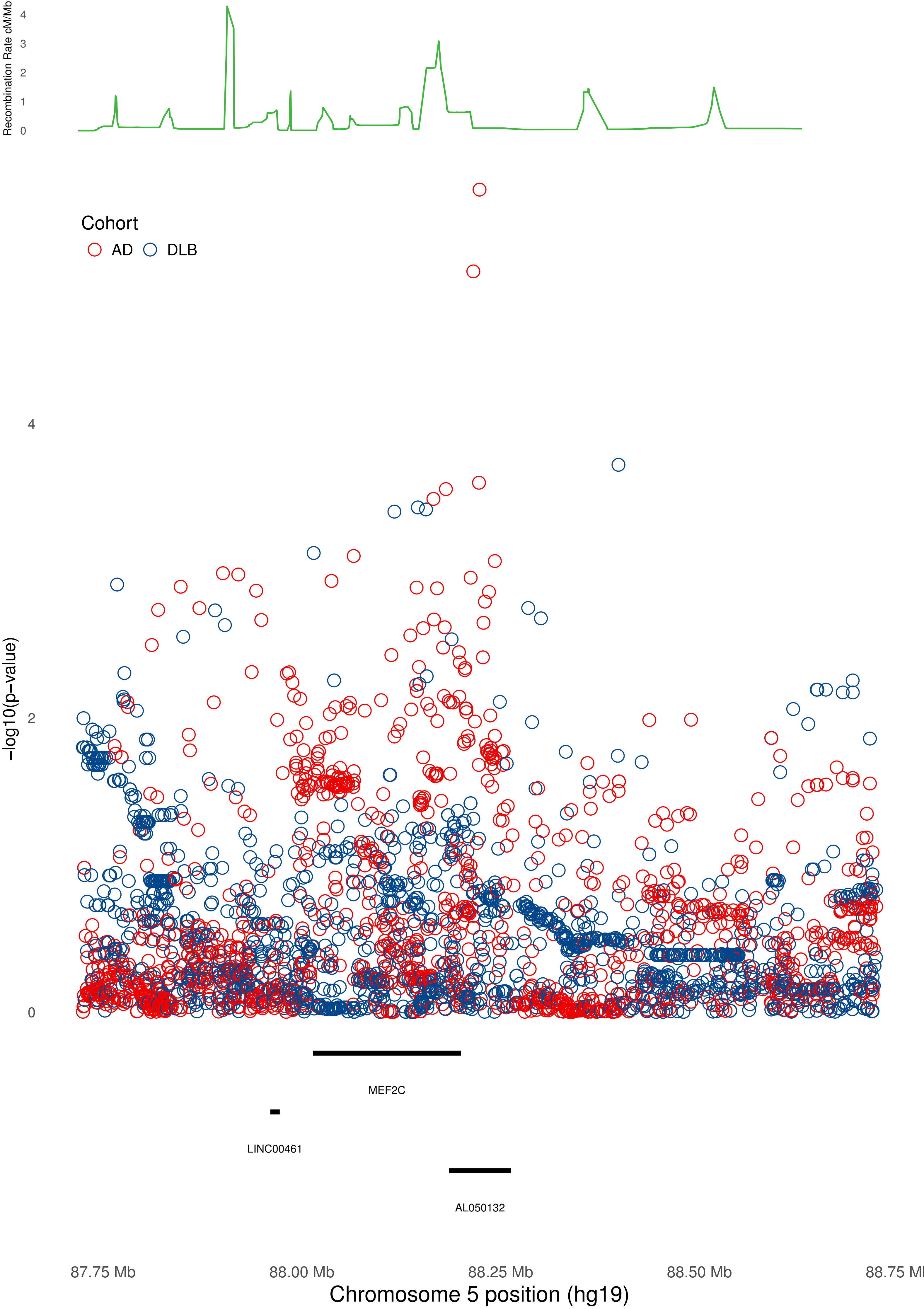
Recombination Rate cM/Mb
4
3
2
1
0
Cohort
AD
DLB
4
2
0
-log10(p-value)
MEF2C
LINC00461
AL050132
87.75 Mb
88.00 Mb
88.25 Mb
88.50 Mb
88.75 Mb
Chromosome 5 position (hg19)

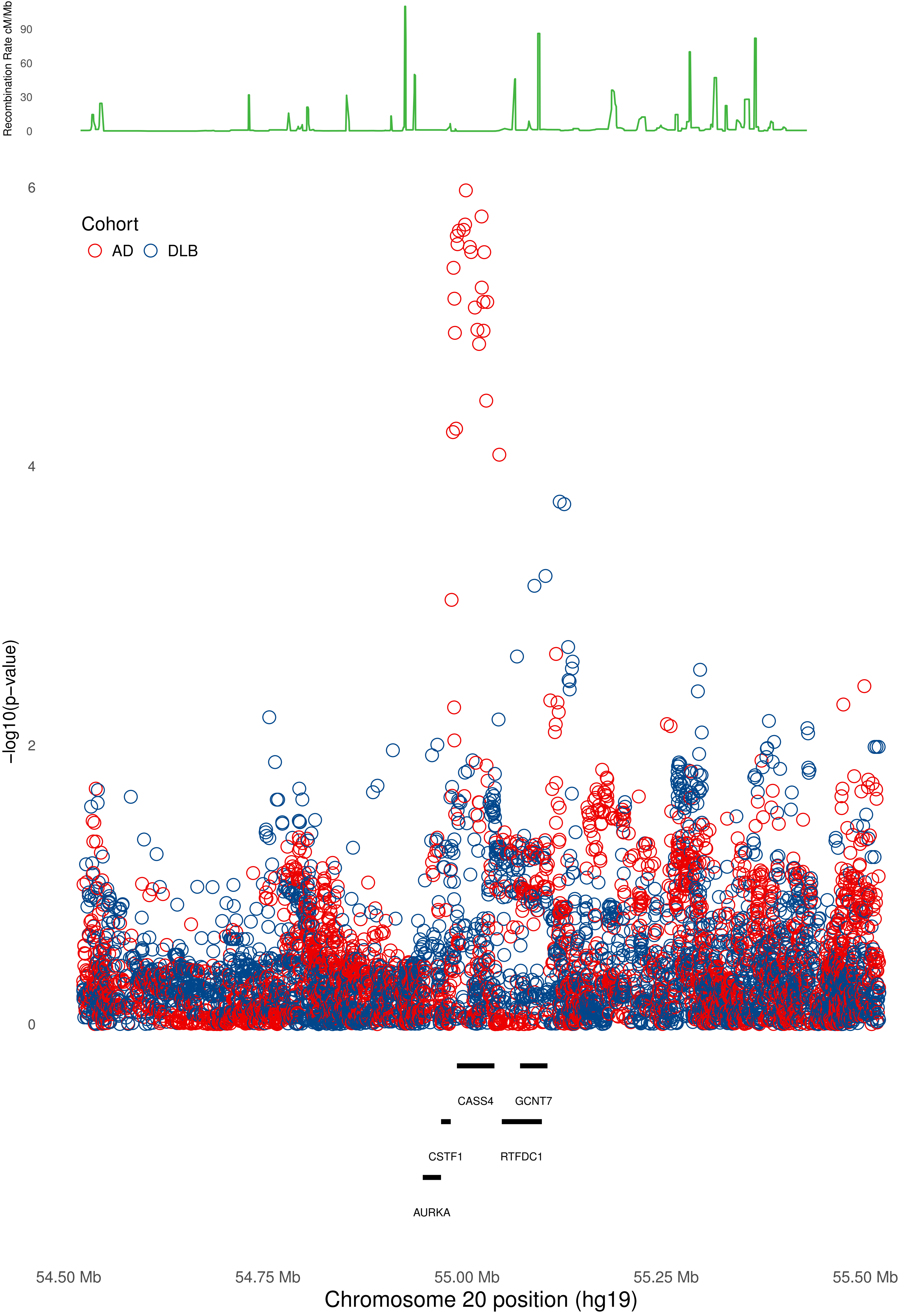
Recombination Rate cM/Mb
90
60
30
0
6
4
2
0
Cohort
AD
DLB
-log10(p-value)
CASS4
GCNT7
CSTF1
RTFDC1
AURKA
54.50 Mb
54.75 Mb
55.00 Mb
55.25 Mb
55.50 Mb
Chromosome 20 position (hg19)

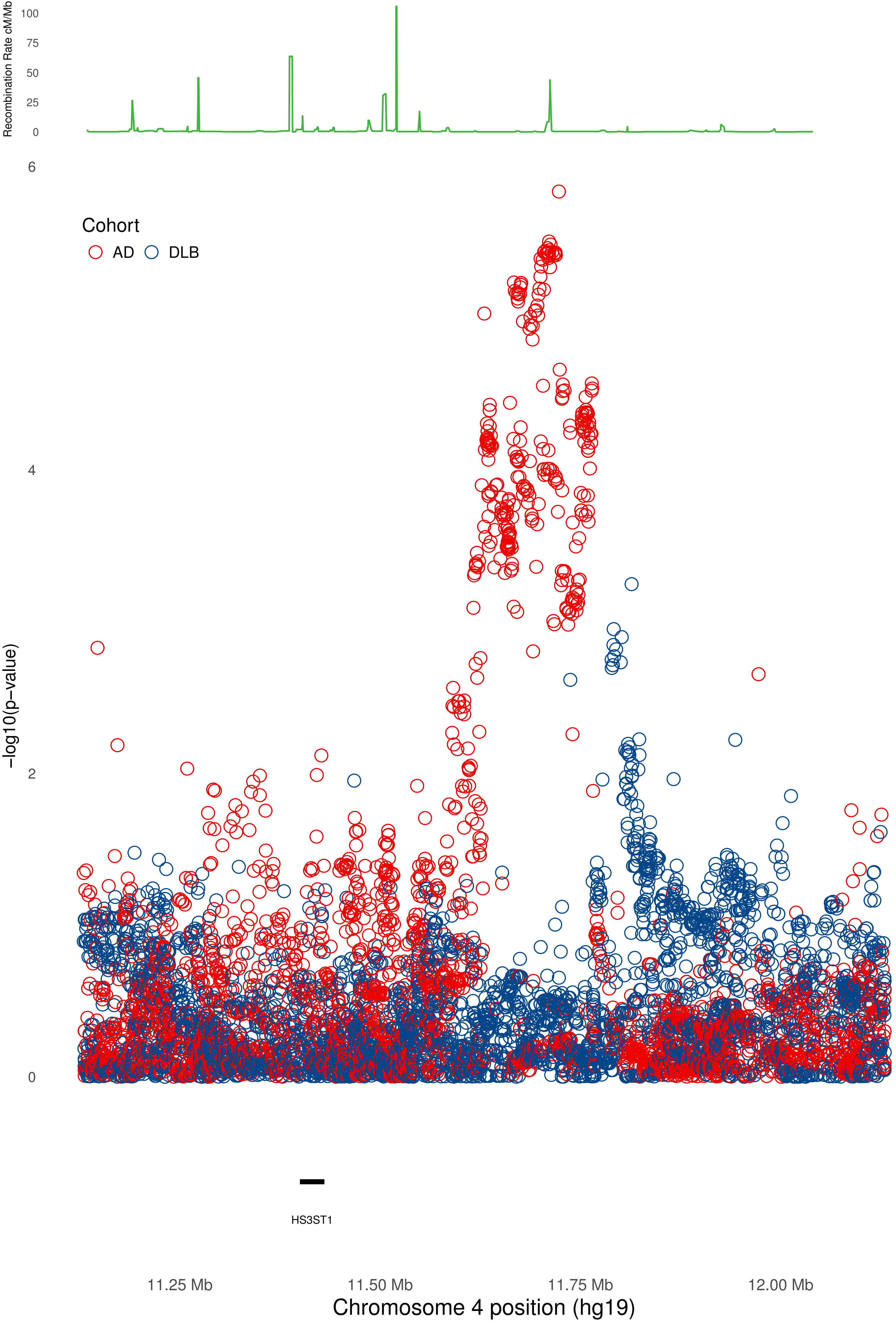
Recombination Rate cM/Mb
100
75
50
25
0
Cohort
AD
DLB
−log10(p−value)
6
4
2
0
HS3ST1
11.25 Mb
11.50 Mb
11.75 Mb
12.00 Mb
Chromosome 4 position (hg19)

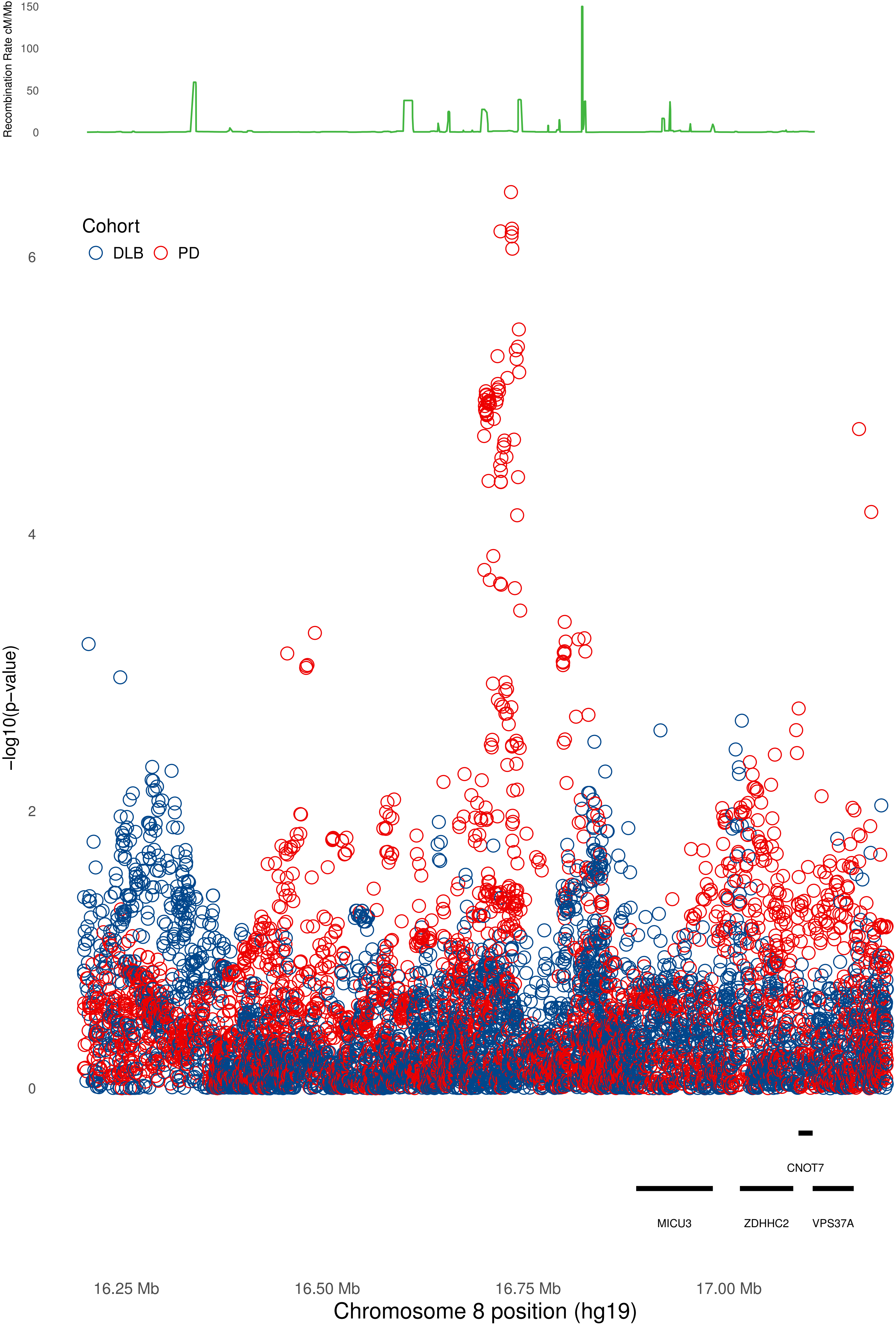
Recombination Rate cM/Mb
150
100
50
0
Cohort
DLB
PD
-log10(p-value)
6
4
2
0
CNOT7
MICU3
ZDHHC2
VPS37A
16.25 Mb
16.50 Mb
16.75 Mb
17.00 Mb
Chromosome 8 position (hg19)

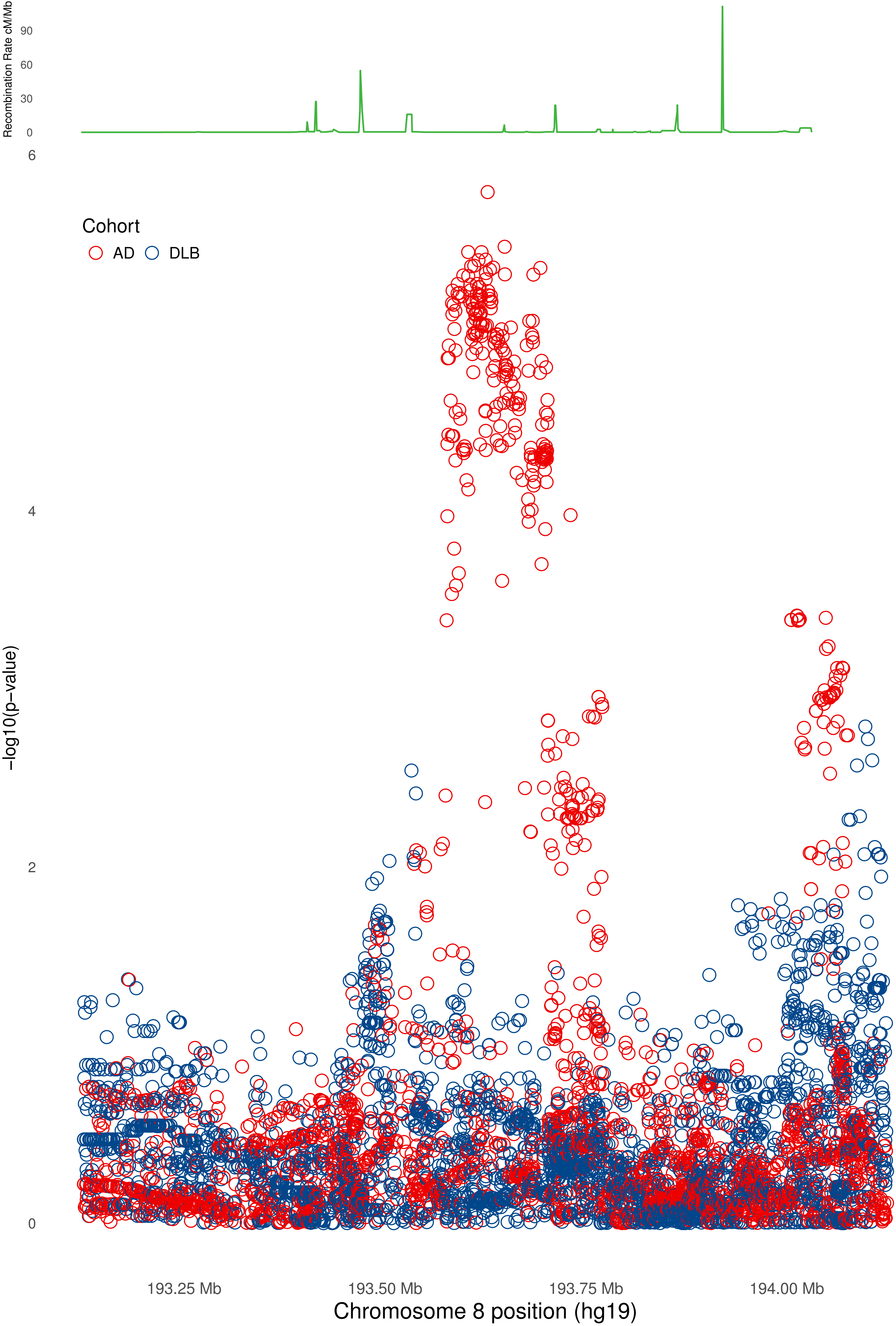
Recombination Rate cM/Mb
90
60
30
0
6
4
2
0
Cohort
AD
DLB
-log10(p-value)
193.25 Mb
193.50 Mb
193.75 Mb
194.00 Mb
Chromosome 8 position (hg19)

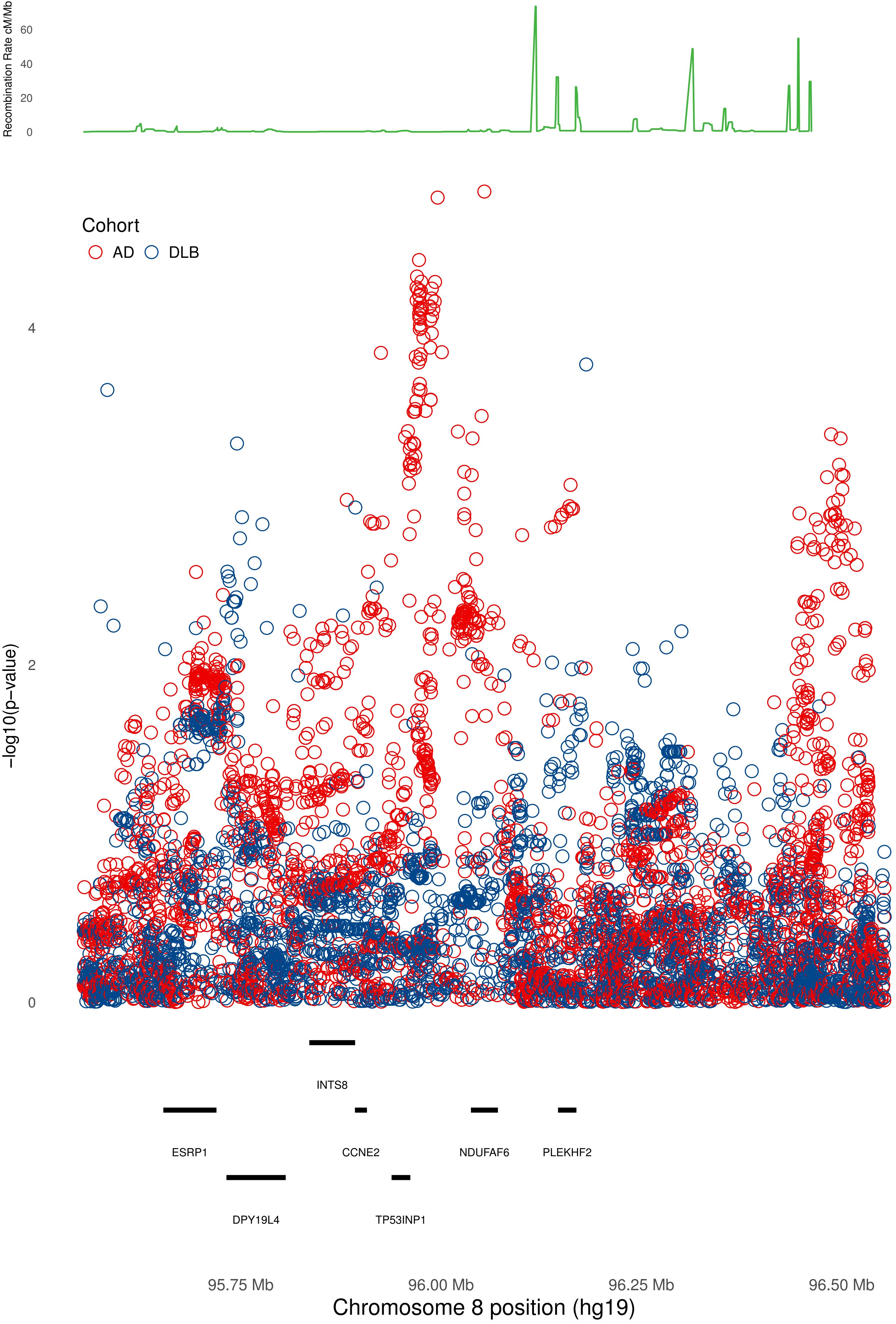
Recombination Rate cM/Mb
60
40
20
0
Cohort
AD
DLB
4
2
0
-log10(p-value)
INTS8
ESRP1
CCNE2
NDUFAF6
PLEKHF2
DPY19L4
TP53INP1
95.75 Mb
96.00 Mb
96.25 Mb
96.50 Mb
Chromosome 8 position (hg19)

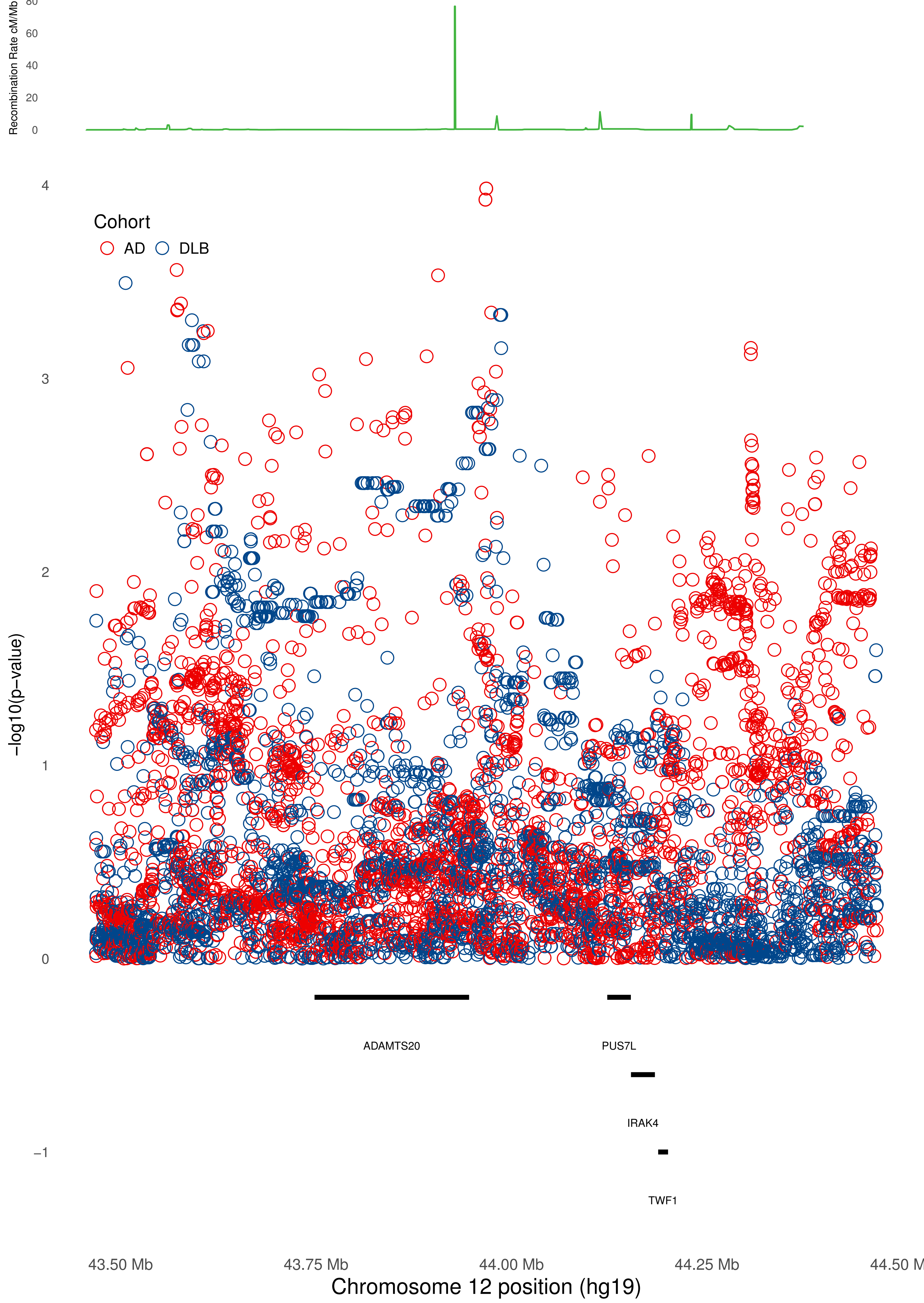
Recombination Rate cM/Mb
80
60
40
20
0
4
3
2
1
0
−1
−log10(p−value)
Cohort
○ AD ○ DLB
ADAMTS20
PUS7L
IRAK4
TWF1
43.50 Mb
43.75 Mb
44.00 Mb
44.25 Mb
44.50 M
Chromosome 12 position (hg19)

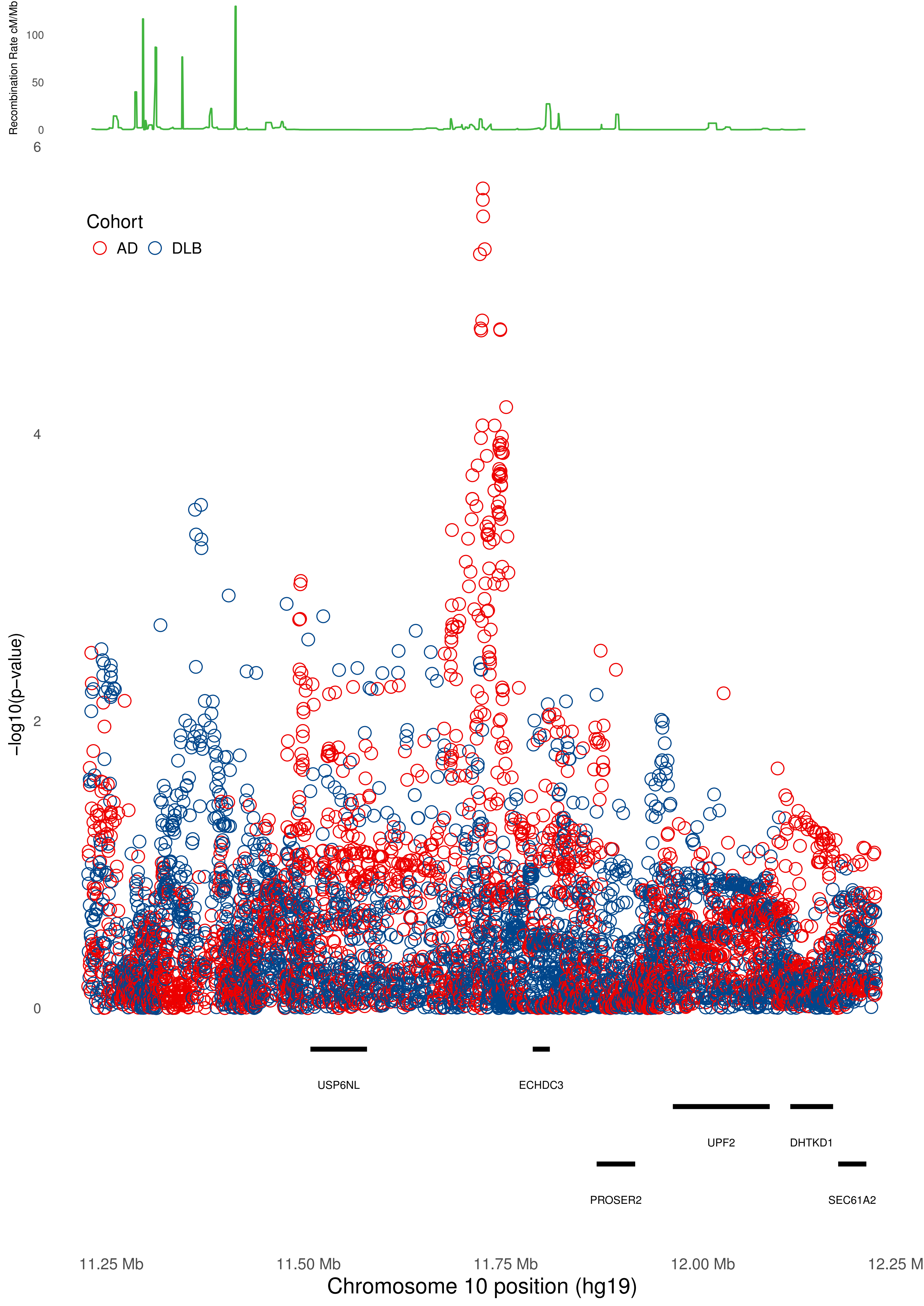
Recombination Rate cM/Mb
100
50
0
6
4
2
0
−log10(p−value)
Cohort
○ AD ○ DLB
USP6NL
ECHDC3
UPF2
DHTKD1
PROSER2
SEC61A2
11.25 Mb
11.50 Mb
11.75 Mb
12.00 Mb
12.25 Mb
Chromosome 10 position (hg19)

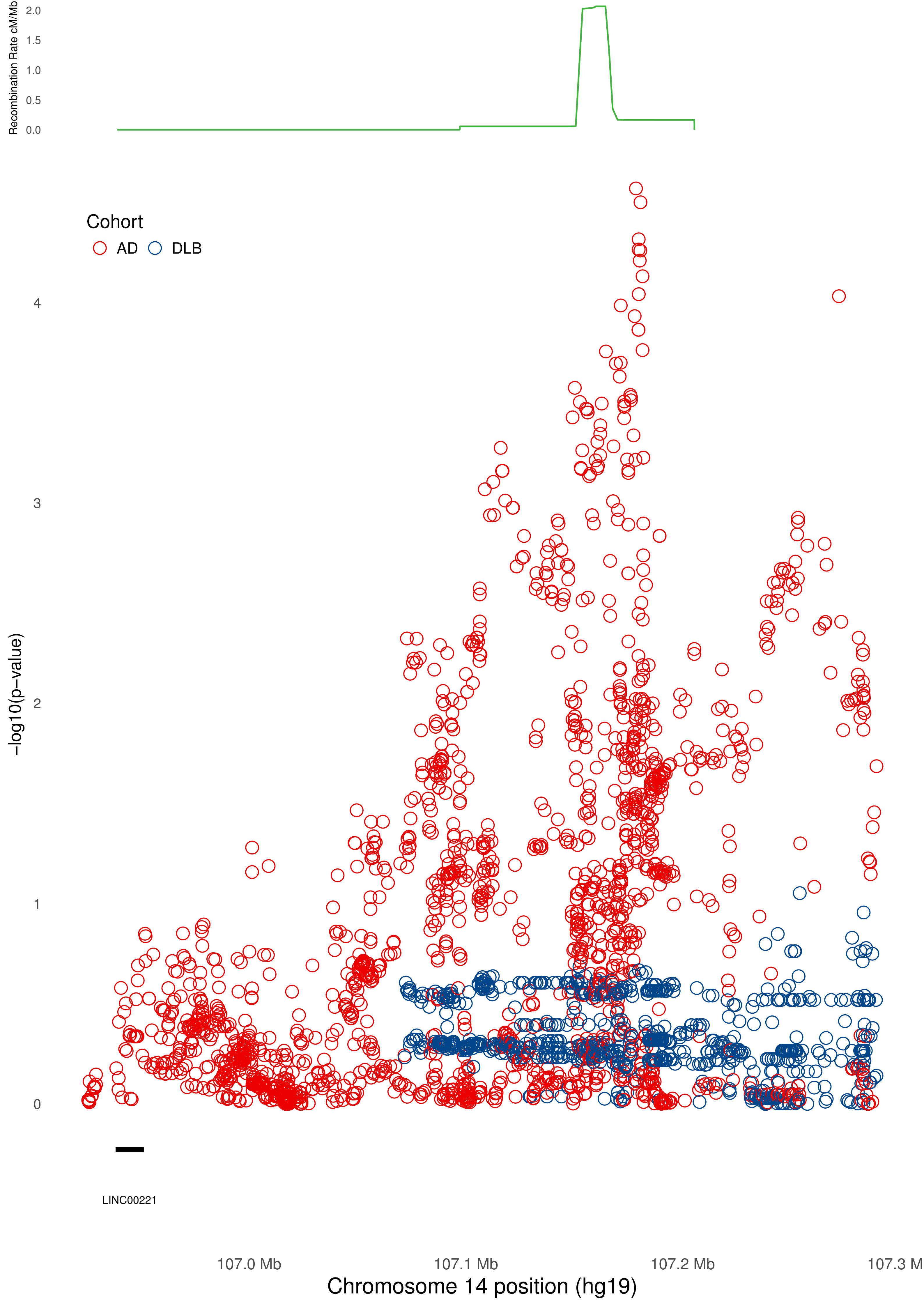
Recombination Rate cM/Mb
2.0
1.5
1.0
0.5
0.0
Cohort
AD
DLB
-log10(p-value)
4
3
2
1
0
LINC00221
107.0 Mb
107.1 Mb
107.2 Mb
107.3 M
Chromosome 14 position (hg19)

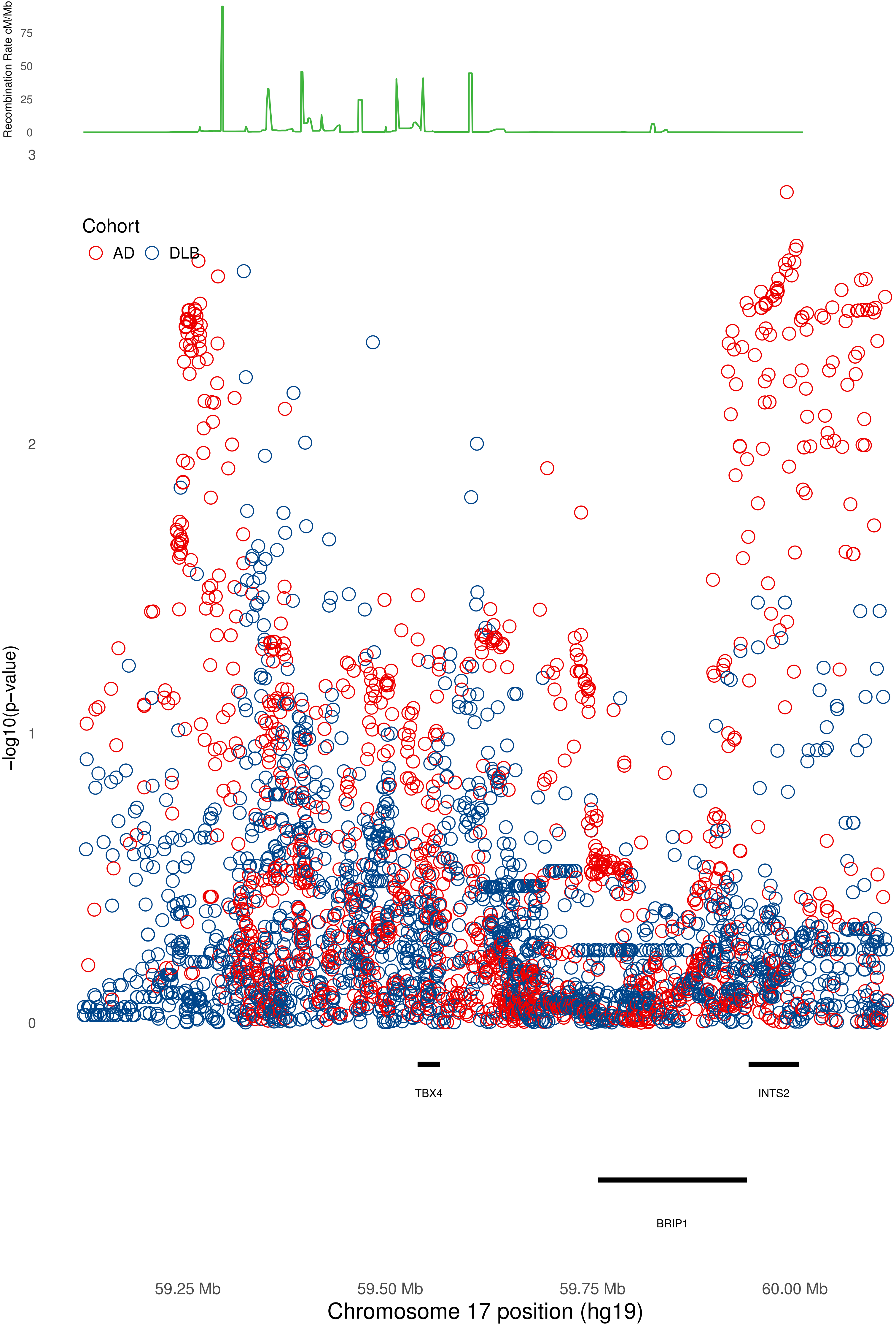
Recombination Rate cM/Mb
75
50
25
0
3
2
1
0
Cohort
AD
DLB
-log10(p-value)
TBX4
INTS2
BRIP1
59.25 Mb
59.50 Mb
59.75 Mb
60.00 Mb
Chromosome 17 position (hg19)

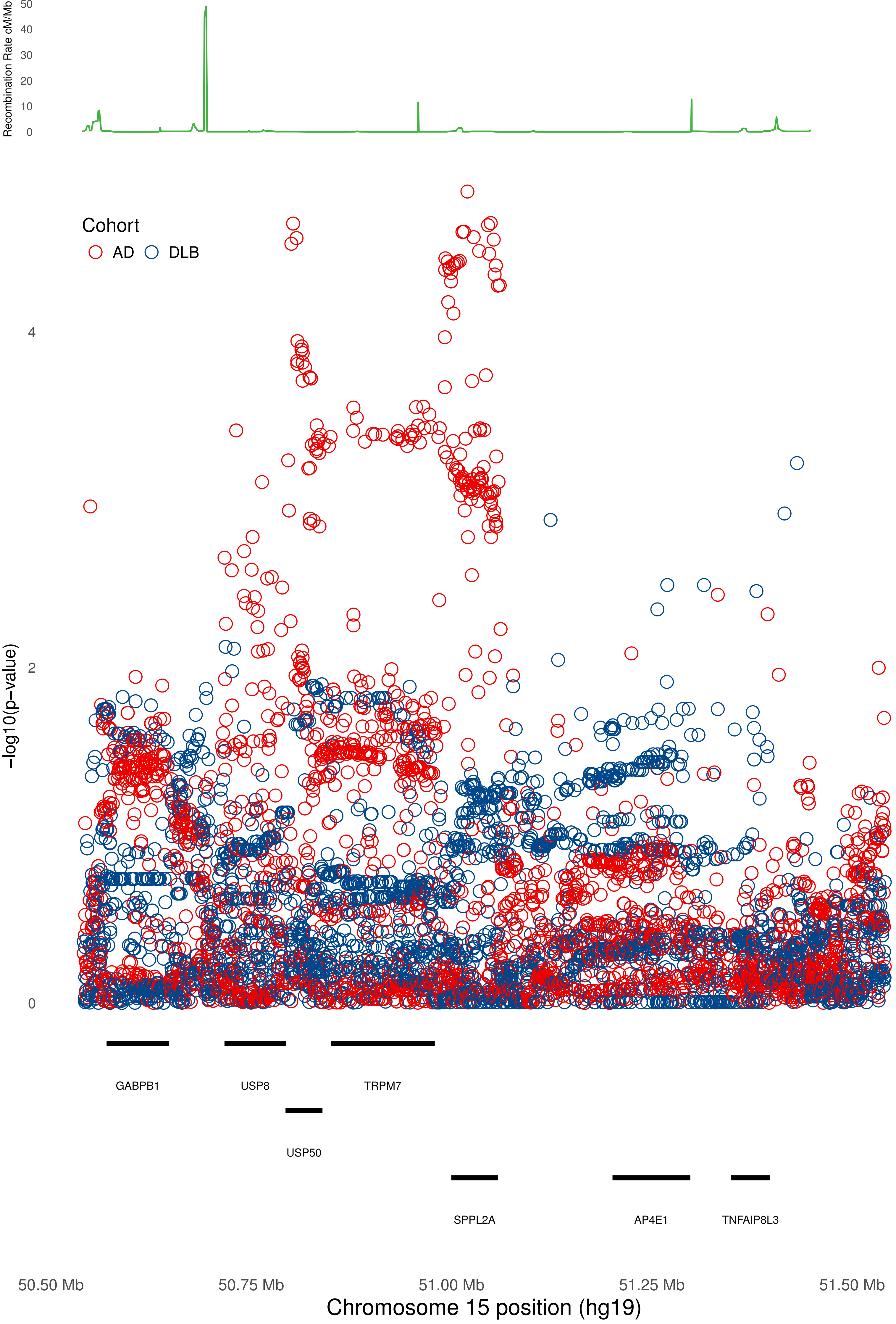
Recombination Rate cM/Mb
50
40
30
20
10
0
Cohort
AD
DLB
−log10(p−value)
4
2
0
GABPB1
USP8
TRPM7
USP50
SPPL2A
AP4E1
TNFAIP8L3
50.50 Mb
50.75 Mb
51.00 Mb
51.25 Mb
51.50 Mb
Chromosome 15 position (hg19)

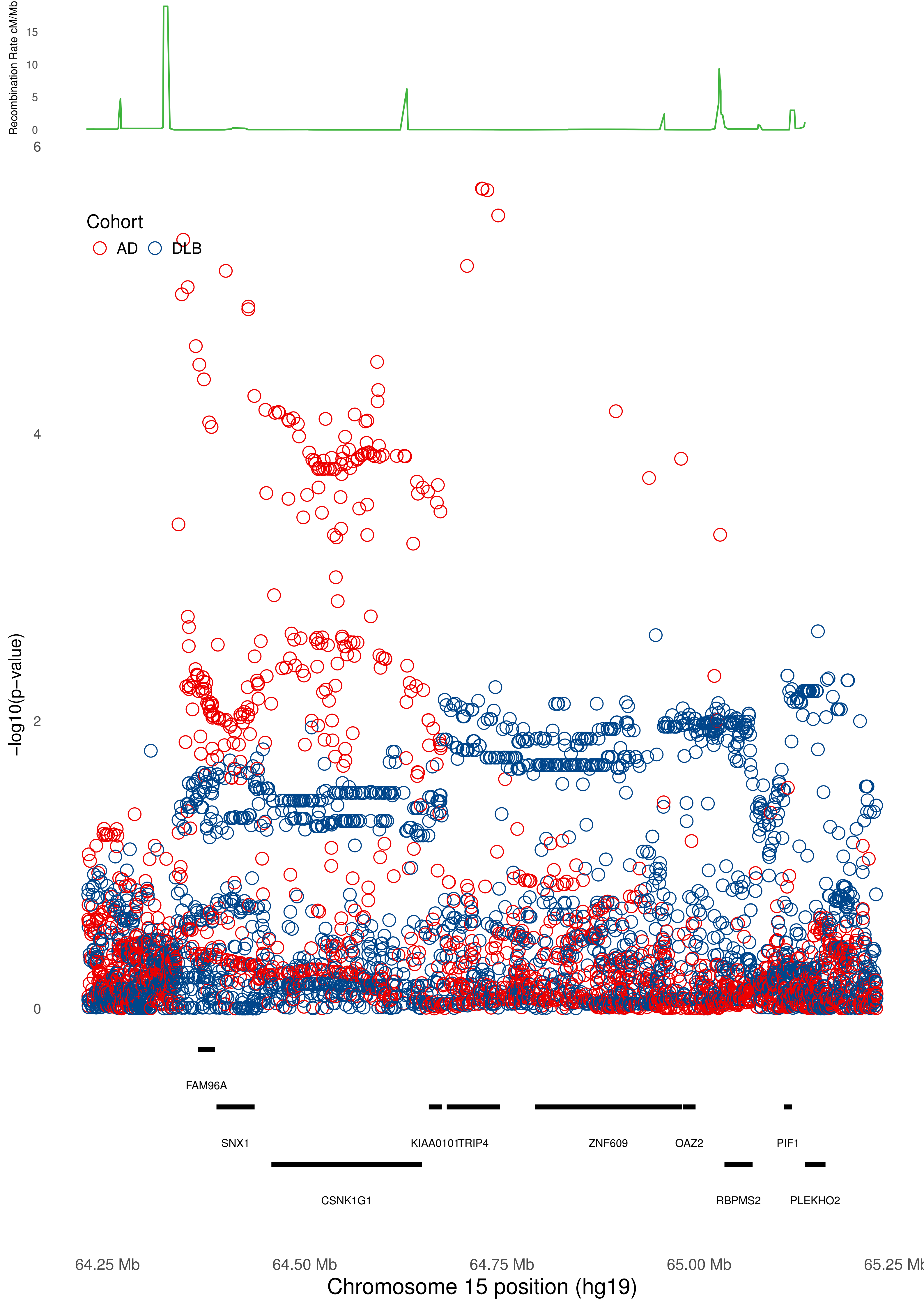
Recombination Rate cM/Mb
15
10
5
0
Cohort
AD
DLB
-log10(p-value)
6
4
2
0
FAM96A
SNX1
KIAA0101
TRIP4
ZNF609
OAZ2
PIF1
CSNK1G1
RBPMS2
PLEKHO2
64.25 Mb
64.50 Mb
64.75 Mb
65.00 Mb
65.25 Mb
Chromosome 15 position (hg19)

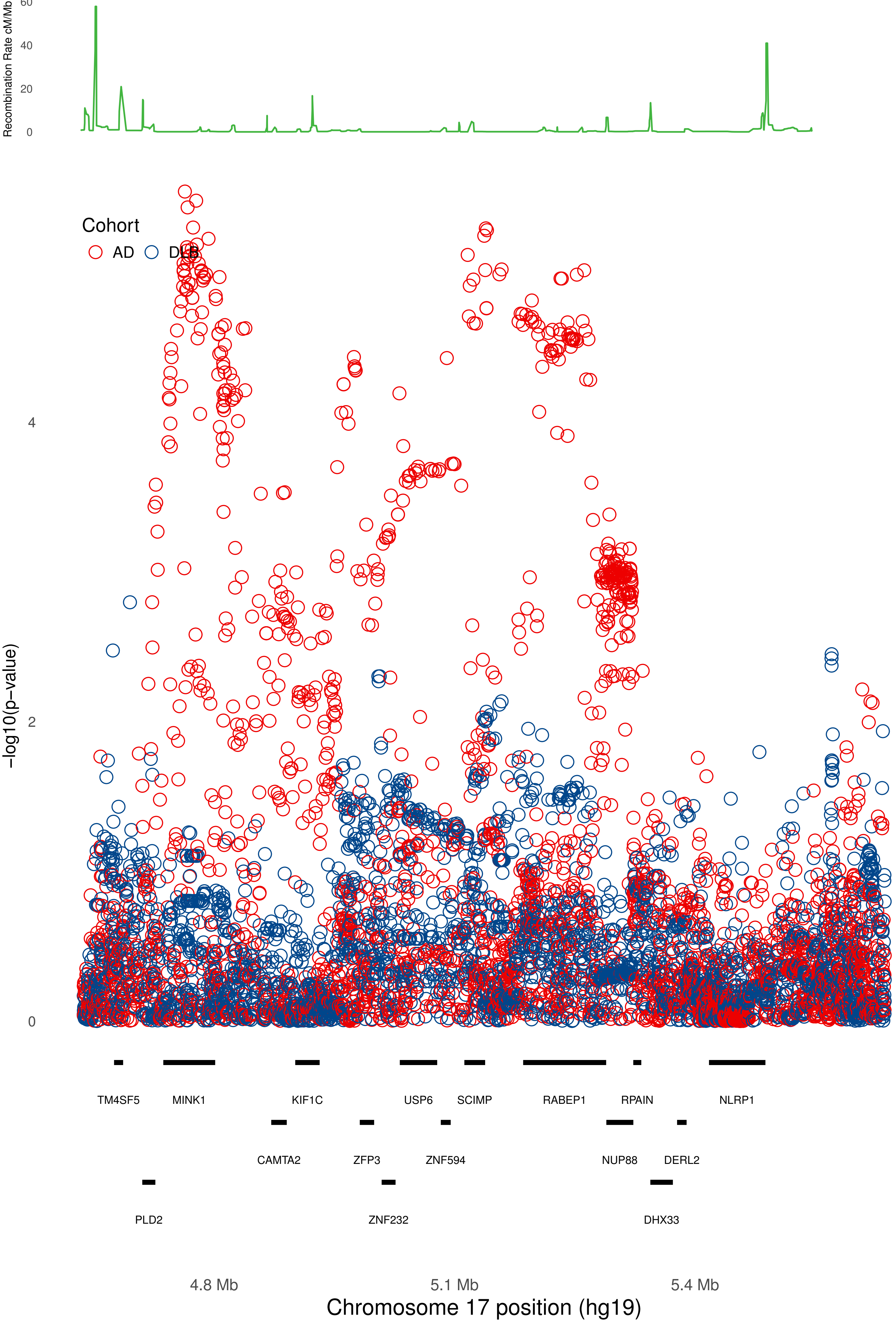
Recombination Rate cM/Mb
60
40
20
0
Cohort
AD
DLB
-log10(p-value)
4
2
0
TM4SF5
MINK1
KIF1C
USP6
SCIMP
RABEP1
RPAIN
NLRP1
CAMTA2
ZFP3
ZNF594
NUP88
DERL2
PLD2
ZNF232
DHX33
4.8 Mb
5.1 Mb
5.4 Mb
Chromosome 17 position (hg19)

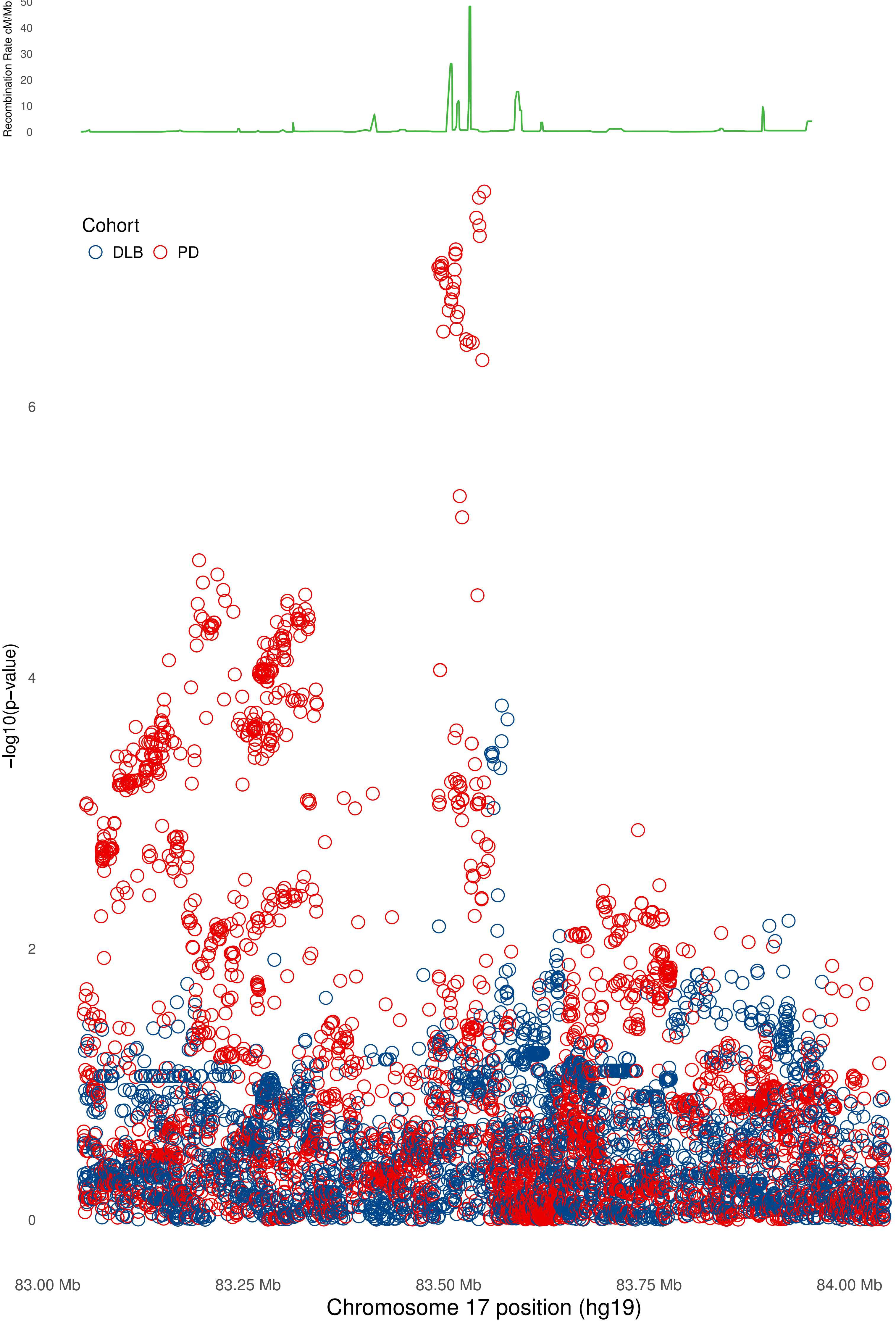
Recombination Rate cM/Mb
50
40
30
20
10
0
Cohort
DLB
PD
-log10(p-value)
6
4
2
0
83.00 Mb
83.25 Mb
83.50 Mb
83.75 Mb
84.00 Mb
Chromosome 17 position (hg19)

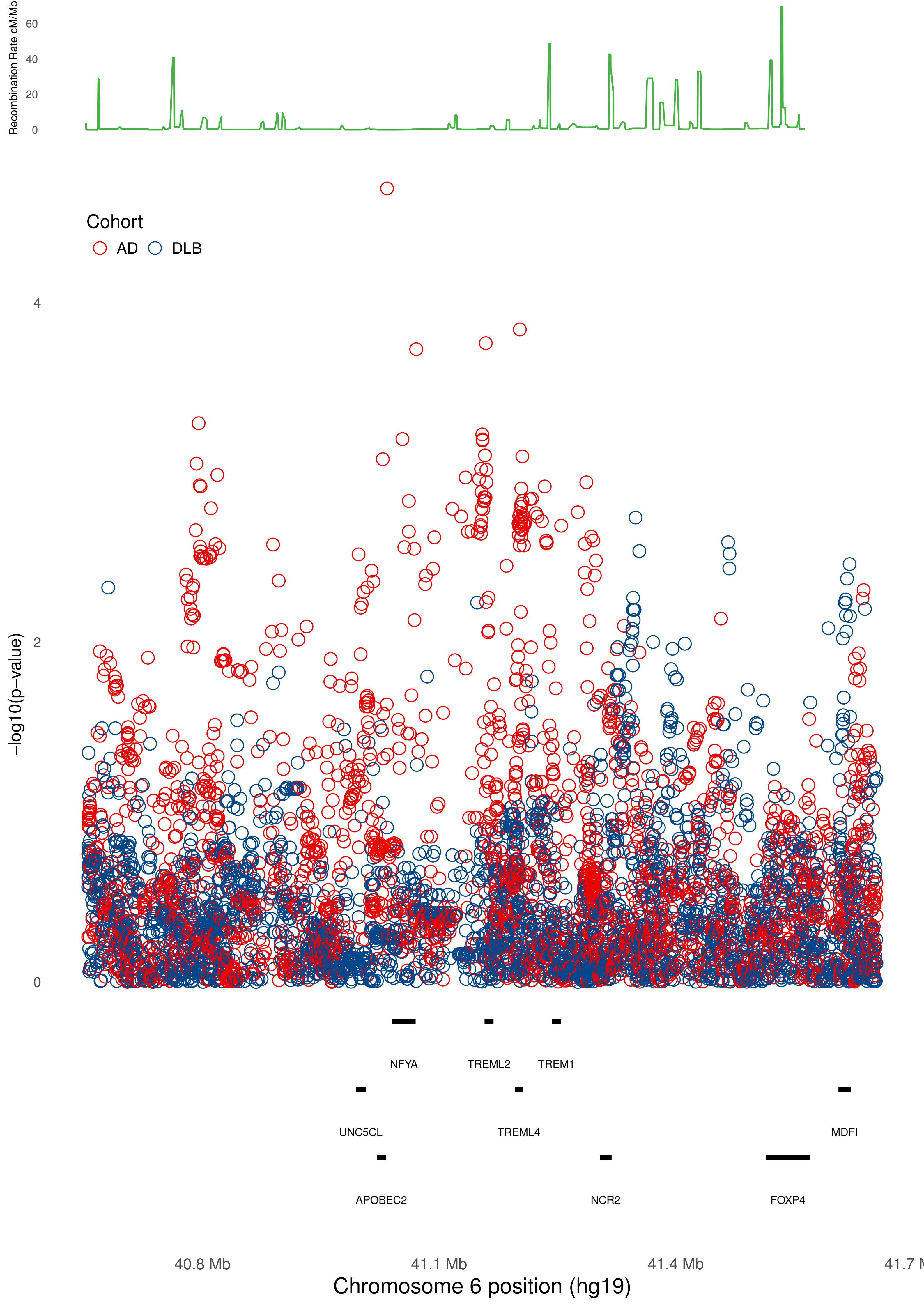
Recombination Rate cM/Mb
60
40
20
0
Cohort
AD
DLB
4
2
0
-log10(p-value)
NFYA
TREML2
TREM1
UNC5CL
TREML4
MDFI
APOBEC2
NCR2
FOXP4
40.8 Mb
41.1 Mb
41.4 Mb
41.7 M
Chromosome 6 position (hg19)

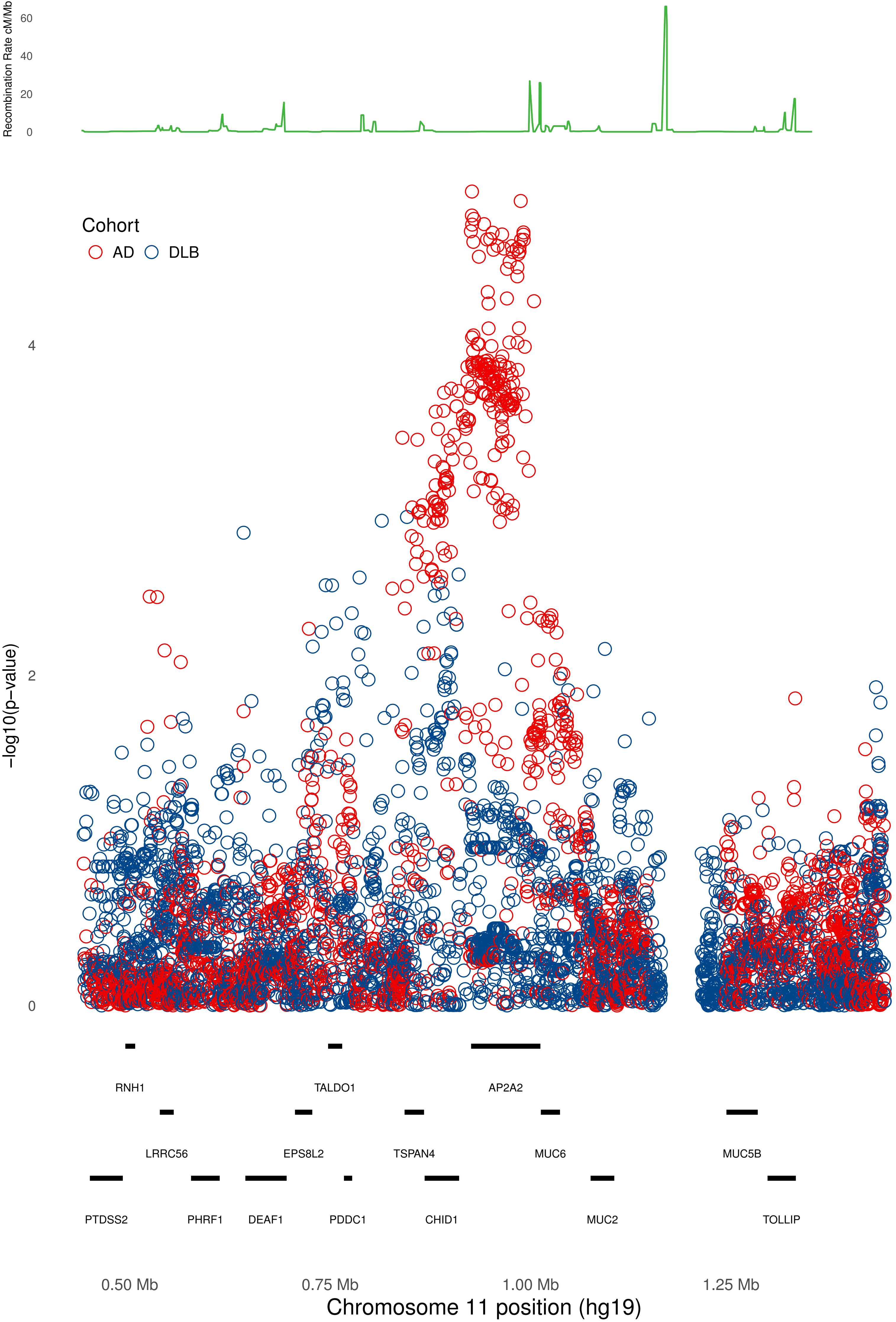

Recombination Rate cM/Mb
60
40
20
0
Cohort
AD
DLB
-log10(p-value)
4
2
0
RNH1
TALDO1
AP2A2
LRRC56
EPS8L2
TSPAN4
MUC6
MUC5B
PTDSS2
PHRF1
DEAF1
PDDC1
CHID1
MUC2
TOLLIP
0.50 Mb
0.75 Mb
1.00 Mb
1.25 Mb
Chromosome 11 position (hg19)

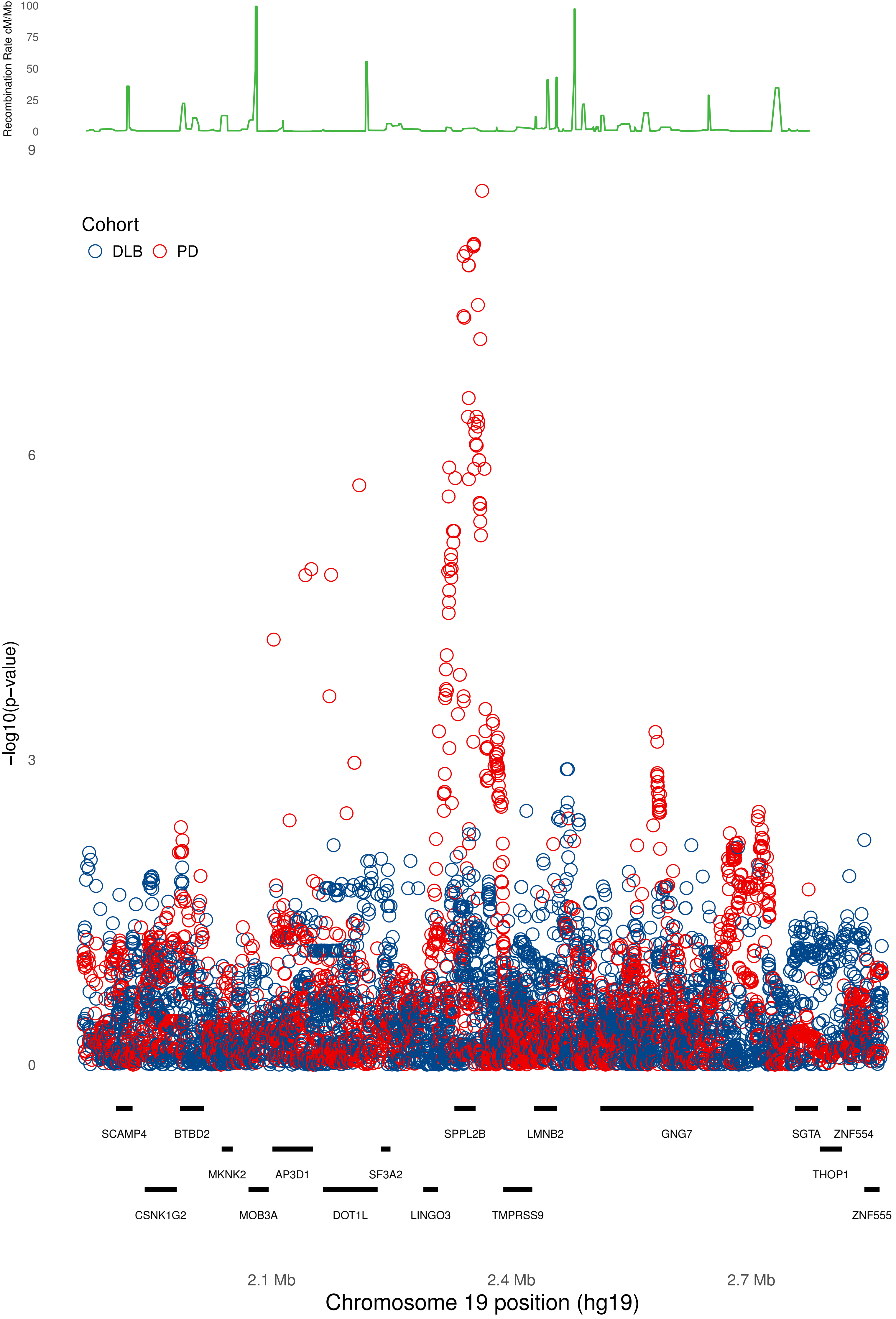
Recombination Rate cM/Mb
100
75
50
25
0
9
6
3
0
−log10(p−value)
Cohort
DLB
PD
SCAMP4
BTBD2
SPPL2B
LMNB2
GNG7
SGTA
ZNF554
MKNK2
AP3D1
SF3A2
THOP1
CSNK1G2
MOB3A
DOT1L
LINGO3
TMPRSS9
ZNF555
2.1 Mb
2.4 Mb
2.7 Mb
Chromosome 19 position (hg19)

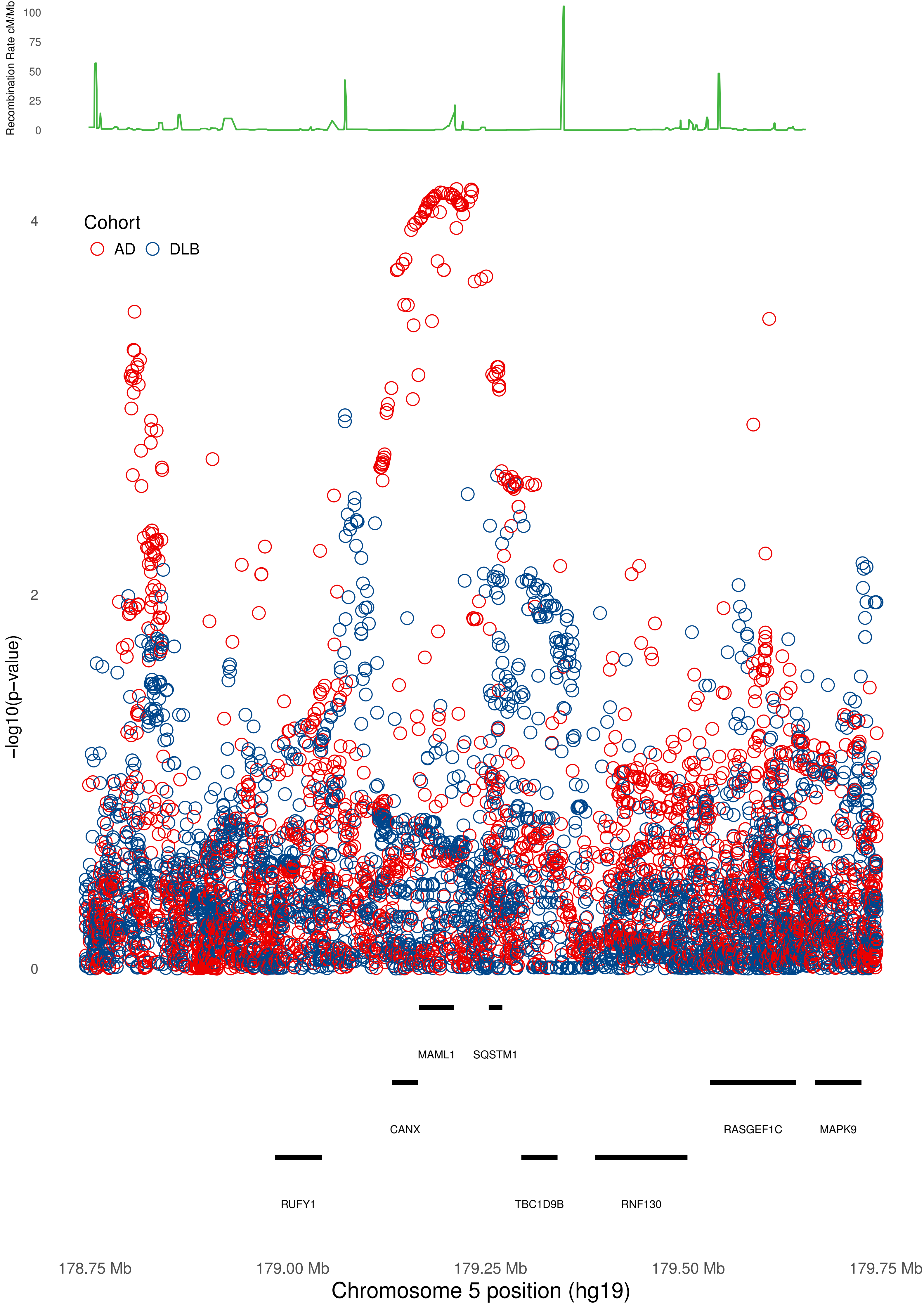
Recombination Rate cM/Mb
100
75
50
25
0
Cohort
AD
DLB
4
2
0
-log10(p-value)
MAML1
SQSTM1
CANX
RASGEF1C
MAPK9
RUFY1
TBC1D9B
RNF130
178.75 Mb
179.00 Mb
179.25 Mb
179.50 Mb
179.75 Mb
Chromosome 5 position (hg19)

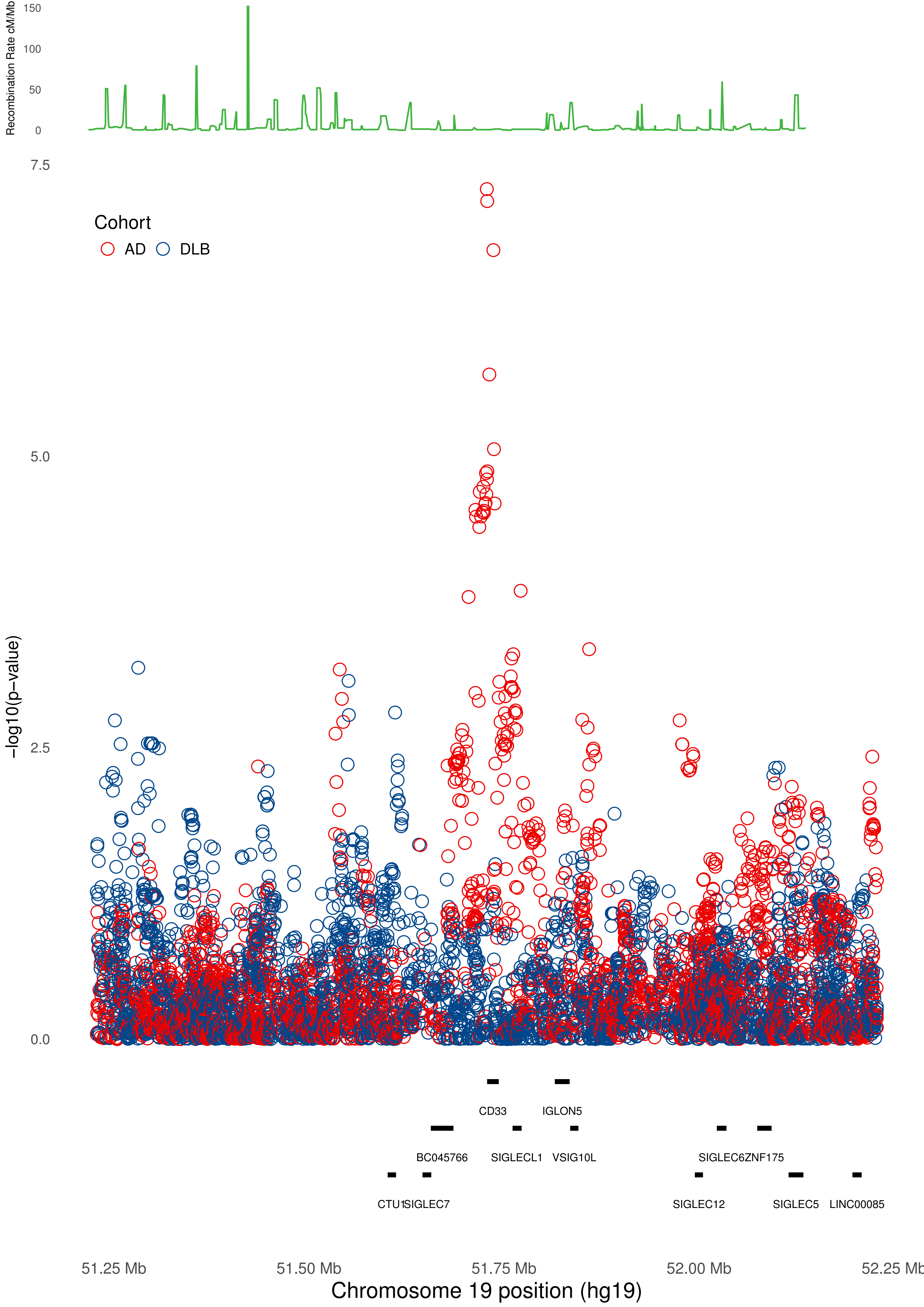
Recombination Rate cM/Mb
150
100
50
0
7.5
5.0
2.5
0.0
-log10(p-value)
Cohort
AD
DLB
CD33
IGLON5
BC045766
SIGLECL1
VSIG10L
SIGLEC6
ZNF175
CTU1
SIGLEC7
SIGLEC12
SIGLEC5
LINC00085
51.25 Mb
51.50 Mb
51.75 Mb
52.00 Mb
52.25 Mb
Chromosome 19 position (hg19)

References

Lambert, J. C., C. A. Ibrahim-Verbaas, D. Harold, A. C. Naj, R. Sims, C. Bellenguez, A. L. DeStafano, et al. 2013. “Meta-Analysis of 74,046 Individuals Identifies 11 New Susceptibility Loci for Alzheimer’s Disease.” Nature Genetics 45 (12): 1452–58.

Nalls, Mike A., Nathan Pankratz, Christina M. Lill, Chuong B. Do, Dena G. Hernandez, Mohamad Saad, Anita L. DeStefano, et al. 2014. “Large-Scale Meta-Analysis of Genome-Wide Association Data Identifies Six New Risk Loci for Parkinson’s Disease.” Nature Genetics 46 (9): 989–93.

Peuralinna, Terhi, Liisa Myllykangas, Minna Oinas, Mike A. Nalls, Hannah A. D. Keage, Veli-Matti Isoviita, Miko Valori, et al. 2015. “Genome-Wide Association Study of Neocortical Lewy-Related Pathology.” Annals of Clinical and Translational Neurology 2 (9): 920–31.